ABSTRACT

Title of Document: PYROLYSIS MODEL PARAMETER OPTIMIZATION USING A CUSTOMIZED STOCHASTIC HILL-CLIMBER ALGORITHM AND BENCH SCALE FIRE TEST DATA

Robert Dale Webster, Jr.
Master of Science, 2009

Directed By: Professor Arnaud Trouvé
Department of Fire Protection Engineering

This study examines the ability of a stochastic hill-climber algorithm to develop an input parameter set to a finite difference one-dimensional model of transient conduction with pyrolysis to match experimentally determined mass loss rates of three sample materials exposed to a range of constant incident heat flux. The results of the stochastic hill-climber algorithm developed as part of the present study are compared to results obtained with genetic algorithms. Graphical documentation of the impact of single parameter mutation is provided. Critical analysis of the physical meaning of parameter sets, and their realistic range of application, is presented. Criteria are also suggested for stability and resolution of solid phase temperature and fuel mass loss rate in an implicit Crank-Nicolson scheme with explicit treatment of the heat generation source term.

PYROLYSIS MODEL PARAMETER OPTIMIZATION USING A CUSTOMIZED STOCHASTIC HILL-CLIMBER ALGORITHM AND BENCH SCALE FIRE TEST DATA

By

Robert Dale Webster Jr.

Thesis submitted to the Faculty of the Graduate School of the
University of Maryland, College Park, in partial fulfillment
of the requirements for the degree of
Master of Science
2009

Advisory Committee:
Professor Arnaud C. Trouvé, Chair
Professor Peter B. Sunderland
Professor James G. Quintiere

Acknowledgements

I would like to thank my thesis advisory committee chair, Dr. Arnaud Trouvé for his mentoring and encouragement. I would like to thank my other committee members Dr. Peter B. Sunderland and Dr. James G. Quintiere for their invaluable instruction during my years as a graduate student in the University of Maryland, Department of Fire Protection Engineering.

I would like to thank Dr. Mariano Lázaro Urrutia. Dr. Lázaro is a researcher at the University of Cantabria, where he performs studies related to fire computer modeling, pyrolysis modeling, dimensional scale fire testing and real scale fire testing. Dr. Lázaro has graciously provided the cone calorimetry test data for all three materials, and the results of implementing Genetic Algorithms used for comparison in the present study.

I would like to thank my co-worker, and 2009 graduate from the University of Maryland, Department of Fire Protection Engineering, Chi T. Do. Chi has been a sounding board for my ideas over the past few months, and has never hesitated to offer constructive criticism.

Most of all, I would like to thank my wife, Ms. Kimberly Webster. Without her support at home in raising our two little girls, Kyliegh and Laurelin, this work would not have been possible.

Table of Contents

Table of Contents
(continued)

List of Figures

List of Figures
(continued)

List of Figures
(continued)

List of Figures
(continued)

List of Figures
(continued)

List of Figures
(continued)

List of Figures
(continued)

List of Figures
(continued)

List of Figures
(continued)

List of Figures
(continued)

List of Figures
(continued)

List of Figures
(continued)

Chapter 1. Introduction

The predictive capability of computer fire models depends on several factors, including the numerical quality of the differential equation solver, the quality of the spatial and temporal resolution, and the fidelity of the sub-models used to represent unresolved physical phenomena. Current models proposed to describe the thermal degradation of solid fuel sources and the associated production of flammable vapors (i.e., the pyrolysis processes) represent one of the major bottlenecks in fire modeling.

In fire safety science and engineering literature, pyrolysis models originate from a variety of approaches ranging from empirical formulations based on experimental data obtained in cone or furniture calorimeter tests, to semi-empirical models [1, 2, 3] that consider transient heat conduction, to comprehensive models [4, 5] based on advanced descriptions of the in-solid heat and mass transfer processes. Comprehensive pyrolysis models adopt a material science perspective, and describe the heat-driven chemical transformation of the virgin solid into solid, liquid and gaseous products. While these models have the ability to capture the influence of the gas-to-solid thermal loading on the rate of production of flammable vapors (i.e., on the fuel mass loss rate), they typically include a large number of unknown parameters that require optimization (calibration).

During parameter optimization, the pyrolysis model parameters are determined by comparisons with experimental data. Unknown model parameters include material properties (e.g., effective values of the mass density, heat capacity, thermal conductivity and emissivity) and parameters of the chemical reactions (e.g., values of the pre-

exponential factors, activation energies, products yields, threshold temperatures and heats of reaction). The experimental data typically come from cone calorimeter tests (the cone calorimeter is a well-established, relatively well-controlled, quasi-one-dimensional configuration) and provide information on the temporal variations of the fuel mass loss rate for different levels of radiant exposure [6].

The present study is focused on an application of the pyrolysis model incorporated into the Fire Dynamics Simulator (Version 5) [4] program; FDS is developed by the Building and Fire Research Laboratory of the U.S. National Institute of Standards and Technology (NIST). More precisely, the present study considers: a one-step Arrhenius-type global pyrolysis reaction for charring materials; cone calorimeter data corresponding to three sample materials (a panel material and a carpet material, both used in commercial aircraft, and a wall material used in metro trains); and 2 optimization techniques for parameter estimation (a stochastic hill-climber algorithm and a genetic algorithm).

Chapter 2. FDS Pyrolysis Model

The solid phase sub-models within FDS [4] were developed by Simo Hostikka, a Senior Research Scientist at VTT Technical Research Centre of Finland. FDS has several approaches for describing the pyrolysis of solids and the evaporation of liquids. The approach to take depends largely on the availability of material properties and the appropriateness of the underlying model. The model evaluated in the present study is referred to in the FDS User Manual [7] as "Solid Fuels that do NOT Burn at a Specified Rate".

2.1 Heat Diffusion

The temperature profile within a body depends upon the rate of its internally-generated heat ($\dot{q}'''_{gen}$), its capacity to store heat ($\rho c \frac{\partial T}{\partial t}$), and the rate of thermal conduction to its boundaries ($k\nabla^2 T$). Mathematically, this is stated by the heat equation [8].

$$\rho c \frac{\partial T}{\partial t} = \nabla \cdot (k \nabla T) + \dot{q}'''_{gen} \qquad (2\text{-}1)$$

FDS employs a one-dimensional transient form of the heat equation with internal generation. In the case of pyrolysis, internal heat generation is a negative term accounting for the amount of energy loss.

$$\rho c \frac{\partial T}{\partial t} = \frac{\partial}{\partial x}\left(k \frac{\partial T}{\partial x} \right) - \dot{q}'''_{reac} \qquad (2\text{-}2)$$

FDS employs finite-rate kinetics, a common technique for comprehensive models [9, 10]. The amount of energy loss due to pyrolysis per cell ($\dot{q}'''_{reac}$) is modeled in FDS as linearly proportional to the rate of mass loss per cell ($\dot{m}'''_{loss}$), where the constant of proportionality is called the heat of reaction (ΔH_R). FDS employs an Arrhenius form of the global reaction rate equation to calculate the rate of mass loss per cell as a function of cell temperature (T).

2.2 Global Reactions

Global reactions are commonly used because they allow for a quick approximation without a full understanding of the intermediate steps or species formed [11]. In chemistry, the overall reaction can be expressed by the global reaction mechanism:

$$Reactant\ A + Reactant\ B \rightarrow Products \tag{2-3}$$

From experimental measurements, the rate at which Reactant A is consumed can be expressed as

$$r = \frac{d}{dt}[X_A] = k_G [X_A]^n [X_B]^m \tag{2-4}$$

where the notation $[X_i]$ denotes the molar concentration of the ith species in the mixture. This equation states that the rate of disappearance of X_A is proportional to the concentration of each of the reactants raised to a power. Because there are two reactants, this is referred to as a bimolecular reaction.

The constant of proportionality k_G, is called the global rate coefficient, and, in general, is not constant, but is rather a strong function of temperature.

The exponents n and m relate to the reaction order. The reaction is nth order with respect to A and mth order with respect to B, and $(n+m)$th order overall. For global reactions, n and m are not necessarily integers and arise from curve fitting experimental data.

2.3 Arrhenius Form

The form of the constant of proportionality k_G, is attributed to Suante Arrhenius, who showed that the thermal behavior for the rate is proportional to $e^{-E/(RT)}$ by the constant B,

$$k_G = Be^{-E/(RT)} \tag{2-5}$$

where R is the universal gas constant and E is the activation energy having units of kJ/kmol. The form of the Arrhenius global reaction rate can be derived by applying basic principles of thermochemistry as follows:

Molecular weight of the ith species is equal to the mass of the ith species divided by the number of moles of the ith species.

$$MW_i = m_i / moles_i \tag{2-6}$$

Mixture density is equal to the mixture mass divided by the mixture volume.

$$\rho_{mix} = m_{mix} / V_{mix} \tag{2-7}$$

Molar concentration is equal to the number of moles of the ith species divided by the mixture volume.

$$[A] = moles_i / V_{mix} \tag{2-8}$$

Mass fraction of the ith species is equal to the mass of the ith species divided by the mixture mass.

$$Y_i = m_i / m_{mix} \tag{2-9}$$

Combining Equations 2-4 through 2-9:

$$r = {Y_A}^n {Y_B}^m A_0 e^{-E/(RT)} \tag{2-10}$$

Where:

$$A_0 = \frac{B{\rho_{mix}}^{n+m}}{{MW_A}^n {MW_B}^m} \tag{2-11}$$

2.4 FDS Model

Pyrolysis in FDS is limited to unimolecular reactions meaning that only one reactant is involved. In addition, a component is added to prohibit reactions below an artificially imposed temperature threshold (T_{thr}), yielding the expression:

$$r = A_0 Y^{ns} e^{(-E/RT)} \max\left[0, T - T_{thr}\right]^{nt} \tag{2-12}$$

Because the mass fractions of individual solid species (Y) are not tracked in FDS, Y is calculated as the species mass per unit volume (ρ) divided by the original mass per unit volume (ρ_0).

$$Y = \frac{\rho}{\rho_0} \tag{2-13}$$

By default, the value of $nt = 0$ and the value of $T_{thr} = -273.15\,\mathrm{K}$, yielding the customary expression:

$$r = A_0 Y^{ns} e^{(-E/RT)} \tag{2-14}$$

The user is given the option of assigning nt a non-zero value, thus making the constant of proportionality of the three parameter functional form:

$$r = A_0 Y^{ns} T^{nt} e^{(-E/RT)} \tag{2-15}$$

In this form, nt should be used to express temperature dependence. Estimations of nt can be obtained from general texts on collision theory, a theory based on gas kinetics. However, it is not uncommon to find implementations of the three parameter functional form applied to solid pyrolysis, for curve fitting purposes.

In the present study, the practice of assigning $ns = 1$, $nt = 0$ and T_{thr} a value equal to the species ignition temperature (T_{ig}) was followed yielding:

$$\text{when } T \le T_{thr}, \text{ then } r = 0 \tag{2-16}$$

$$\text{when } T > T_{thr}, \text{ then } r = YA_0 e^{(-E/RT)} \tag{2-17}$$

Chapter 3. Evolutionary Algorithms

Evolutionary Algorithms (EA's) are optimization techniques inspired by the theory of evolution proposed by Charles Darwin in "The Origin of Species by Means of Natural Selection" [12]. Evolutionary algorithms differ from more traditional optimization approaches in that they seek to optimize a population rather than a single individual.

Evolutionary algorithms start with a genetically diverse population (i.e. each individual in a population has unique traits). With each consecutive generation, those individuals that are better adapted survive, pass their traits on to their offspring. After many generations, the entire population trends toward convergence on a set of common traits which have allowed them to be well adapted to the conditions of their environment.

When evolutionary algorithms are applied to pyrolysis model parameter optimization; the "traits" refer to the magnitudes of unknown parameters, "individuals" represent combinations of parameters (or parameter sets), and the "conditions of the environment" are a measure of fitness to experimental test data.

In the present study, a distinction is made between the terms "parameters" and "properties" in that "parameters" refers to unknown inputs to the model, and "properties" are well defined, measured quantities.

Several different types of evolutionary algorithms have been developed for a wide range of application. Some of these algorithms include Genetic Programming (GP),

which evolve programs, Evolutionary Programming (EP), which focuses on optimizing continuous functions without recombination, Evolutionary Strategies (ES), which focuses on optimizing continuous functions with recombination, and Genetic Algorithms (GA), which focus on optimizing general combinatorial problems.

To date, all moderately successful optimization for pyrolysis model input has been conducted using Genetic Algorithms (GA) [13]. For a detailed explanation of use of genetic algorithms for pyrolysis model parameter optimization, refer to "A Generalized Pyrolysis Model for Combustible Solids", by Christopher Lautenberger [5], and other notable works [14-18].

3.1 Computational Efficiency

In computing, there are circumstances in which the outputs of all procedures solving a particular type of problem are statistically identical. The customary way of describing such a circumstance, introduced by Wolpert and Macready [19, 20] in connection with the problems of search and optimization, is to say that there is No Free Lunch (NFL).

NFL establishes that in the absence of prior knowledge of the evaluation function for a problem and when all possible evaluation functions for a problem are considered, no technique will perform better over the complete set of evaluation functions than any other technique. It is not the intent of the present study to derive the NFL criteria; however, mathematically it is expressed as:

$$\sum_f P\left(h_m^y \middle| f, m, a_1\right) = \sum_f P\left(h_m^y \middle| f, m, a_2\right) \tag{3-18}$$

Thus, in the absence of knowledge, blind or random search is exactly as efficient as any other optimization technique.

Proponents of evolutionary algorithms argue, however, that it is reasonable to use evolutionary algorithms as an initial strategy in preference to blind search. This is supported by the assumption that a small amount of knowledge of the evaluation function is gained with each successive evolution.

3.2 Parameter Optimization

Prior studies that have applied evolutionary algorithms to the problem of pyrolysis modeling have received a significant amount of criticism from the traditional fire protection community. The reason being, of course, that it is questionable that the parameters attained through random mutation could have any physical meaning, and it is questionable that these parameters could have any application outside of the calibrated range.

The general procedure for creating empirical models of pyrolysis is to (1) identify well defined, measurable quantities, (2) propose a mathematical model that relates those quantities and then (3) determine curve fitting coefficients that provide the best fit to experimental data.

Alternatively, use of the comprehensive models (with parameter optimization) requires the user to (1) propose a mathematical model, (2) determine curve fitting parameters that provide the best fit to experimental data and (3) assume a relationship exists between the modeled parameters and the actual physical properties.

When implementing evolutionary algorithms, there is no experimental link between parameters attained and actual physical properties. However, proponents of evolutionary algorithms have argued that their use is equivalent to conducting experiments, and that the solution parameter sets actually have physical meaning. The present study seeks to investigate the physical meaning of parameter sets, and their realistic range of application.

Chapter 4. Contributors to the Field of Parameter Optimization

The following paragraphs summarize the contributions of those currently applying evolutionary algorithms to the problem of pyrolysis parameter optimization.

4.1 Lautenberger w/ Fernandez–Pello

Dr. Lautenberger's primary research interest is computer modeling of fires and related solid-phase (pyrolysis) processes. His Ph.D. dissertation [5] involved formulation and coding of a generalized pyrolysis model to simulate the pyrolysis and gasification of a variety of solid combustibles encountered in fires, development of a material property estimation technique to quantify solid combustibles in terms of the material properties needed by this pyrolysis model, and fire development modeling over a range of length scales using this pyrolysis model coupled to FDS.

Dr. Lautenberger is working at UC Berkeley as a post doctoral researcher in the Department of Mechanical Engineering in the Combustion Processes Laboratory. His research project is, "Tackling CFD Modeling of Flame Spread on Practical Solid Combustibles," (PI Carlos Fernandez-Pello). As part of this work, techniques initially proposed in his dissertation to estimate material properties from flammability test data will be extended and improved. This aspect of the work will disseminated via Google Code, see http://code.google.com/p/gpyro for details. The ultimate goal of this research is to tackle CFD-based prediction of room-scale fire growth on real world fuels.

4.2 Matala w/ Ehtamo & Hostikka

Matala's M.S. thesis in 2008 was entitled "Estimation of Solid Phase Reaction Parameters for Fire Simulation". The goal of the thesis was to study and build an effective application of genetic algorithms, and to use it for estimating the parameters of a pyrolysis model. Genetic algorithms proved to be a very practical tool for this research, making it possible to estimate several parameters simultaneously.

The effects of thermal parameters were also studied and a guide for estimating them manually was developed. Thermal parameters were estimated both with the genetic algorithm, and without, using the guide. Both methods had their advantages: The genetic algorithm was capable of handling the estimation process without user's participation, but the process was quite slow. On the other hand, finding the parameters manually was quicker, but required significant user interaction.

Ms. Matala continues to fine tune her computational methodology in her career at VTT Finland, and in her pursuit of a PhD at the Helsinki University of Technology.

4.3 Dembsey w/ Janssens & Hurley

NIST has funded a multi-year effort (2008-2011) Entitled “Development of Guidelines for Obtaining Material Parameters for Input into Fire Models”. The work is being conducted by Nicholas Dembsey at WPI with sub-awards to Marc Janssens at SwRI and Morgan Hurley at SFPE. The objective of the project is to create a SFPE Guidance Document for fire pyrolysis model parameter estimation.

Chapter 5. Genetic Algorithms

The logic of genetic algorithms can be described in four distinct processes; (1) initialization, (2) selection, (3) reproduction and (4) termination. The following paragraphs summarize typical implementation of genetic algorithms for the purposes of comparison. However, specific applications of genetic algorithms may vary.

5.1 Initialization

The initial traits of individuals within a population are customarily randomly generated within a user defined parameter space. The intent of generating random traits is to impose genetic diversity throughout the population. Population size is also a user defined quantity, and depending on the problem, can range from hundreds to tens of thousands of individuals.

5.2 Selection

With each successive generation, a percentage of the population is selected for reproduction. Probability of selection is customarily based on fitness. Fitness functions quantify the extent to which individuals are adapted to the conditions of their environment. Generally these functions are a simple error quantifier. Where multiple environmental conditions are present, fitness functions typically employ a weighted mean. In the present study, the term "goal" is used synonymously with environmental conditions, and the term "competing goals" is meant to indicate a weighted mean of multiple goals. Although the probability of selection is based on fitness, there is a random

component so that a small percentage of less fit individuals are selected. This functionality keeps the population diverse, preventing premature convergence on a local optimum. The term "local optimum" is used in the present study to reference a parameter set which satisfies the fitness function better than closely related parameter sets; however, is not the parameter set which best satisfies the fitness function, known as the global optimum.

5.3 Reproduction

Reproduction is the process by which a new generation is derived from a previous one. Reproduction is conducted on a per child basis, and is accomplished through the genetic processes of crossover (also called recombination), and/or mutation. For each new "child" to be produced, a pair of "parents" is selected for breeding. Crossover is the process by which traits of the parents are passed to the child. Mutation is the process introducing small random variations in the traits of children. Each child typically has a unique set of parents. The process of producing children is continued until the population of the new generation is equal to the population of the previous one. In the present study, the term "iteration" is used synonymously with generation.

5.4 Termination

The evolutionary process is continued until a termination condition is reached. Customary termination conditions include when; (1) a solution is found that satisfies minimum criteria, (2) a fixed number of generations are reached, (3) an allocated budget (computation time) has been reached or (4) a combination of the above.

Chapter 6. Stochastic Hill-Climber Algorithm

The following paragraphs summarize the stochastic hill-climber algorithm "HC-PYRO", developed as part of the present study. Source code, written in an application specific LISP programming language, is provided in Appendix B. This chapter is organized so that a comparison can be made to genetic algorithms.

6.1 Initialization

Using stochastic hill-climber algorithms, the initial parameter sets should be chosen based on informed engineering judgment. This could mean knowledge of the actual thermophysical properties of the material in question. However, experience indicates that hand picking material properties does not increase the probability that the resulting mass loss rate curve will have any of the characteristics of the desired curve.

The desired method for initial parameter selection, and the one used in the present study, is based on selection of curve characteristics rather than the value of any one parameter. In other words, it's much more computationally efficient to start with a curve that looks good with incorrect parameters, than one that looks bad with correct parameters.

For more information regarding the characteristic mass loss rate curves for pyrolysis of solids, refer to "A Semi-Quantitative Model for the Burning Rate of Solid Materials", by Dr. James Quintiere [1]. For recommended procedures on manually

developing characteristic curves (shown below), refer to "Estimation of Solid Phase Reaction Parameters for Fire Simulation" by Anna Matala [14].

Effect	k_{solid}	$c_{p,solid}$	k_{char}	$c_{p,char}$	ΔH	ΔH_c
Time of ignition (T_{ign})	+	+	0	0	0	0
1st peak (width) (w_1)	0	0	+	0	(-)	0
1st peak (height) (h_1)	0	0	0	0	(-)	+
Depth of valley (d)	0	+	-	0	+	+
2nd peak (time) (T_2)	-	+	-	0	0	+
2nd peak (height) (h_2)	+	+	+	-	-	+

Figure 6-1. Effect of Increasing Select Parameters on the Characteristic Mass Loss Rate Curve (Matala)

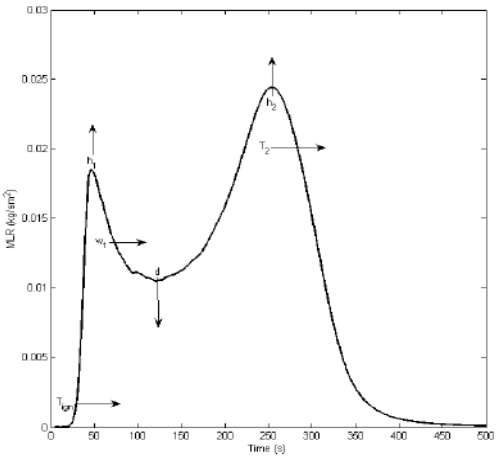

Figure 6-2. Meaning and Positive Directions of Effects on the Characteristic Mass Loss Rate Curve (Matala)

The timing of the second peak in the figure above is coincident with the back face reaching the threshold temperature. For the purposes of the present study, the term "thermally-thick" is used to indicate a characteristic curve where the second peak is temporally separated from the first peak. Simply stated, thermally-thick means that it takes a long time for heat to penetrate the depth of the specimen. Conversely, the term "thermally-thin" is used in the present study to indicate a condition where the first and second peaks are coincident.

6.2 Selection

The fitness function used in the present study is simply the coefficient of determination, commonly referred to as the "R-squared" (R^2) value.

$$R^2 \equiv 1 - \frac{SS_{err}}{SS_{tot}} \tag{6-19}$$

and

$$SS_{err} = \sum_i (y_i - f_i)^2 \quad \text{and} \quad SS_{tot} = \sum_i (y_i - \bar{y})^2 \tag{6-20}$$

where f_i are the modeled values, y_i are the observed values from cone calorimetry, and $\bar{y}_i$ is the average value from cone calorimetry. The coefficient of determination (R^2) is a statistical measure of how well the model approximates the test data. An R^2 value of 1.0 (or 100%) indicates that the model perfectly fits the test data. For detailed information on the coefficient of determination (R^2), refer to general texts on probability and statistics.

6.3 Reproduction

The basic principle of stochastic hill-climbing is searching for successively better fit parameter sets through random mutation. Making a comparison to genetic algorithms, stochastic hill-climbing is a genetic algorithm without cross-mutation and a population of 2, parent and child. Stochastic hill-climbing is also unique in that the parents outlive the children if they are better adapted to the environment.

In stochastic hill-climbing, children only differ from the parents by the magnitude of the mutation. In the present study, the magnitude of the mutation of any parameter for each iteration, excluding those parameters with defined targets (see Section 10.1), is a random function of the normalized mutation magnitude and the iteration number.

6.3.1 Normalization

To keep any single parameter from dominating the solution, the magnitude of the mutation for any parameter is limited to that which results in a maximum 5% change in the accuracy of primary curve. This is accomplished by systematically stepping through each parameter of the set and adjusting that parameter until a 5% change in the accuracy of the solution is achieved. The following figures are examples of mutations with normalized impact:

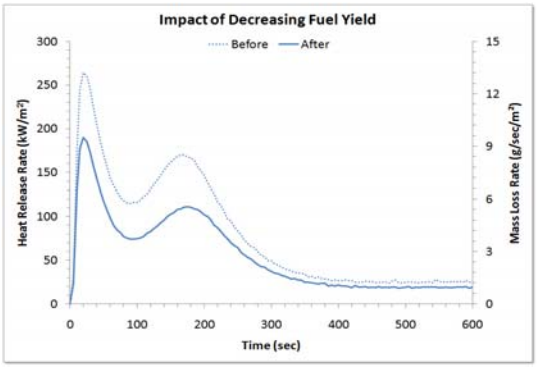

Figure 6-3. Normalized Impact of Decreasing Fuel Yield on the Characteristic Mass Loss Rate Curve

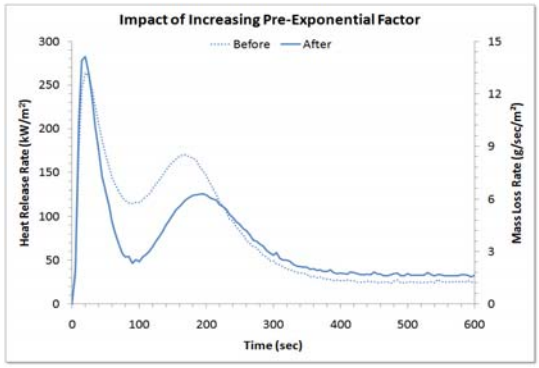

Figure 6-4. Normalized Impact of Increasing Pre-Exponential Factor on the Characteristic Mass Loss Rate Curve

The above figures illustrate mutations in fuel yield and in pre-exponential factor. For the purpose of illustration, the magnitude of each mutation is such that the solution is reduced 50% in accuracy. The magnitude of the mutation is the integer 2, raised to some integer exponent (2^n). As an example, the normalized mutation magnitude for fuel yield may be 2%, and the normalized mutation magnitude for the pre-exponential factor may be 64%.

6.3.2 Iteration Number

A relationship exists between the magnitude of mutations and the probability that mutations will result in a better fit solution. Because of this, the magnitude of each mutation (as determined by the normalized impact) is multiplied by a scalar which decreases the magnitude of the mutations with each unsuccessful iteration, and increases the magnitude with each successful one.

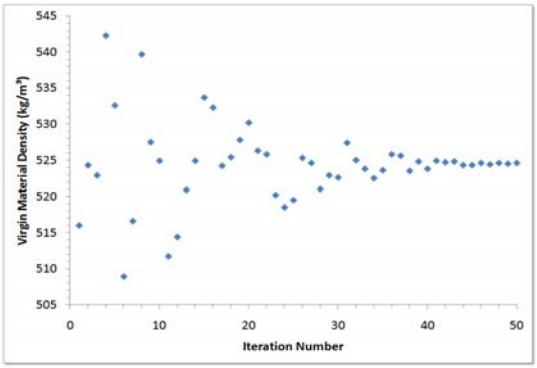

Figure 6-5. Example of Density Mutation Magnitude as a Function of Iteration Number

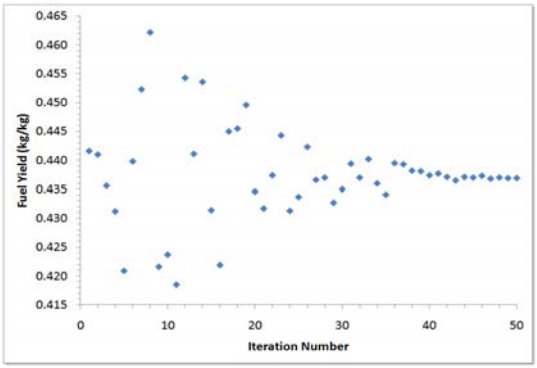

Figure 6-6. Example of Fuel Yield Mutation Magnitude as a Function of Iteration Number

The above figures illustrate the decrease in mutation magnitude as a function of the number of unsuccessful iterations (Iteration Number). These figures are typical of the last 50 iterations before optimization termination.

6.4 Termination

When the iteration number increases to a point where further variation in the parameter set cannot produce better fit solutions, then the algorithm terminates. This indicates that an optimum condition has been reached. The following figures illustrate the typical evolution of the stochastic hill-climber algorithm HC-PYRO:

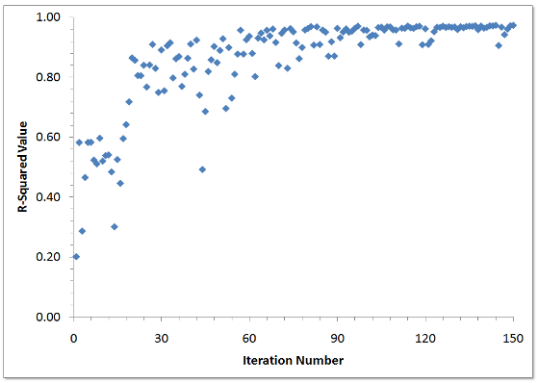

Figure 6-7. Evolution of the R-squared Value as a Function of Iteration Number for HC-PYRO (Example 1)

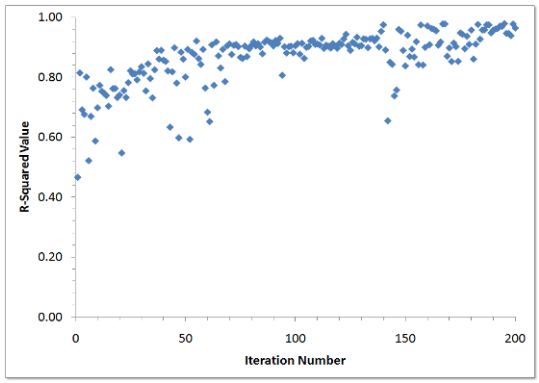

Figure 6-8. Evolution of the R-squared Value as a Function of Iteration Number for HC-PYRO (Example 2)

For any application specific algorithm, the outcome is highly dependent on programming nuances. The results documented in the present study should not be construed to imply any broad conclusion about all stochastic hill-climbing or genetic algorithms.

Chapter 7. Cone Calorimetry Test Data

Material test data used in the present study has been provided by Dr. Mariano Lázaro Urrutia, Research Engineer, GIDAI - Fire Safety - Research and Technology, Dept. of Transport and Technology Projects and Processes, University of Cantabria.

7.1 Test Methodology

These tests were based on the observation that, generally, the net heat of combustion is directly related to the amount of oxygen required for combustion. Approximately 13.1×10^3 kJ of heat are released per 1 kg of oxygen consumed. Specimens in the test were burned in ambient air conditions while subjected to a prescribed external heat flux.

The heat release was determined by measurement of the oxygen consumption, as determined by the oxygen concentration and flow rate in the combustion product stream, consistent with the requirements of ASTM Test Method E 1354 [6], "Standard Test Method for Heat and Visible Smoke Release Rates for Materials and Products Using an Oxygen Consumption Calorimeter".

The primary measurements were oxygen concentration and exhaust gas flow rate. Additional measurements included the mass loss rate of the specimen, time to sustained flaming (or time to ignition), and effective heat of combustion.

7.2 Carpet Material

The "carpet material" referenced in the present study is a carpet sample, commonly used in commercial aircraft. In commercial aircraft, the type of floor covering used depends on the location within the aircraft. Carpet covers most of the cabin floor, including the aisle and under the seats. Most aircraft have wool or nylon-face yarns with a polyester, polypropylene, cotton, or fiberglass backing and a fire-retardant back coating. Wool-face yarned carpets, as tested in the present study, are also treated with a fire retardant. The carpet material sample thickness in the present study was approximately 6.0 mm, and the virgin material density was approximately 450 kg/m³.

7.2.1 Test Results

At exposure heat fluxes greater than or equal to 50 kW/m², the carpet material was observed to burn efficiently, leaving behind only a white powdery residue, as illustrated in the following figures.

Figure 7-1. Photograph of the Carpet Material Before the Cone Calorimetry Test

Figure 7-2. Photograph of the Carpet Material After the Cone Calorimetry Test

In tests with a lower exposure heat flux, a yellow fluid (assumed to be resin treatment) was observed draining from the material. This occurrence could have contributed to error in the mass loss rate data.

The cone calorimetry tests for the carpet material produced heat release rate and mass loss rate curves with two distinct peaks. These results are consistent with that of a residue producing, thermally thick material with insulated backing. For the purposes of the present study, the term "residue" is meant to include char.

At higher heat flux, mass loss rates were greater in magnitude. Additionally, at higher heat flux, the second peak was observed to occur much earlier in time. At lower heat flux, the time to ignition was observed to be greater.

7.2.2 Selection of Data

The carpet material was subjected to six constant heat flux exposures ranging from 25 kW/m² to 75 kW/m². Three tests were conducted at each exposure. For each test, the rate of oxygen consumption was used as an indicator of the heat release rate, recorded in units of kW/m². Mass of the specimen was logged at each time interval, and was used as an indicator of the fuel mass loss rate, recorded in units of g/m²/sec.

Selection of the carpet material data used in the present study was based on whether the data was characteristic of apparent trends throughout the range of exposures, and proportionality of the recorded heat release rate with mass loss rate. The following figures identify the data selected for analysis for each exposure.

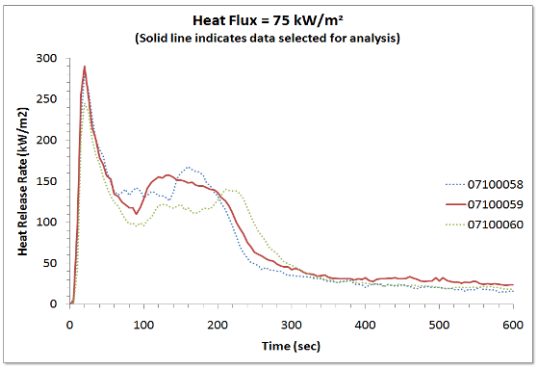

Figure 7-3. Time Variation of the Heat Release Rate in Cone Calorimeter Tests for the Carpet Material Under a 75 kW/m² Radiant Exposure

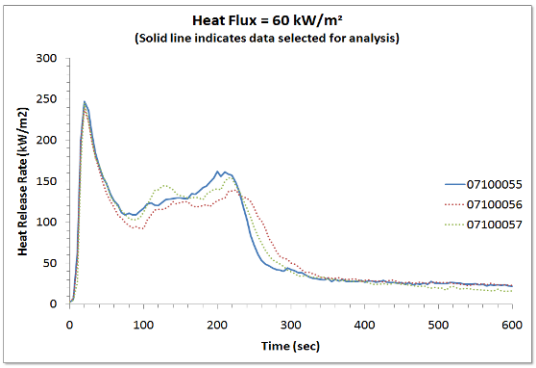

Figure 7-4. Time Variation of the Heat Release Rate in Cone Calorimeter Tests for the Carpet Material Under a 60 kW/m² Radiant Exposure

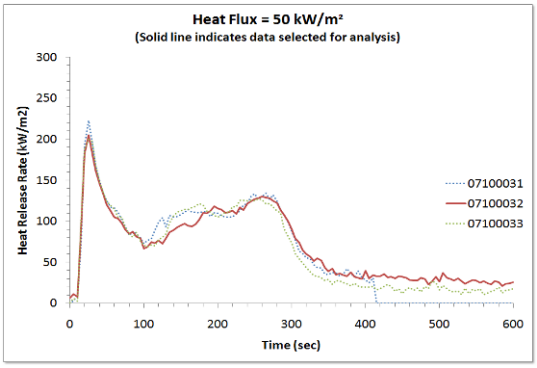

Figure 7-5. Time Variation of the Heat Release Rate in Cone Calorimeter Tests for the Carpet Material Under a 50 kW/m² Radiant Exposure

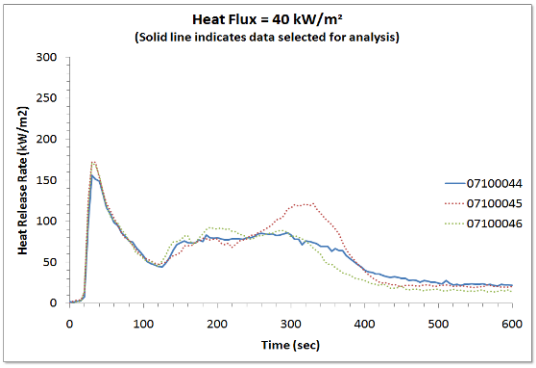

Figure 7-6. Time Variation of the Heat Release Rate in Cone Calorimeter Tests for the Carpet Material Under a 40 kW/m² Radiant Exposure

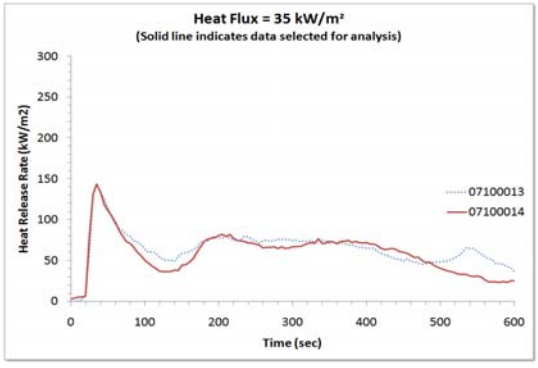

Figure 7-7. Time Variation of the Heat Release Rate in Cone Calorimeter Tests for the Carpet Material Under a 35 kW/m² Radiant Exposure

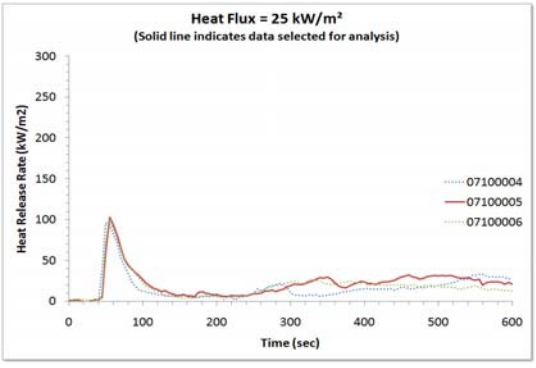

Figure 7-8. Time Variation of the Heat Release Rate in Cone Calorimeter Tests for the Carpet Material Under a 25 kW/m² Radiant Exposure

7.2.3 Heat of Combustion Estimation

It is customary to model the heat release rate as linearly proportional to the mass loss rate, where the constant of proportionality is called the heat of combustion [21, 22], measured in units of kJ/kg. For the purposes of the present study, heat of combustion was estimated semi-quantitatively by comparing the proportionality of the heat release rate with that of mass loss rate. The following figures illustrate the relationship between the heat release rate and mass loss rate for a heat of combustion of 20,000 kJ/kg.

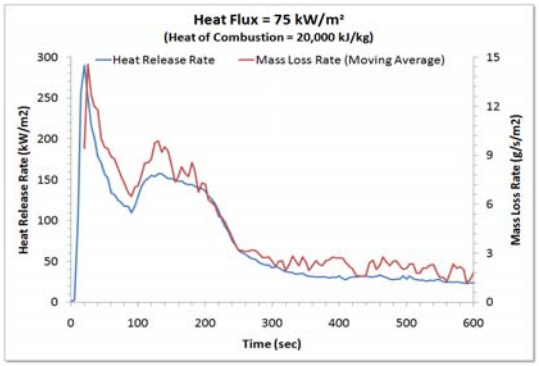

Figure 7-9. Time Variation of the Heat Release Rate and Mass Loss Rate in a Cone Calorimeter Test for the Carpet Material Under a 75 kW/m² Radiant Exposure

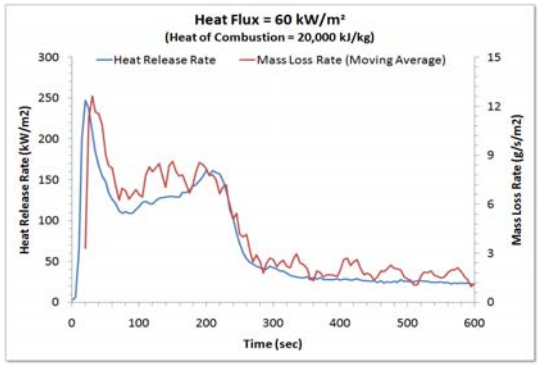

Figure 7-10. Time Variation of the Heat Release Rate and Mass Loss Rate in a Cone Calorimeter Test for the Carpet Material Under a 60 kW/m² Radiant Exposure

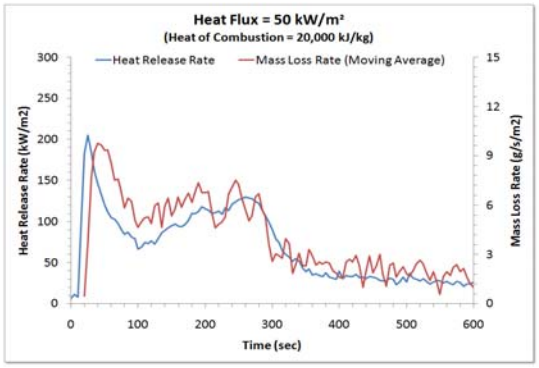

Figure 7-11. Time Variation of the Heat Release Rate and Mass Loss Rate in a Cone Calorimeter Test for the Carpet Material Under a 50 kW/m² Radiant Exposure

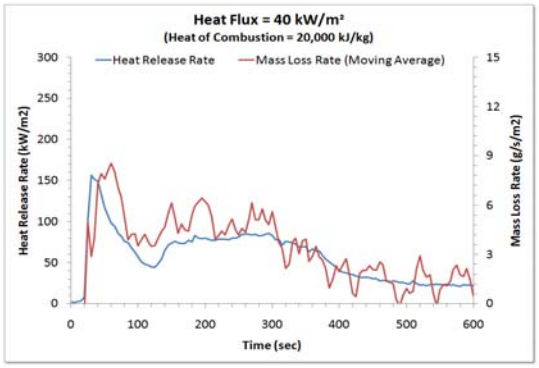

Figure 7-12. Time Variation of the Heat Release Rate and Mass Loss Rate in a Cone Calorimeter Test for the Carpet Material Under a 40 kW/m² Radiant Exposure

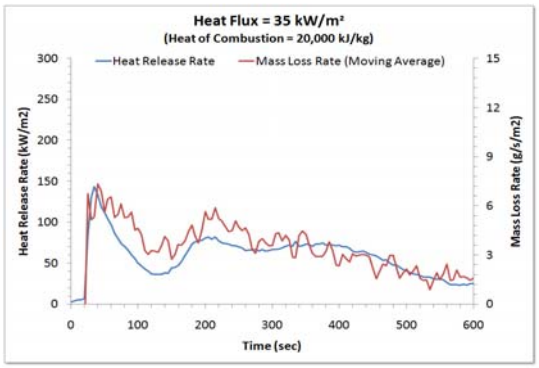

Figure 7-13. Time Variation of the Heat Release Rate and Mass Loss Rate in a Cone Calorimeter Test for the Carpet Material Under a 35 kW/m² Radiant Exposure

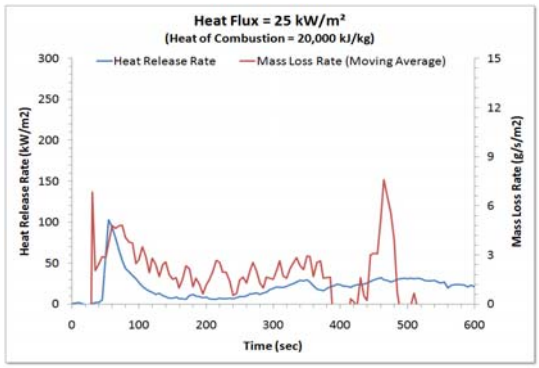

Figure 7-14. Time Variation of the Heat Release Rate and Mass Loss Rate in a Cone Calorimeter Test for the Carpet Material Under a 25 kW/m² Radiant Exposure

7.3 Wall Material

The "wall material" referenced in the present study is a sample of a fireproof polyester wall, reinforced with fiberglass, mixed with SMC (Sheet Molding Compound), commonly mounted to the walls of metro trains. The wall material sample thickness in the present study was approximately 2.4 mm, and the virgin material density was approximately 2,000 kg/m³.

7.3.1 Test Results

At exposure heat fluxes greater than or equal to 50 kW/m², the wall material was observed to burn efficiently, leaving behind only a white powdery residue, as illustrated in the following figures.

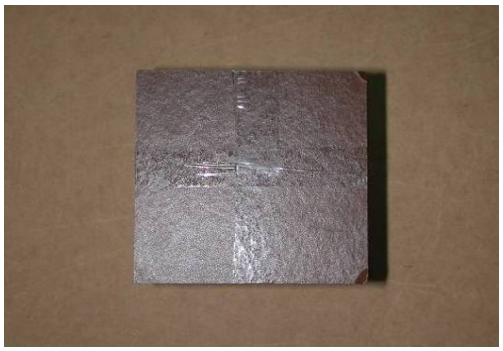

Figure 7-15. Photograph of the Wall Material Before the Cone Calorimetry Test

Figure 7-16. Photograph of the Wall Material After the Cone Calorimetry Test

The cone calorimetry tests for the wall material produced heat release rate and mass loss rate curves with two peaks of minimal separation. These results are consistent with that of a residue producing, relatively thermally-thin material with insulated backing.

At higher heat flux, mass loss rates were greater in magnitude and the second peak was observed to be coincident with the first peak. At lower heat flux, the time to ignition was observed to be greater.

7.3.2 Selection of Data

The wall material was subjected to six constant heat flux exposures ranging from 20 kW/m² to 80 kW/m². As with the carpet material, three tests were conducted at each exposure. The following figures identify the data selected for analysis for each exposure.

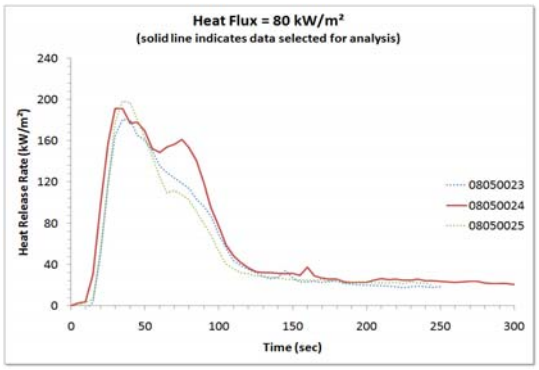

Figure 7-17. Time Variation of the Heat Release Rate in Cone Calorimeter Tests for the Wall Material Under an 80 kW/m² Radiant Exposure

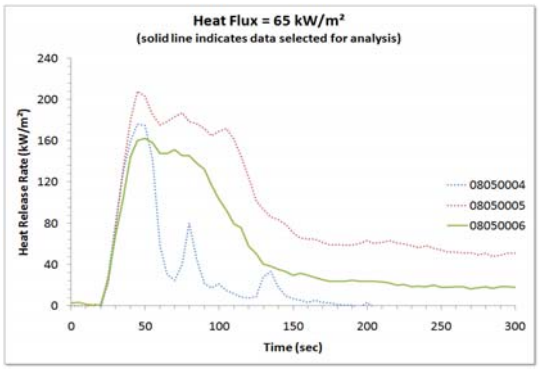

Figure 7-18. Time Variation of the Heat Release Rate in Cone Calorimeter Tests for the Wall Material Under a 65 kW/m² Radiant Exposure

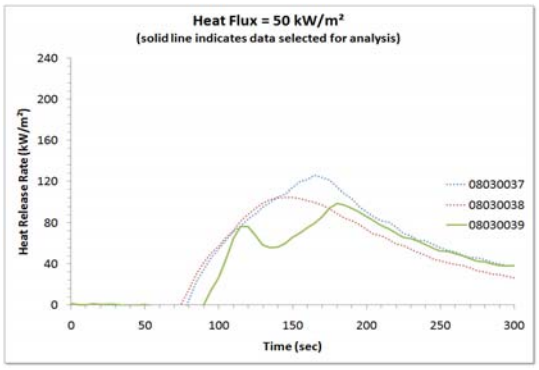

Figure 7-19. Time Variation of the Heat Release Rate in Cone Calorimeter Tests for the Wall Material Under a 50 kW/m² Radiant Exposure

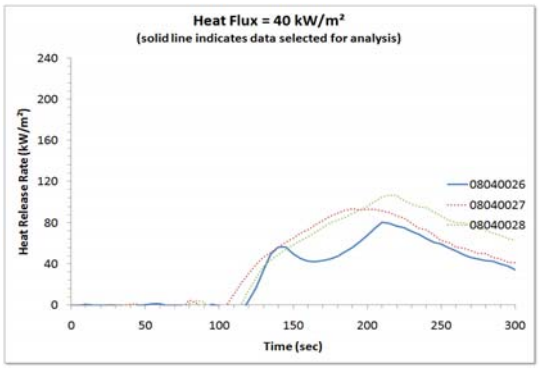

Figure 7-20. Time Variation of the Heat Release Rate in Cone Calorimeter Tests for the Wall Material Under a 40 kW/m² Radiant Exposure

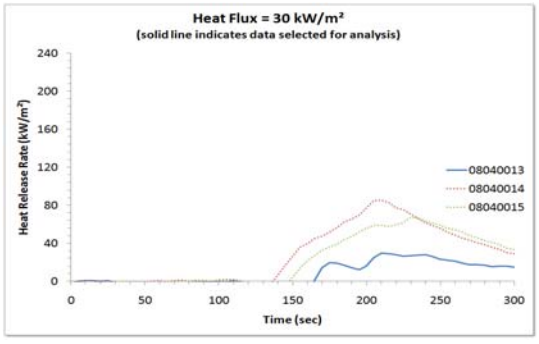

Figure 7-21. Time Variation of the Heat Release Rate in Cone Calorimeter Tests for the Wall Material Under a 30 kW/m² Radiant Exposure

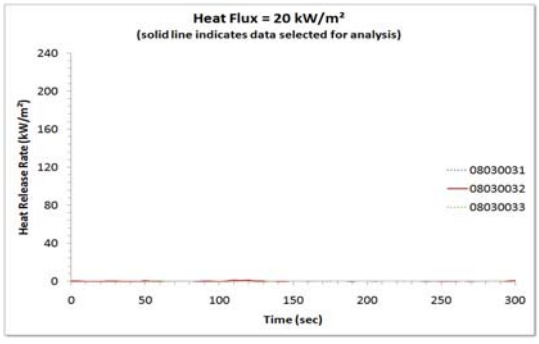

Figure 7-22. Time Variation of the Heat Release Rate in Cone Calorimeter Tests for the Wall Material Under a 20 kW/m² Radiant Exposure

7.3.3 Heat of Combustion Estimation

For the purposes of the present study, heat of combustion was estimated semi-quantitatively by comparing the proportionality of the heat release rate with that of mass loss rate. The following figures illustrate the relationship between the heat release rate and mass loss rate for a heat of combustion of 8,000 kJ/kg.

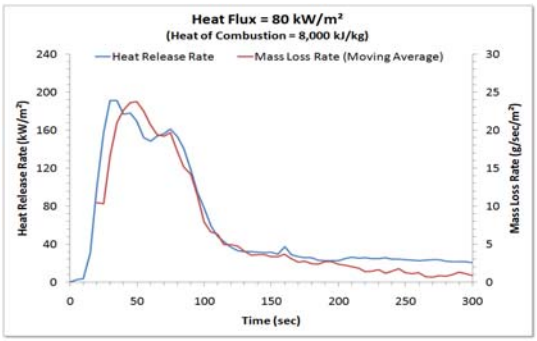

Figure 7-23. Time Variation of the Heat Release Rate and Mass Loss Rate in a Cone Calorimeter Test for the Wall Material Under an 80 kW/m² Radiant Exposure

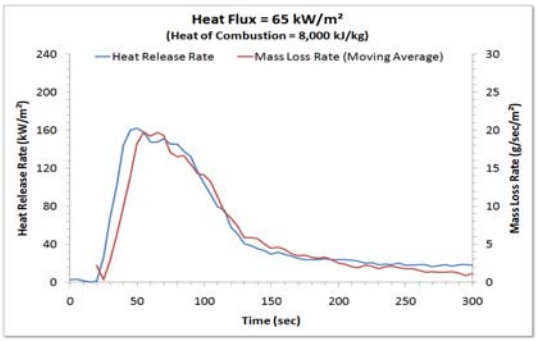

Figure 7-24. Time Variation of the Heat Release Rate and Mass Loss Rate in a Cone Calorimeter Test for the Wall Material Under a 65 kW/m² Radiant Exposure

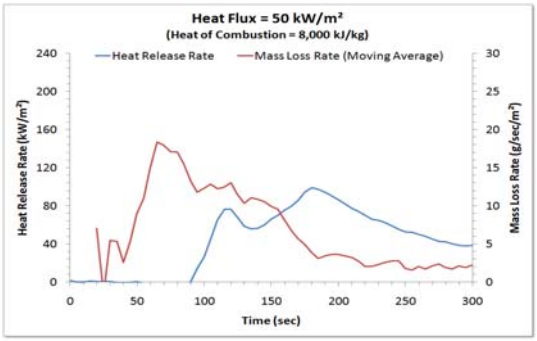

Figure 7-25. Time Variation of the Heat Release Rate and Mass Loss Rate in a Cone Calorimeter Test for the Wall Material Under a 50 kW/m² Radiant Exposure

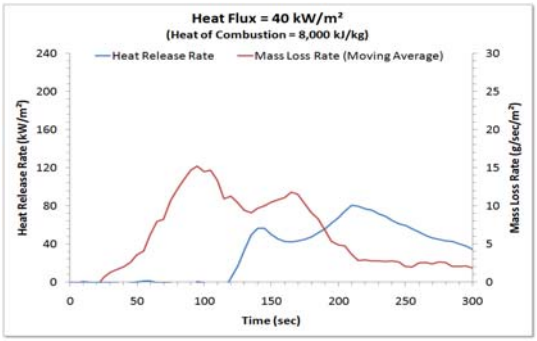

Figure 7-26. Time Variation of the Heat Release Rate and Mass Loss Rate in a Cone Calorimeter Test for the Wall Material Under a 40 kW/m² Radiant Exposure

There appears to be a timing discrepancy between the mass loss rate and heat release rate data from the cone calorimeter. This discrepancy cannot be explained by any physical mechanism, and is most likely an error in data collection.

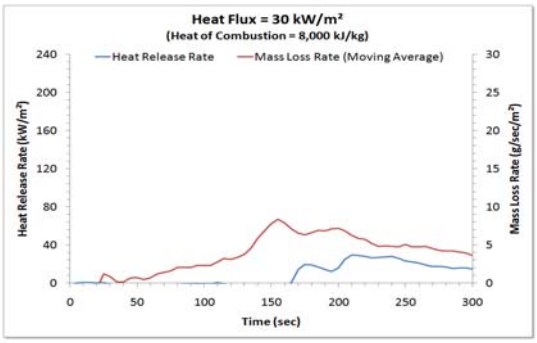

Figure 7-27. Time Variation of the Heat Release Rate and Mass Loss Rate in a Cone Calorimeter Test for the Wall Material Under a 30 kW/m² Radiant Exposure

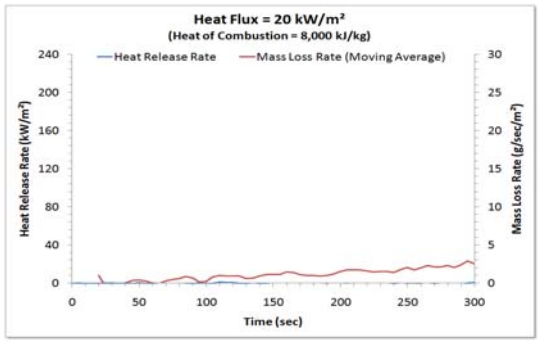

Figure 7-28. Time Variation of the Heat Release Rate and Mass Loss Rate in a Cone Calorimeter Test for the Wall Material Under a 20 kW/m² Radiant Exposure

7.4 Panel Material

The "panel material" referenced in the present study is a panel sample commonly used in commercial aircraft. Although a few monolithic laminate panels are used, most panels used in airplane interiors are sandwich structures. This type of construction is preferred for its high strength and stiffness to weight ratio. These panels are made of face sheets, adhesives, core, and decorative coverings, with small variations that depend on the requirements for the individual application. Panels are used for ceilings, galleys, lavatories, sidewalls, baggage racks, floors, partitions, and closets.

The core in a sandwich panel is most often a "honeycomb" structure to achieve the best physical properties at the minimum weight. Aluminum honeycomb has been used in cabin interiors; however, the most common type, and the one tested in the present study is an aramid-based paper coated with a phenolic resin to stabilize the paper. The panel material sample thickness in the present study was approximately 6.0 mm, and the virgin material density was approximately 315 kg/m³.

7.4.1 Test Results

At exposure heat fluxes greater than or equal to 50 kW/m², the panel material was observed to burn efficiently, as illustrated in the following figures.

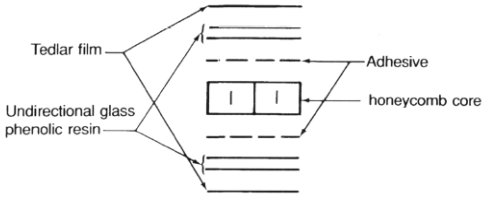

Figure 7-29. Schematic Cross-Section of the Panel Material

Figure 7-30. Photograph of the Panel Material After the Cone Calorimetry Test

The cone calorimetry tests for the panel material produced heat release rate and mass loss rate curves with one peak. These results are consistent with that of a residue producing, thermally-thin material with insulated backing.

At higher heat flux, mass loss rates were greater in magnitude. At all levels of heat flux, there was no differentiable second peak. At lower heat flux, the time to ignition was observed to be greater.

7.4.2 Selection of Data

The panel material was subjected to six constant heat flux exposures ranging from 25 kW/m² to 75 kW/m². Similar to the carpet and wall materials, three tests were conducted at each exposure. The following figures identify the data selected for analysis for each exposure.

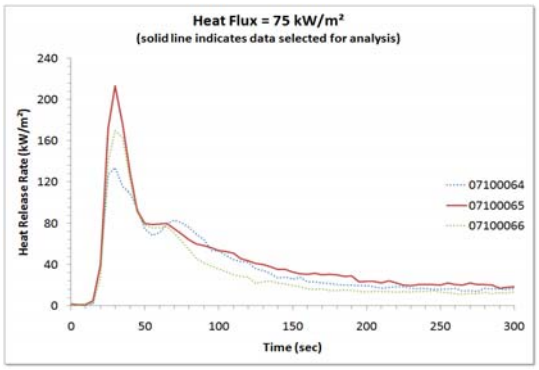

Figure 7-31. Time Variation of the Heat Release Rate in Cone Calorimeter Tests for the Panel Material Under a 75 kW/m² Radiant Exposure

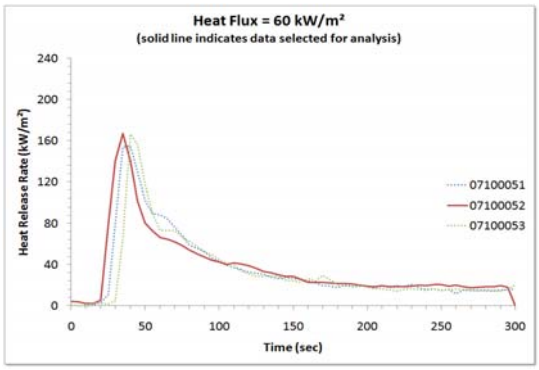

Figure 7-32. Time Variation of the Heat Release Rate in Cone Calorimeter Tests for the Panel Material Under a 60 kW/m² Radiant Exposure

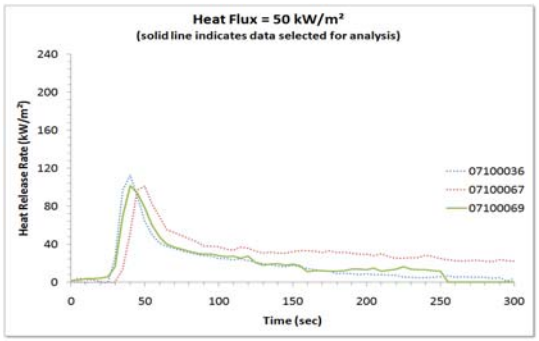

Figure 7-33. Time Variation of the Heat Release Rate in Cone Calorimeter Tests for the Panel Material Under a 50 kW/m² Radiant Exposure

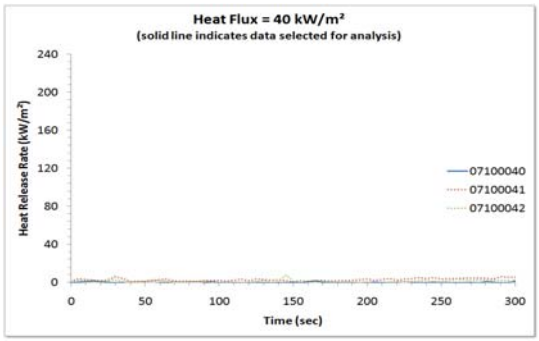

Figure 7-34. Time Variation of the Heat Release Rate in Cone Calorimeter Tests for the Panel Material Under a 40 kW/m² Radiant Exposure

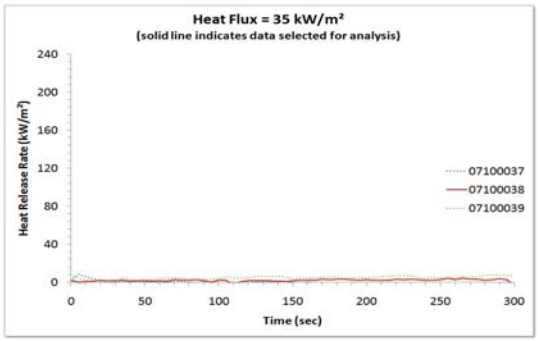

Figure 7-35. Time Variation of the Heat Release Rate in Cone Calorimeter Tests for the Panel Material Under a 35 kW/m² Radiant Exposure

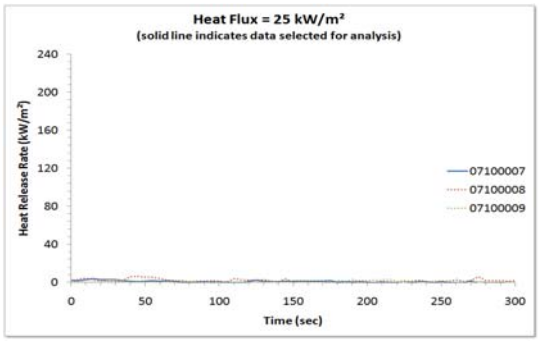

Figure 7-36. Time Variation of the Heat Release Rate in Cone Calorimeter Tests for the Panel Material Under a 25 kW/m² Radiant Exposure

7.4.3 Heat of Combustion Estimation

For the purposes of the present study, heat of combustion was estimated semi-quantitatively by comparing the proportionality of the heat release rate with that of mass loss rate. The following figures illustrate the relationship between the heat release rate and mass loss rate for a heat of combustion of 20,000 kJ/kg.

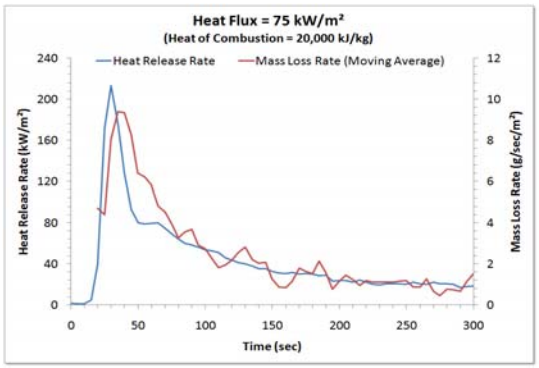

Figure 7-37. Time Variation of the Heat Release Rate and Mass Loss Rate in a Cone Calorimeter Test for the Panel Material Under a 75 kW/m² Radiant Exposure

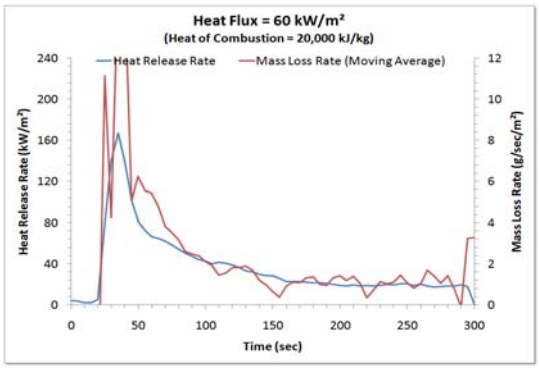

Figure 7-38. Time Variation of the Heat Release Rate and Mass Loss Rate in a Cone Calorimeter Test for the Panel Material Under a 60 kW/m² Radiant Exposure

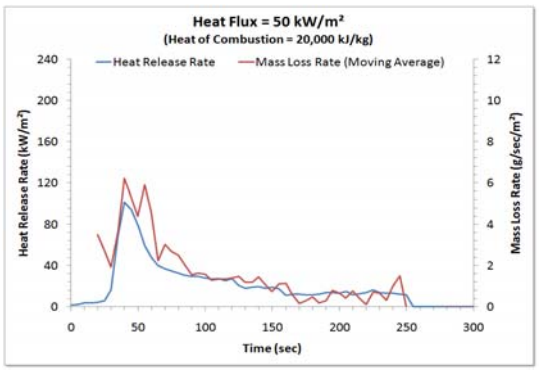

Figure 7-39. Time Variation of the Heat Release Rate and Mass Loss Rate in a Cone Calorimeter Test for the Panel Material Under a 50 kW/m² Radiant Exposure

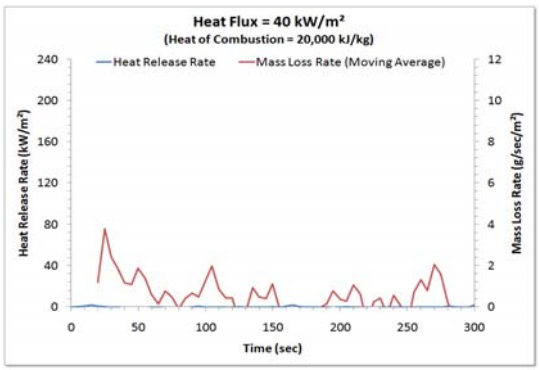

Figure 7-40. Time Variation of the Heat Release Rate and Mass Loss Rate in a Cone Calorimeter Test for the Panel Material Under a 40 kW/m² Radiant Exposure

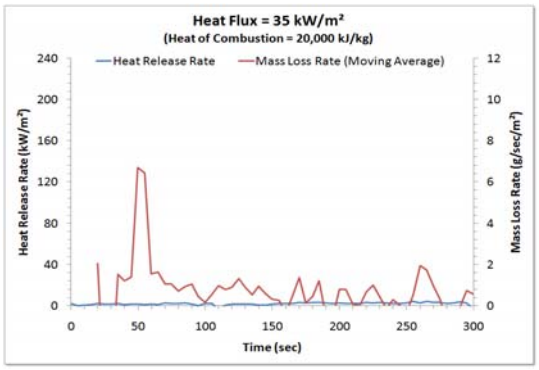

Figure 7-41. Time Variation of the Heat Release Rate and Mass Loss Rate in a Cone Calorimeter Test for the Panel Material Under a 35 kW/m² Radiant Exposure

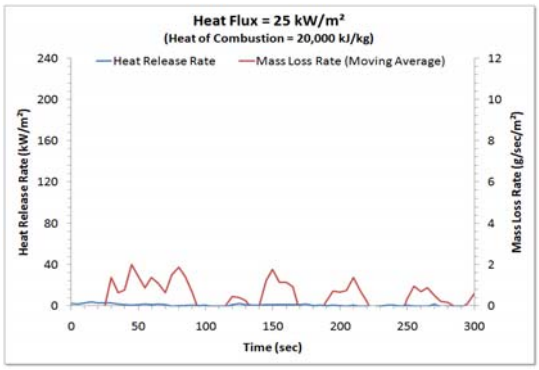

Figure 7-42. Time Variation of the Heat Release Rate and Mass Loss Rate in a Cone Calorimeter Test for the Panel Material Under a 25 kW/m² Radiant Exposure

Note: There appears to be a discrepancy in the fluctuations of mass loss rate and heat release rate data collected from cone calorimetry. These fluctuations are most likely a sensitivity error in data collection, and no physical meaning should be assumed.

Chapter 8. Methodology

The objectives of the present study are to (1) present an algorithm for generating FDS input parameters for pyrolysis, which produce a set of mass loss rate curves that correlate well with actual material test data under similar exposures, (2) examine the extent to which input parameters can be assumed equivalent to actual physical properties and (3) examine the accuracy of extrapolations to other radiant exposures.

The present study differs in philosophy from previous studies [16] in that it is not the intention of the present study to estimate thermophysical properties.

8.1 Modeled Parameters

The present study approaches the problem of parameter optimization from a mathematically unbiased perspective. One bias reducing factor previously discussed is the normalization of parameters. Parameter normalization has the impact of releasing dependency of the mass loss rate curve to select parameters. For example, if decreasing residue thermal conductivity by 64% has an equivalent impact on the mass loss rate curve as increasing the heat of reaction by 2%, then the probability either one happening is equal.

The present study treats all FDS input parameters as variable, i.e. those that could be reasonably estimated including the virgin material emissivity, species yields, ignition temperature and thermal conductivity, as well as those that are well known, such as virgin material thickness and density. Prior studies that have attempted to estimate the actual

thermophysical properties assume a number of known parameters. However, as the intent of the present work is to examine the extent to which the input parameters can be assumed equivalent to actual physical properties, all input parameters are assumed unknown, so that comparisons can be made to the actual values. The solution parameter sets obtained by this methodology are not limited by any preconception about what values are realistic or unrealistic for a given material.

The solution parameter sets obtained are also not limited by any preconception about what values are realistic or unrealistic for a given parameter. The advantage is that parameter values are free to mutate in the direction that produces the best curve fit. However, the disadvantage is that the parameters that produce the best curve fit may be utterly unrealistic.

Following are the 14 FDS input parameters that compose the parameter set used for calibration in the present study.

VIRGIN MATERIAL	REACTION	RESIDUE MATERIAL
DENSITY (kg/m^3)	HEAT_OF_REACTION (kJ/kg)	DENSITY (kg/m^3)
SPECIFIC_HEAT (kJ/kg/K)	NU_FUEL	SPECIFIC_HEAT (kJ/kg/K)
CONDUCTIVITY (w/m/K)	THRESHOLD_TEMPERATURE (°C)	CONDUCTIVITY (w/m/K)
EMISSIVITY	A (1/s)	EMISSIVITY
THICKNESS (m)	E (kJ/kmol)	

Figure 8-1. FDS Input Parameters that compose the Parameter Set used for Calibration

It should be noted, however, that for the purposes of creating an efficient algorithm, the parameters A and E were not directly calibrated. Rather two substitute parameters were introduced: (1) "RR", the reaction rate at the threshold temperature, and (2) "DRR", the change in the reaction rate one degree above the threshold temperature. Additionally, residue yield is assumed to be 1 minus the fuel yield.

8.2 Pyrolysis Model

The present study considers a one-step Arrhenius-type global pyrolysis reaction for residue producing materials in a single layer. For the purposes of comparison, the same model is consistently applied to each material. It is recognized however that the actual physical processes for the materials in question would be better described by more complex models.

In the present study, the term "model" is only meant to imply the application of the FDS pyrolysis model used. Therefore, the conclusions of this study cannot be extrapolated to imply broad conclusions about other applications of the model, or about the FDS pyrolysis model in general.

8.3 Boundary Conditions

The present study examines the ability of a stochastic hill-climber algorithm to develop an input parameter set to a finite difference one-dimensional model of transient conduction with pyrolysis; however, there is no gas phase treatment. The modeled boundary condition of the exposed surface is that of a constant irradiation (EXTERNAL_FLUX):

$$\dot{q}_r'' / \varepsilon + \sigma\left(T_w{}^4 - T_\infty{}^4\right) = \text{EXTERNAL\_FLUX} \qquad (8\text{-}21)$$

where $\dot{q}_r''$ is the net radiative flux, ε is the emissivity, σ is the Stefan-Boltzmann constant, T_w is the exposed surface temperature, and T_∞ is the temperature of the environment. The modeled boundary condition for the back surface ($x = L$) is insulated:

$$\left.\frac{\partial T}{\partial x}\right|_{x=L} = \frac{\partial T}{\partial n} = 0 \qquad (8\text{-}22)$$

Additionally, this model neglects convection losses and radiation from flame. It is recognized that these assumptions could have a significant impact on internal temperatures, and therefore, on the subsequent fuel mass loss rate.

8.4 Empirical Constants

The application of the FDS pyrolysis model used in the present study assumes a threshold temperature (T_{thr}), below which the fuel mass loss rate is explicitly zero. It should be noted that while imposing a threshold temperature is prudent for use of the Arrhenius equation in FDS (because of the implications of injecting fuel into the computational domain at low temperatures), threshold temperature is not included in all applications of the Arrhenius equation. Therefore, it is reasonable to assume that customary combinations of the pre-exponential factor (A_0) and the activation energy (E) have limited application in the FDS pyrolysis model, if any. Furthermore, it is reasonable to expect that well-fit combinations of A_0 and E in the FDS model could be vastly different from customary combinations of these parameters.

8.5 Constant Properties

The application of FDS used in the present study assumes constant material properties. It is recognized however that the assumption of constant material thermal properties may not be valid for the possible temperature ranges encountered during pyrolysis.

Chapter 9. Comparison of Algorithm Results

Stochastic hill-climber algorithm results are based on the HC-PYRO algorithm developed in the present study. Genetic Algorithm (GA) results were provided by and used with permission from Dr. Mariano Lázaro Urrutia, Research Engineer, GIDAI - Fire Safety - Research and Technology, Dept. of Transport and Technology Projects and Processes, University of Cantabria.

Each of the HC-PYRO parameter calibrations in this section were concluded in approximately 4 hours time. This includes roughly 1500 simulations at 10 seconds per simulation. For an example of the FDS model input syntax, refer to Appendix A.

9.1 Carpet Material

For the carpet material, results were significantly better for the stochastic hill-climber algorithm, as illustrated in the following figures:

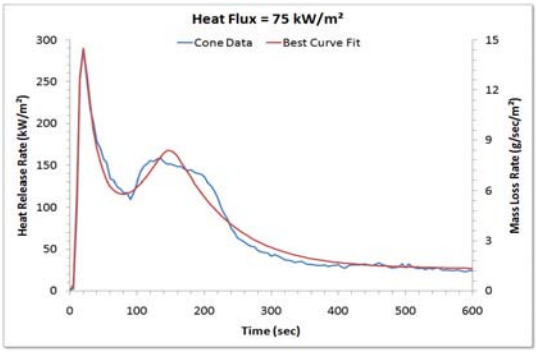

Figure 9-1. Comparison of the Heat Release Rate from Cone Calorimetry and the Mass Loss Rate from FDS for the Carpet Material under a 75 kW/m² Radiant Exposure using Parameters Obtained from a Stochastic Hill-Climber Algorithm

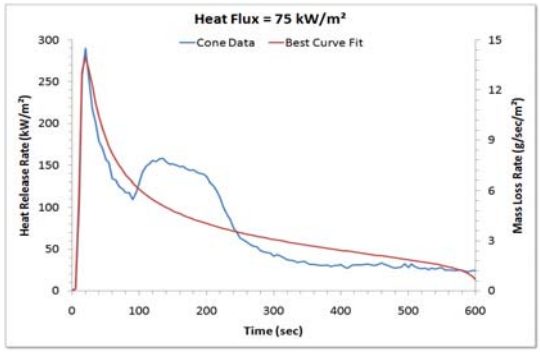

Figure 9-2. Comparison of the Heat Release Rate from Cone Calorimetry and the Mass Loss Rate from FDS for the Carpet Material under a 75 kW/m² Radiant Exposure using Parameters Obtained from a Genetic Algorithm

In the above figures, the R-squared value for the stochastic hill-climber algorithm was 98.05%, and 81.15% for the genetic algorithm. The results indicate that the stochastic hill-climber algorithm is able to match mass loss rate curves with secondary peaks, characteristic of thermally thick char producing materials with insulated backing. This is primarily a result of the initial characteristic curve selected.

These results do not indicate that genetic algorithms cannot find parameter combinations that produce secondary peaks. However, after several weeks of computation, a secondary peak was not found with the genetic algorithm. These results suggest at a minimum, that the stochastic hill-climber algorithm was much more efficient.

This also highlights the limitation to which NFL refers; without any knowledge of the combination of parameters that produces a secondary peak, the probability that a genetic algorithm will find the right combination is not greater than the probability of a blind or random search.

9.2 Wall Material

For the wall material, results were also significantly better for the stochastic hill-climber algorithm, as illustrated in the following figures:

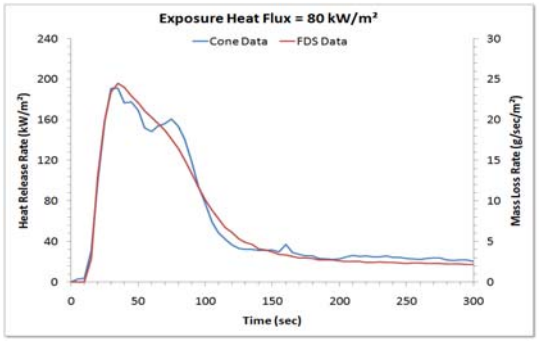

Figure 9-3. Comparison of the Heat Release Rate from Cone Calorimetry and the Mass Loss Rate from FDS for the Wall Material under an 80 kW/m² Radiant Exposure using Parameters Obtained from a Stochastic Hill-Climber Algorithm

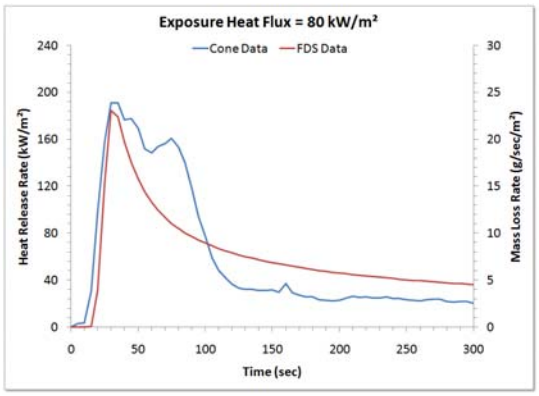

Figure 9-4. Comparison of the Heat Release Rate from Cone Calorimetry and the Mass Loss Rate from FDS for the Wall Material under an 80 kW/m² Radiant Exposure using Parameters Obtained from a Genetic Algorithm

For the wall material, the R-squared value for the stochastic hill-climber algorithm was 98.29%, and 79.27% for the genetic algorithm.

9.3 Panel Material

For the panel material, results were marginally better for the stochastic hill-climber algorithm, as illustrated in the following figures:

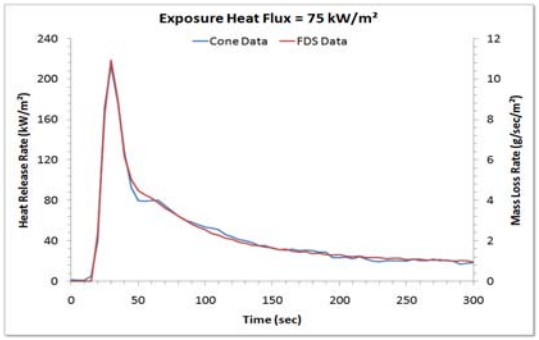

Figure 9-5. Comparison of the Heat Release Rate from Cone Calorimetry and the Mass Loss Rate from FDS for the Panel Material under a 75 kW/m² Radiant Exposure using Parameters Obtained from a Stochastic Hill-Climber Algorithm

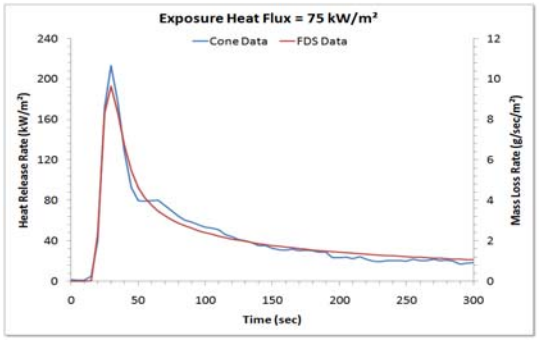

Figure 9-6. Comparison of the Heat Release Rate from Cone Calorimetry and the Mass Loss Rate from FDS for the Panel Material under a 75 kW/m² Radiant Exposure using Parameters Obtained from a Genetic Algorithm

For the panel material, the R-squared value for the stochastic hill-climber algorithm was 99.39%, and 98.18% for the genetic algorithm. It is clear that both algorithms are able to match mass loss rate curves with a single peak, characteristic of thermally thin char forming materials. The benefit of the stochastic hill-climber algorithm highlighted in this example is its ability to narrow in on a particular solution.

Chapter 10. Physical Meaning of Parameters

The following plots illustrate the normalized impact of single parameter mutation. These graphs can serve as a complement to work done by Matala [14] in manually developing characteristic curves. Characteristic fuel mass loss rate curves are based on data from FDS for the carpet material under a 75 kW/m² radiant exposure.

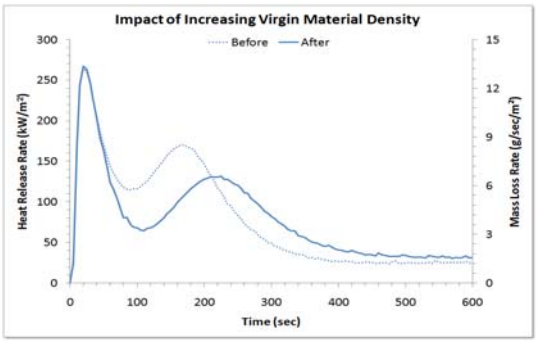

Figure 10-1. Normalized Impact of Increasing Virgin Material Density on the Characteristic Mass Loss Rate Curve

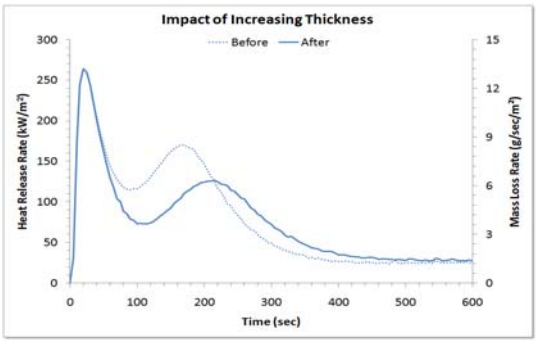

Figure 10-2. Normalized Impact of Increasing Thickness on the Characteristic Mass Loss Rate Curve

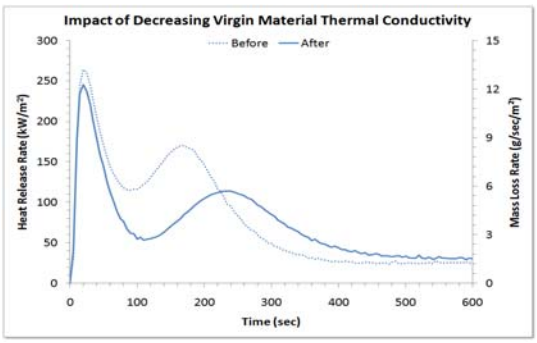

Figure 10-3. Normalized Impact of Decreasing Virgin Material Thermal Conductivity on the Characteristic Mass Loss Rate Curve

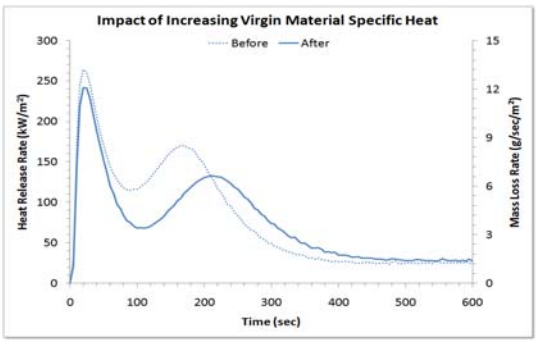

Figure 10-4. Normalized Impact of Increasing Virgin Material Specific Heat on the Characteristic Mass Loss Rate Curve

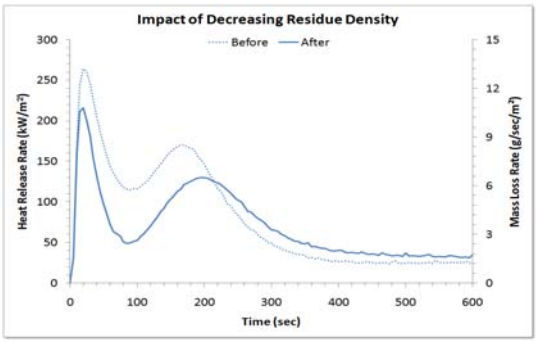

Figure 10-5. Normalized Impact of Decreasing Residue Density on the Characteristic Mass Loss Rate Curve

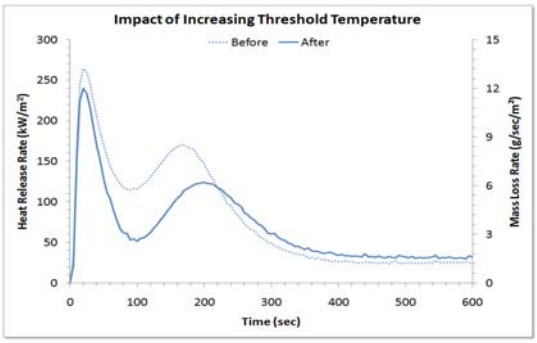

Figure 10-6. Normalized Impact of Increasing Threshold Temperature on the Characteristic Mass Loss Rate Curve

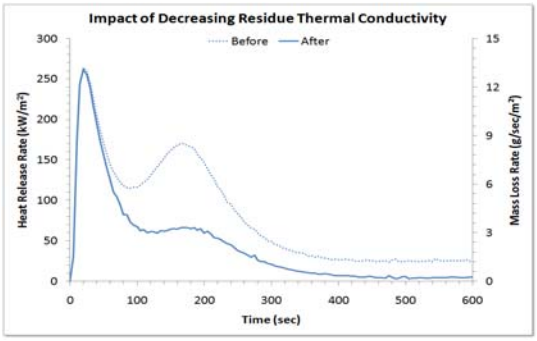

Figure 10-7. Normalized Impact of Decreasing Residue Thermal Conductivity on the Characteristic Mass Loss Rate Curve

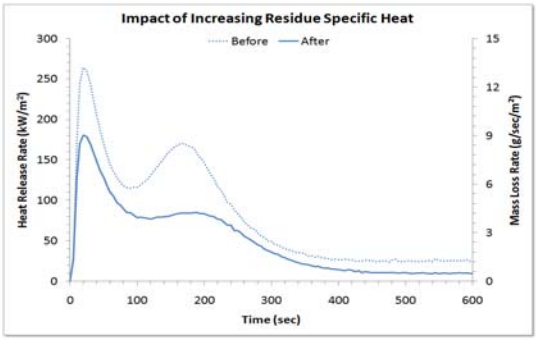

Figure 10-8. Normalized Impact of Increasing Residue Specific Heat on the Characteristic Mass Loss Rate Curve

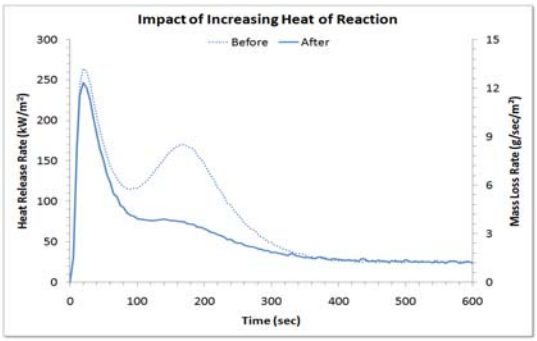

Figure 10-9. Normalized Impact of Increasing Heat of Reaction on the Characteristic Mass Loss Rate Curve

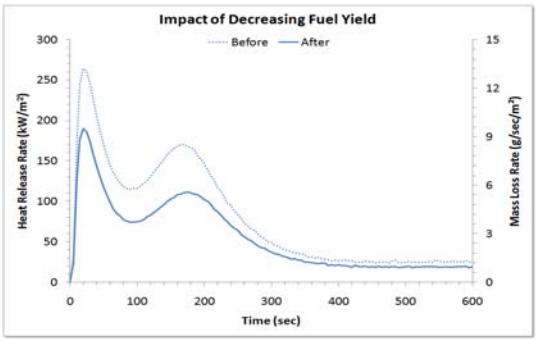

Figure 10-10. Normalized Impact of Decreasing Fuel Yield on the Characteristic Mass Loss Rate Curve

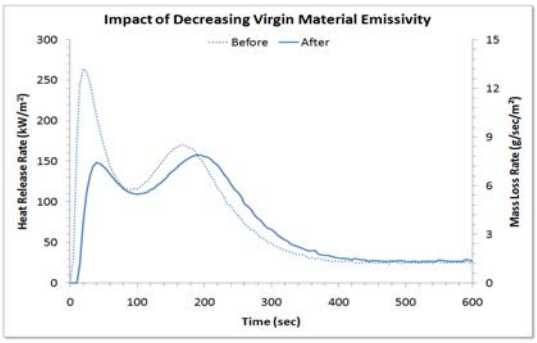

Figure 10-11. Normalized Impact of Decreasing Virgin Material Emissivity on the Characteristic Mass Loss Rate Curve

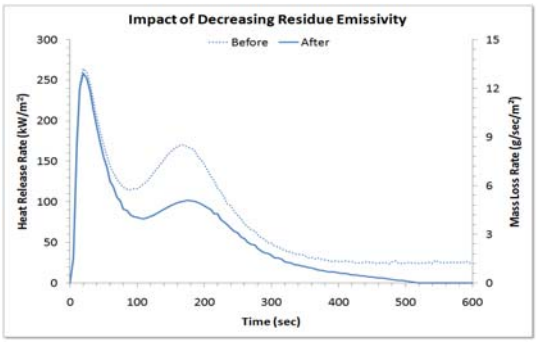

Figure 10-12. Normalized Impact of Decreasing Residue Emissivity on the Characteristic Mass Loss Rate Curve

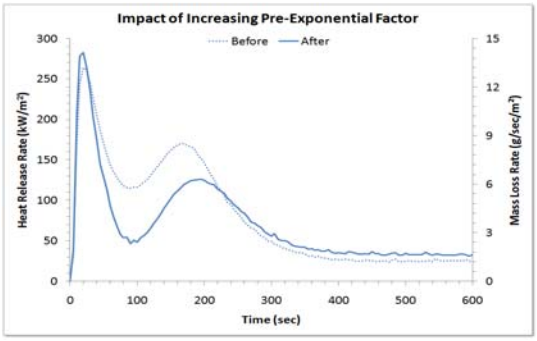

Figure 10-13. Normalized Impact of Increasing Pre-Exponential Factor on the Characteristic Mass Loss Rate Curve

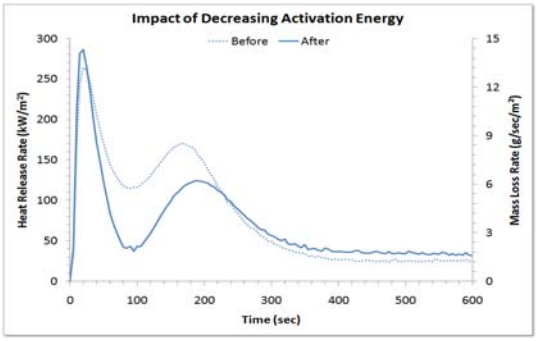

Figure 10-14. Normalized Impact of Decreasing Activation Energy on the Characteristic Mass Loss Rate Curve

From the above graphs, it is clear that the impacts of certain parameters are indistinguishable. To proponents of genetic algorithms, this highlights the need to identify as many known parameters as possible. The thought is that by reducing the number of unknowns that the possible sources of error are minimized, and consequently, the unknown parameters take on more physical meaning.

10.1 Specifying Known Parameters

Functionality is included in the stochastic hill-climber algorithm HC-PYRO, to allow target parameter values to be specified. If certain parameter values are well-known, then those parameters can be identified, and the algorithm will increment the solution toward those values, allowing non-specified parameters to compensate. The algorithm will increment toward the target values regardless of whether the solution accuracy is increased.

In reality, information is typically available about the materials virgin material density, emissivity, thickness, species yields, ignition temperature, in some cases, thermal conductivity. In the following example, known quantities are identified as "targets" in hopes of reducing the magnitude of the error in the unknown parameters by reducing the sources of error.

The following figures are a summary of the parameter solution sets with and without defined targets.

```
VIRGIN MATERIAL
DENSITY=5.294E+02
SPECIFIC_HEAT=4.205E-01
CONDUCTIVITY=4.087E-01
EMISSIVITY=8.509E-01
THICKNESS=1.619E-02

REACTION
HEAT_OF_REACTION=6.965E+01
NU_FUEL=4.318E-01
THRESHOLD_TEMPERATURE=4.374E+02
A=2.946E+06
E=1.095E+05

RESIDUE MATERIAL
DENSITY=3.697E+03
SPECIFIC_HEAT=3.911E+01
CONDUCTIVITY=1.285E-01
EMISSIVITY=1.760E+00
```

Figure 10-15. FDS Input Parameters Obtained from the Stochastic Hill-Climber Algorithm with no Target Values Specified

```
VIRGIN MATERIAL
DENSITY=4.500E+02
SPECIFIC_HEAT=1.342E+00
CONDUCTIVITY=1.209E-01
EMISSIVITY=9.000E-01
THICKNESS=6.000E-03

REACTION
HEAT_OF_REACTION=2.126E+02
NU_FUEL=9.000E-01
THRESHOLD_TEMPERATURE=4.000E+02
A=7.865E+00
E=3.665E+04

RESIDUE MATERIAL
DENSITY=4.217E+01
SPECIFIC_HEAT=2.900E+02
CONDUCTIVITY=4.427E-02
EMISSIVITY=1.261E+01
```

Figure 10-16. FDS Input Parameters Obtained from the Stochastic Hill-Climber Algorithm with Target Values Specified

In the figures above, target values are shown in green, and select "unrealistic" values are shown in red. The following figures illustrate the impact of specifying target values on the mass loss rate curve.

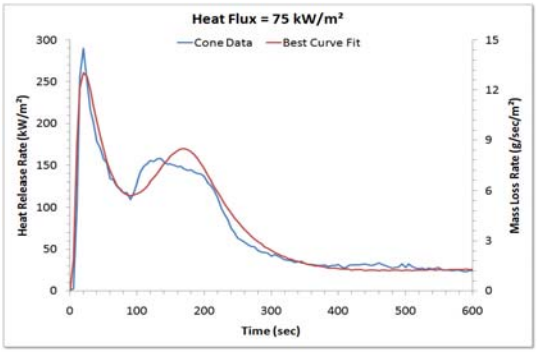

Figure 10-17. Comparison of the Heat Release Rate from Cone Calorimetry and the Mass Loss Rate from FDS for the Carpet Material under a 75 kW/m² Radiant Exposure with no Target Values Specified

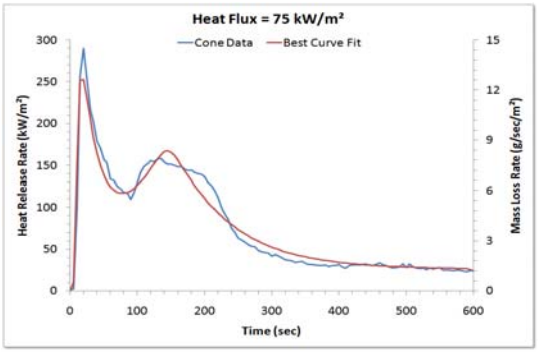

Figure 10-18. Comparison of the Heat Release Rate from Cone Calorimetry and the Mass Loss Rate from FDS for the Carpet Material under a 75 kW/m² Radiant Exposure with Target Values Specified

It is clear in this example, that the exercise of defining targets has no quantitative impact on the accuracy of the mass loss rate curve. It is clear that without defined targets, parameter values do not trend toward the known target values. It is also clear that defining targets does not increase the physical meaning of the other parameters.

For example, the specific heat of the virgin material is observed to increase from 0.4205 kJ/kg/K to 13.42 kJ/kg/K, specific heat of the residue increases from 39.11 kJ/kg/K to 290.0 kJ/kg/K and emissivity of the residue increases from 1.760 to 12.61. Clearly, the solution parameter set values do not trend toward realistic values.

To many, this divergence from realistic parameter values is justification for limiting the range of the parameter set. On the other hand, if using an optimization algorithm requires limiting the range of parameters to arrive at realistic solutions, then the model employed must not be representative of the actual physics of the problem.

It is difficult to assume physical meaning from the values in the solution parameter set. This is because an error in one solution parameter is balanced by errors in the remaining parameters as a consequence of the over-specified conditions of the problem. In the present study, the term "over-specified" indicates that the model uses too many parameters to describe the physics of the problem.

This could mean either that the contributions of some parameters are not differentiated by the limited number of observations, or that some parameters do not have a unique contribution to the parameter set. In either case, the result is that an equivalent mass loss rate curve can be generated by more than one solution parameter set.

However, the magnitude and direction of parameter mutation may also provide insight. Referring back to the figures illustrating the impact of single parameter mutation, it is possible to glean knowledge about why the parameters were forced in a particular direction.

For instance, a 220% increase in the virgin material specific heat was observed. To explain why, it is necessary to examine the defined targets. Thickness was decreased to approximately 40% of its original value. Decreasing thickness decreases the magnitude of the second peak in the mass loss rate curve (Figure 10-2). Increasing virgin material specific heat has the impact of increasing the magnitude of the second peak (Figure 10-4), thus balancing the impact of the change in thickness.

Even though these two parameters have very different physical meanings, their contribution to the shape of the fuel mass loss rate curve is similar. Consequently, when one is modified, the other is forced to compensate.

Chapter 11. Range of Validity of Solutions Sets

It's is necessary to know how well heat release rates and mass loss rates produced by the optimized parameter set extrapolate, because if they do not extrapolate well, then they have very minimal application outside of the range of calibration.

11.1 Extrapolation from High Exposure Heat Flux

Following are extrapolations to a low radiant exposure for a mass loss rate curve that is well fit at the maximum radiant exposure.

11.1.1 Carpet Material

The following figures compare the heat release rate from cone calorimetry and the mass loss rate from FDS for the carpet material under a range of radiant exposures using parameters obtained from calibrating the 75 kW/m² exposure (with defined targets).

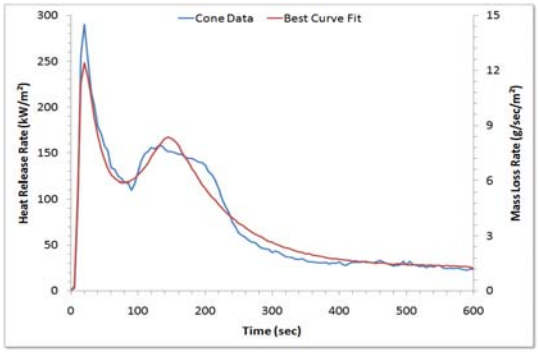

Figure 11-1. Comparison of the Heat Release Rate from Cone Calorimetry and the Mass Loss Rate from FDS for the Carpet Material under a 75 kW/m² Radiant Exposure using Parameters Obtained from a Stochastic Hill-Climber Algorithm

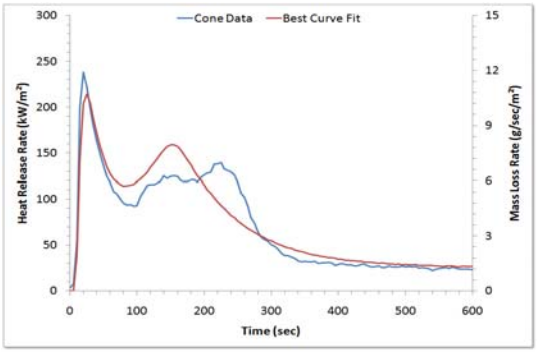

Figure 11-2. Comparison of the Heat Release Rate from Cone Calorimetry and the Mass Loss Rate from FDS for the Carpet Material under a 60 kW/m² Radiant Exposure using Parameters Obtained from calibrating a 75 kW/m² Exposure

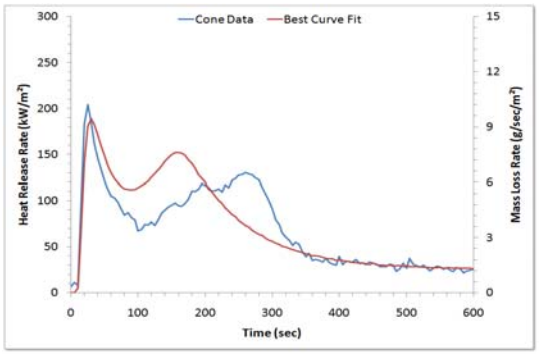

Figure 11-3. Comparison of the Heat Release Rate from Cone Calorimetry and the Mass Loss Rate from FDS for the Carpet Material under a 50 kW/m² Radiant Exposure using Parameters Obtained from calibrating a 75 kW/m² Exposure

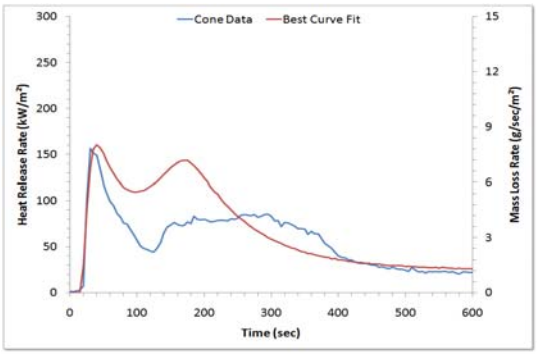

Figure 11-4. Comparison of the Heat Release Rate from Cone Calorimetry and the Mass Loss Rate from FDS for the Carpet Material under a 40 kW/m² Radiant Exposure using Parameters Obtained from calibrating a 75 kW/m² Exposure

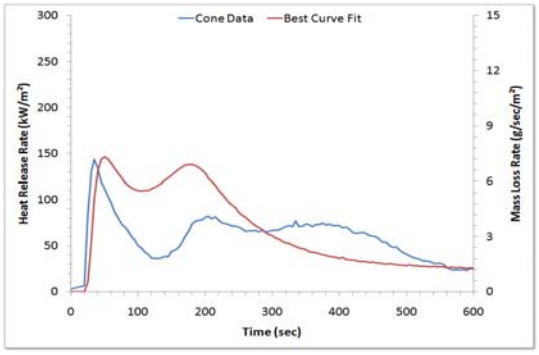

Figure 11-5. Comparison of the Heat Release Rate from Cone Calorimetry and the Mass Loss Rate from FDS for the Carpet Material under a 35 kW/m² Radiant Exposure using Parameters Obtained from calibrating a 75 kW/m² Exposure

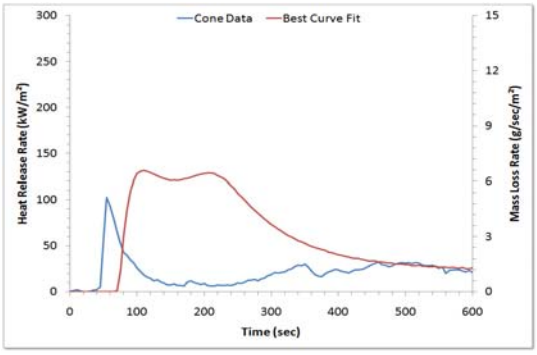

Figure 11-6. Comparison of the Heat Release Rate from Cone Calorimetry and the Mass Loss Rate from FDS for the Carpet Material under a 25 kW/m² Radiant Exposure using Parameters Obtained from calibrating a 75 kW/m² Exposure

Extrapolation from a single known exposure was qualitatively poor, especially as it relates to the timing and magnitude of the second peak, even when known material properties were defined.

Following are the FDS input parameters used for extrapolation.

```
VIRGIN_MATERIAL
DENSITY=4.500E+02
SPECIFIC_HEAT=1.342E+00
CONDUCTIVITY=1.209E-01
EMISSIVITY=9.000E-01
THICKNESS=6.000E-03

REACTION
HEAT_OF_REACTION=2.126E+02
NU_FUEL=9.000E-01
THRESHOLD_TEMPERATURE=4.000E+02
A=7.865E+00
E=3.665E+04

RESIDUE_MATERIAL
DENSITY=4.217E+01
SPECIFIC_HEAT=2.900E+02
CONDUCTIVITY=4.427E-02
EMISSIVITY=1.261E+01
```

Figure 11-7. FDS Input Parameters Obtained by the Stochastic Hill-Climber Algorithm for the Carpet Material Under an 75 kW/m² Radiant Exposure

In the figures above, target values are shown in green, and select "unrealistic" values are shown in red.

11.1.2 Wall Material

The following figures compare the heat release rate from cone calorimetry and the mass loss rate from FDS for the wall material under a range of radiant exposures using parameters obtained from calibrating the 80 kW/m² exposure.

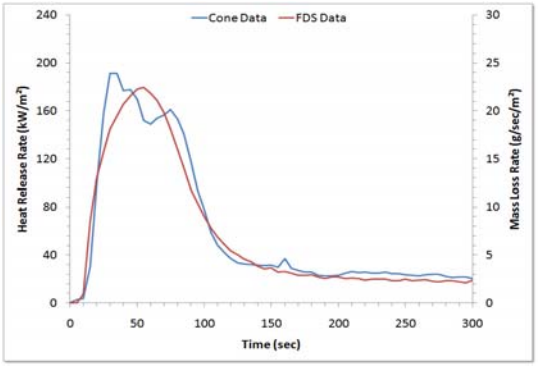

Figure 11-8. Comparison of the Heat Release Rate from Cone Calorimetry and the Mass Loss Rate from FDS for the Wall Material under an 80 kW/m² Radiant Exposure using Parameters Obtained from a Stochastic Hill-Climber Algorithm

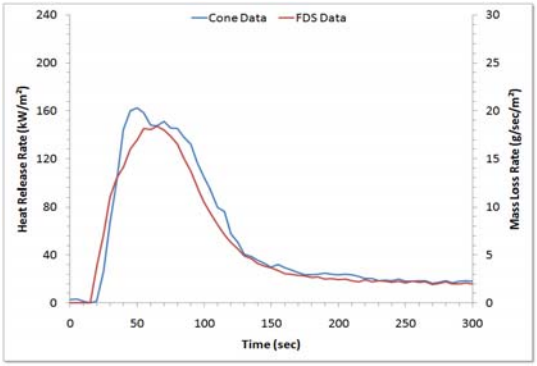

Figure 11-9. Comparison of the Heat Release Rate from Cone Calorimetry and the Mass Loss Rate from FDS for the Wall Material under a 65 kW/m² Radiant Exposure using Parameters Obtained from calibrating a 80 kW/m² Exposure

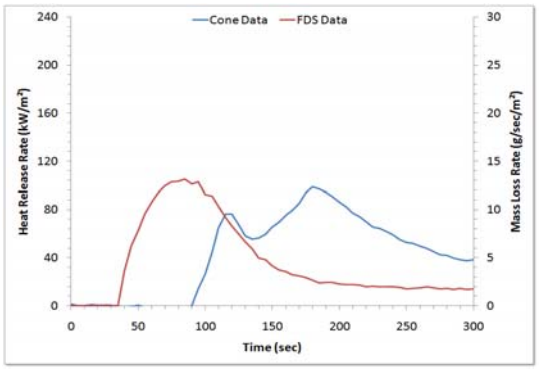

Figure 11-10. Comparison of the Heat Release Rate from Cone Calorimetry and the Mass Loss Rate from FDS for the Wall Material under a 50 kW/m² Radiant Exposure using Parameters Obtained from calibrating a 80 kW/m² Exposure

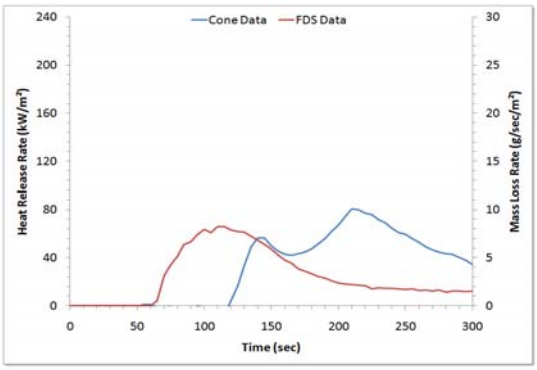

Figure 11-11. Comparison of the Heat Release Rate from Cone Calorimetry and the Mass Loss Rate from FDS for the Wall Material under a 40 kW/m² Radiant Exposure using Parameters Obtained from calibrating a 80 kW/m² Exposure

A significant finding illustrated above is that even though the fuel mass loss rate was well matched at the 80 kW/m² exposure, the characteristics of the second peak were not differentiable from general fluctuations in the test data. Consequently, there is no second peak in the extrapolation. The error in the timing of ignition at mid-range heat flux is most likely because of an error in data collection.

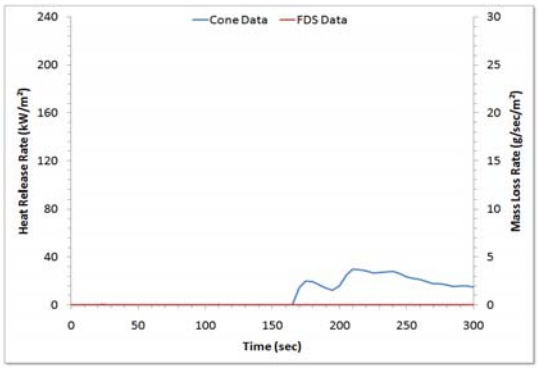

Figure 11-12. Comparison of the Heat Release Rate from Cone Calorimetry and the Mass Loss Rate from FDS for the Wall Material under a 30 kW/m² Radiant Exposure using Parameters Obtained from calibrating a 80 kW/m² Exposure

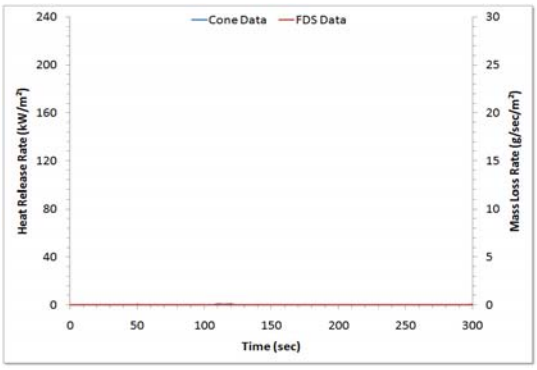

Figure 11-13. Comparison of the Heat Release Rate from Cone Calorimetry and the Mass Loss Rate from FDS for the Wall Material under a 20 kW/m² Radiant Exposure using Parameters Obtained from calibrating a 80 kW/m² Exposure

As illustrated in the above figures, the extrapolation was not able to predict the critical heat flux, as quantified by the threshold temperature.

Following are the FDS input parameters used for extrapolation.

```
VIRGIN_MATERIAL                REACTION                          RESIDUE_MATERIAL
DENSITY=4.309E+02              HEAT_OF_REACTION=7.979E+02        DENSITY=3.218E+02
SPECIFIC_HEAT=9.423E-01        NU_FUEL=9.869E-01                 SPECIFIC_HEAT=2.173E-02
CONDUCTIVITY=3.738E-01         THRESHOLD_TEMPERATURE=5.406E+02   CONDUCTIVITY=3.421E-02
EMISSIVITY=1.109E+00           A=2.227E-01                       EMISSIVITY=1.107E+00
THICKNESS=7.743E-03            E=7.551E+03
```

Figure 11-14. FDS Input Parameters Obtained by the Stochastic Hill-Climber Algorithm for the Wall Material Under an 80 kW/m² Radiant Exposure

In the figures above, no targets were defined, and select "highly unrealistic" values are shown in red. The actual wall material sample thickness in the present study was approximately 2.4 mm, and the virgin material density was approximately 2,000 kg/m³.

11.1.3 Panel Material

The following figures compare the heat release rate from cone calorimetry and the mass loss rate from FDS for the panel material under a range of radiant exposures using parameters obtained from calibrating the 75 kW/m² exposure.

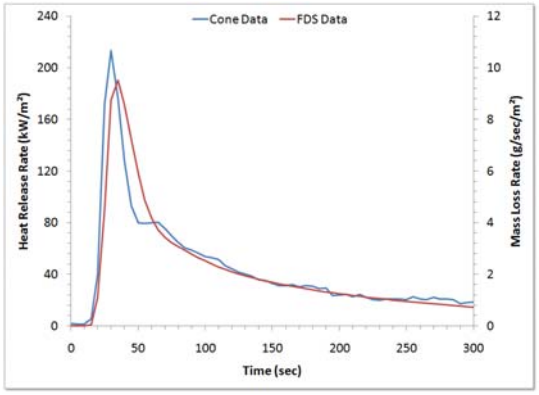

Figure 11-15. Comparison of the Heat Release Rate from Cone Calorimetry and the Mass Loss Rate from FDS for the Panel Material under a 75 kW/m² Radiant Exposure using Parameters Obtained from a Stochastic Hill-Climber Algorithm

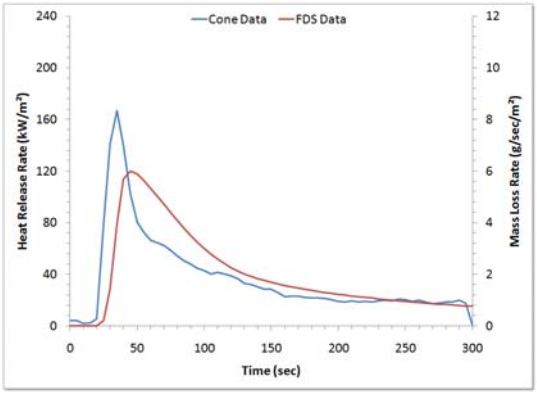

Figure 11-16. Comparison of the Heat Release Rate from Cone Calorimetry and the Mass Loss Rate from FDS for the Panel Material under a 60 kW/m² Radiant Exposure using Parameters Obtained from calibrating a 75 kW/m² Exposure

The figures above illustrate a significant error in extrapolation, even at an exposures close to the calibrated exposure.

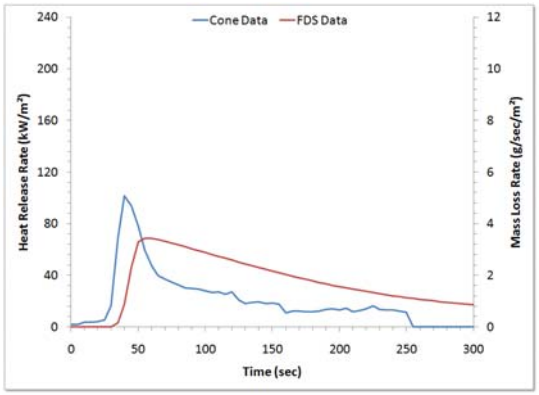

Figure 11-17. Comparison of the Heat Release Rate from Cone Calorimetry and the Mass Loss Rate from FDS for the Panel Material under a 50 kW/m² Radiant Exposure using Parameters Obtained from calibrating a 75 kW/m² Exposure

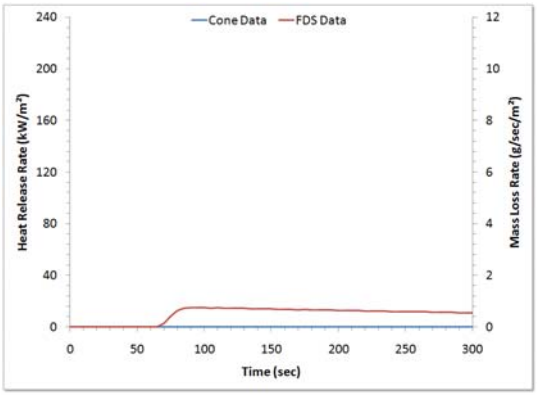

Figure 11-18. Comparison of the Heat Release Rate from Cone Calorimetry and the Mass Loss Rate from FDS for the Panel Material under a 40 kW/m² Radiant Exposure using Parameters Obtained from calibrating a 75 kW/m² Exposure

As illustrated in the above figures, the extrapolation was not able to predict the critical heat flux, as quantified by the threshold temperature.

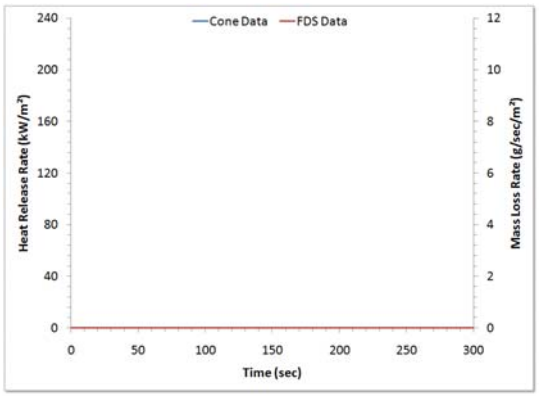

Figure 11-19. Comparison of the Heat Release Rate from Cone Calorimetry and the Mass Loss Rate from FDS for the Panel Material under a 35 kW/m² Radiant Exposure using Parameters Obtained from calibrating a 75 kW/m² Exposure

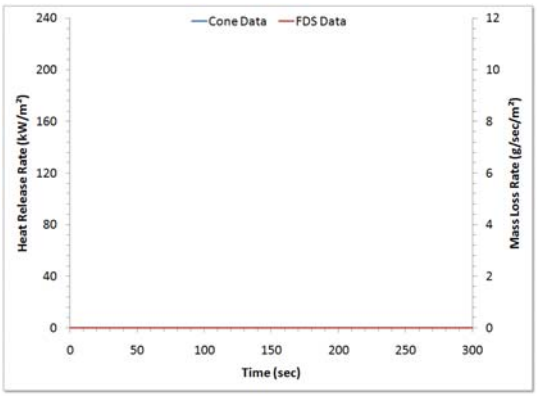

Figure 11-20. Comparison of the Heat Release Rate from Cone Calorimetry and the Mass Loss Rate from FDS for the Panel Material under a 25 kW/m² Radiant Exposure using Parameters Obtained from calibrating a 75 kW/m² Exposure

Following are the FDS input parameters used for extrapolation.

```
VIRGIN MATERIAL
DENSITY=4.290E+02
SPECIFIC_HEAT=1.460E+00
CONDUCTIVITY=1.940E-01
EMISSIVITY=9.000E-01
THICKNESS=2.360E-03

REACTION
HEAT_OF_REACTION=1.000E+03
NU_FUEL=6.990E-01
THRESHOLD_TEMPERATURE=5.860E+02
A=6.060E+12
E=2.520E+05

RESIDUE MATERIAL
DENSITY=1.060E+02
SPECIFIC_HEAT=2.240E-01
CONDUCTIVITY=1.010E-02
EMISSIVITY=9.000E-01
```

Figure 11-21. FDS Input Parameters Obtained by the Stochastic Hill-Climber Algorithm for the Panel Material Under a 75 kW/m² Radiant Exposure

In the figures above, no targets were defined, and select "highly unrealistic" values are shown in red. The actual panel material sample thickness in the present study was approximately 6.0 mm, and the virgin material density was approximately 315 kg/m³.

11.2 Extrapolation from Low Exposure Heat Flux

The following case is provided as an example of extrapolation to high heat flux for a fuel mass loss rate curve that is well fit at a low radiant exposure. The wall material was the only material that had characteristics at low heat fluxes that were not apparent at high heat fluxes, i.e. the second peak. Therefore this material was chosen for extrapolation.

The following figures compare the heat release rate from cone calorimetry and the mass loss rate from FDS for the wall material under a range of radiant exposures using parameters obtained from calibrating the 40 kW/m² exposure.

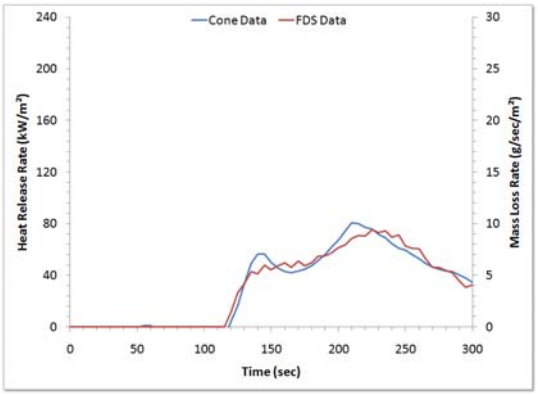

Figure 11-22. Comparison of the Heat Release Rate from Cone Calorimetry and the Mass Loss Rate from FDS for the Wall Material under an 40 kW/m² Radiant Exposure using Parameters Obtained from a Stochastic Hill-Climber Algorithm

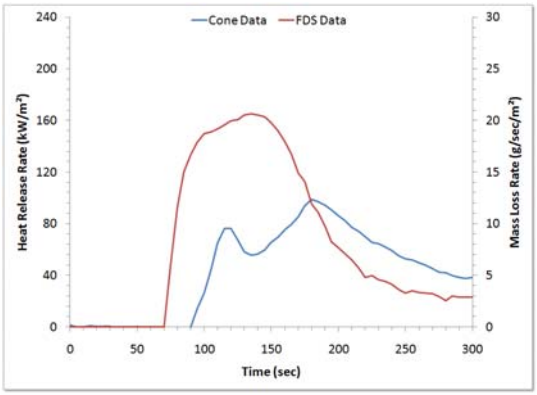

Figure 11-23. Comparison of the Heat Release Rate from Cone Calorimetry and the Mass Loss Rate from FDS for the Wall Material under a 50 kW/m² Radiant Exposure using Parameters Obtained from calibrating a 40 kW/m² Exposure

The figures above illustrate a significant error in extrapolation, even at an exposures close to the calibrated exposure.

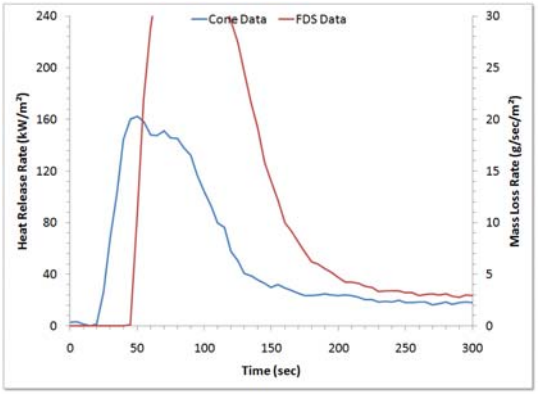

Figure 11-24. Comparison of the Heat Release Rate from Cone Calorimetry and the Mass Loss Rate from FDS for the Wall Material under a 65 kW/m² Radiant Exposure using Parameters Obtained from calibrating a 40 kW/m² Exposure

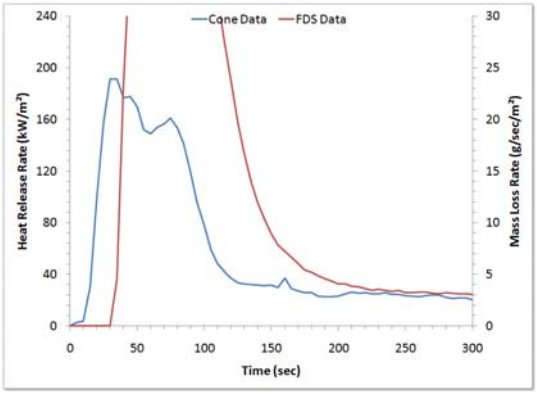

Figure 11-25. Comparison of the Heat Release Rate from Cone Calorimetry and the Mass Loss Rate from FDS for the Wall Material under a 80 kW/m² Radiant Exposure using Parameters Obtained from calibrating a 40 kW/m² Exposure

Generally speaking, the percentage error associated with extrapolation to high exposure heat flux is on the same order of magnitude as extrapolation in the other direction. However, at high heat flux, the error is magnified by the magnitude of the mass loss rate.

Following are the FDS input parameters used for extrapolation.

```
VIRGIN MATERIAL                 REACTION                          RESIDUE MATERIAL
DENSITY=3.210E+02               HEAT_OF_REACTION=6.938E+02        DENSITY=6.056E+02
SPECIFIC_HEAT=8.327E-01         NU_FUEL=9.592E-01                 SPECIFIC_HEAT=1.109E-02
CONDUCTIVITY=2.980E+00          THRESHOLD_TEMPERATURE=5.740E+02   CONDUCTIVITY=1.331E-01
EMISSIVITY=9.848E-01            A=5.639E-01                       EMISSIVITY=1.515E+00
THICKNESS= 1.571E-02            E=1.568E+04
```

Figure 11-26. FDS Input Parameters Obtained by the Stochastic Hill-Climber Algorithm for the Wall Material Under an 40 kW/m² Radiant Exposure

In the figures above, no targets were defined, and select "highly unrealistic" values are shown in red. The actual wall material sample thickness in the present study was approximately 2.4 mm, and the virgin material density was approximately 2,000 kg/m³.

Chapter 12. Multi-Goal Fitness Functions

Common fitness functions for genetic algorithms take the form of a weighted mean: $F = A(x) + B(y) + C(z) + \ldots$, where A, B and C are weight factors, and x, y and z are curve fitting goals. For the purposes of the present study, the term "competing goals" is used to describe fitness functions that seek to minimize error between multiple goals.

Because of the complexity of the carpet material mass loss rate curve, this material was chosen to illustrate the typical results for competing goal type fitness functions. These figures compare the heat release rate from cone calorimetry and the mass loss rate from FDS for the carpet material under a range of radiant exposures using parameters obtained from calibrating the 50 kW/m² and 60 kW/m² exposures.

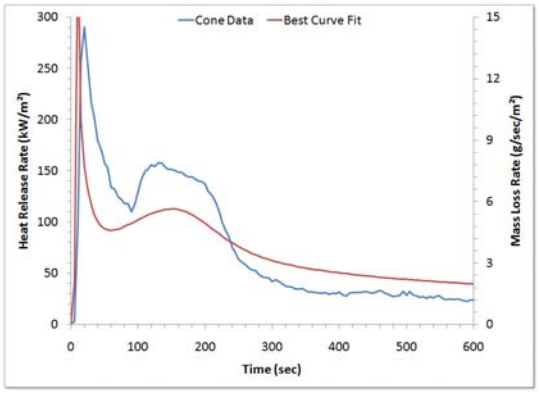

Figure 12-1. Comparison of the Heat Release Rate from Cone Calorimetry and the Mass Loss Rate from FDS for the Carpet Material under a 75 kW/m² Radiant Exposure using Parameters Obtained from calibrating the 50 kW/m² and 60 kW/m² Exposures

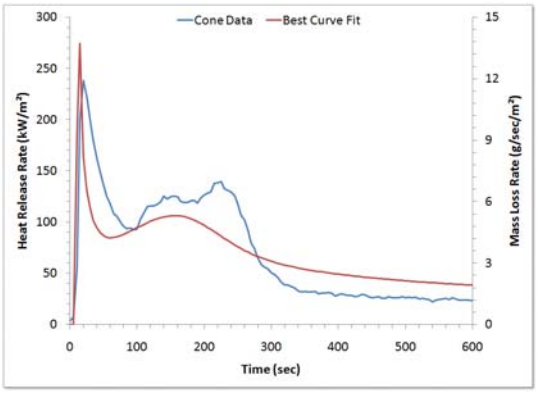

Figure 12-2. Comparison of the Heat Release Rate from Cone Calorimetry and the Mass Loss Rate from FDS for the Carpet Material under a 60 kW/m² Radiant Exposure using Parameters Obtained from a Stochastic Hill-Climber Algorithm with Competing Goals

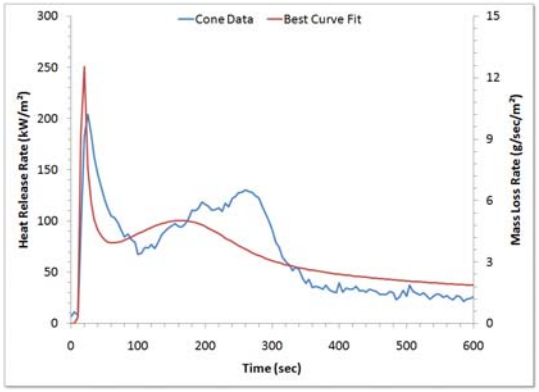

Figure 12-3. Comparison of the Heat Release Rate from Cone Calorimetry and the Mass Loss Rate from FDS for the Carpet Material under a 50 kW/m² Radiant Exposure using Parameters Obtained from a Stochastic Hill-Climber Algorithm with Competing Goals

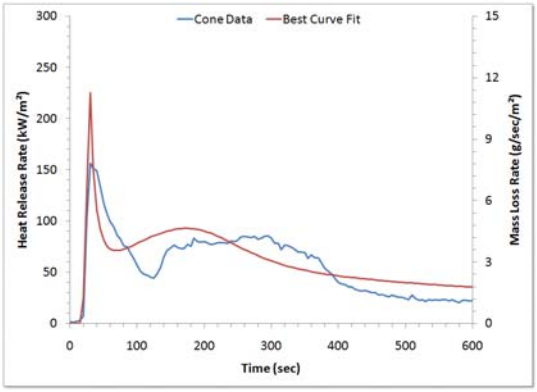

Figure 12-4. Comparison of the Heat Release Rate from Cone Calorimetry and the Mass Loss Rate from FDS for the Carpet Material under a 40 kW/m² Radiant Exposure using Parameters Obtained from calibrating the 50 kW/m² and 60 kW/m² Exposures

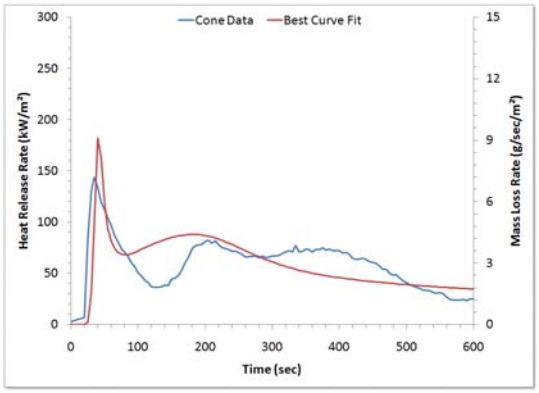

Figure 12-5. Comparison of the Heat Release Rate from Cone Calorimetry and the Mass Loss Rate from FDS for the Carpet Material under a 35 kW/m² Radiant Exposure using Parameters Obtained from calibrating the 50 kW/m² and 60 kW/m² Exposures

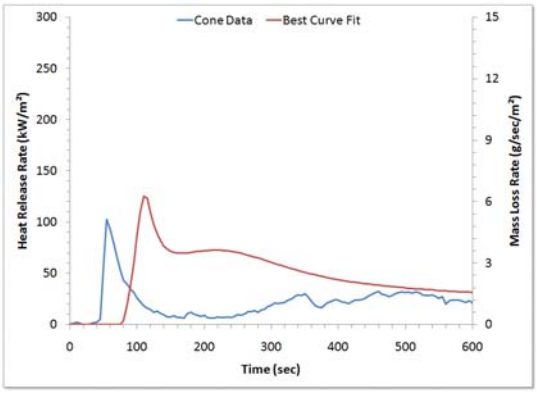

Figure 12-6. Comparison of the Heat Release Rate from Cone Calorimetry and the Mass Loss Rate from FDS for the Carpet Material under a 25 kW/m² Radiant Exposure using Parameters Obtained from calibrating the 50 kW/m² and 60 kW/m² Exposures

Following are the FDS input parameters used for extrapolation.

```
VIRGIN MATERIAL
DENSITY=4.187E+02
SPECIFIC_HEAT=6.121E-01
CONDUCTIVITY=3.426E-01
EMISSIVITY=9.443E-01
THICKNESS=1.558E-02

REACTION
HEAT_OF_REACTION=1.946E+02
NU_FUEL=3.817E-01
THRESHOLD_TEMPERATURE=4.059E+02
A=2.117E+16
E=2.347E+05

RESIDUE MATERIAL
DENSITY=5.622E+02
SPECIFIC_HEAT=7.751E+00
CONDUCTIVITY=1.115E-01
EMISSIVITY=1.837E+00
```

Figure 12-7. FDS Input Parameters Obtained by the Stochastic Hill-Climber Algorithm for the Carpet Material Under 50 kW/m² and 60 kW/m² Radiant Exposures with Competing Goals

In the figures above, no targets were defined, and select "highly unrealistic" values are shown in red.

Imposing competing goals generally produces results that trend toward a local optimum conditions, partially satisfying each goal. In this example, the competing goals are both mass loss rate curves. However, it is reasonable to conclude that the same principle applies if the competing goals are exposed face temperatures, back face temperatures, measured mass loss rates, oxygen consumption rates, etc., if the model doesn't extrapolate well with test data. The following figures illustrate the inherent flaw in competing goal fitness functions.

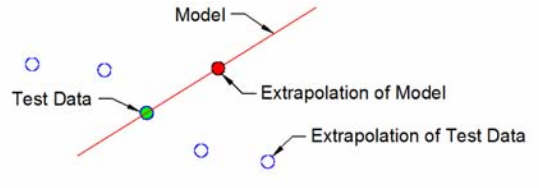

Figure 12-8. Schematic Illustrating Extrapolation from a Model Fit with One Goal

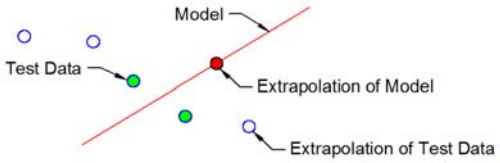

Figure 12-9. Schematic Illustrating Extrapolation from a Model Fit with Competing Goals

The inherent flaw in fitness functions with competing goals is that if the model doesn't extrapolate well with test data, using multiple goals will only result in a statistical average. Alternatively, imposing non-competing goals should allow mitigating the possibility of arriving at a local optimum, producing results which iterate toward satisfying both goals individually.

Consequently, the main routine for stochastic hill-climber algorithm HC-PYRO, takes the form of a nested loop. The inner loop performs a curve fit on the mass loss rate of the primary curve(s) (Goal 1), and the outer loop performs a curve fit to the mass loss

rate of secondary curve(s) (Goal 2). The following figures schematically illustrate non-competing goals.

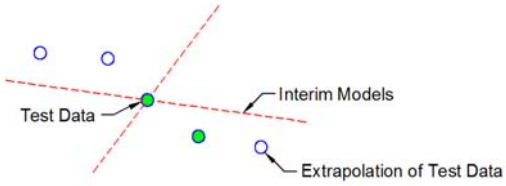

Figure 12-10. Schematic Illustrating Extrapolation from Interim Models for Non-Competing Goals

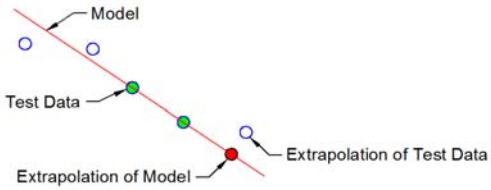

Figure 12-11. Schematic Illustrating Final Extrapolation from a Model with Non-Competing Goals

Imposing non-competing goals takes advantage of the over-specified nature of the problem. Because equivalent solutions can be reached with different combinations of parameters, it is possible to allow parameters to be modified while maintaining the accuracy of the primary goal (interim models schematically shown above). This characteristic allows examination of the impact of changing parameters on the accuracy of the secondary curve, without trending toward a weighted mean between multiple goals.

Chapter 13. Calibration Results

The results presented in this chapter entail use of the stochastic hill-climber algorithm HC-PYRO, with parameter normalization, iteration dependent mutation magnitudes and multiple non-competing goals. Each of the parameter calibrations in this section were concluded in approximately 3 days time. This includes roughly 25,000 simulations at 10 seconds per simulation. For an example of the FDS model input syntax, refer to Appendix A.

13.1 Carpet Material

The following figures compare the heat release rate from cone calorimetry and the mass loss rate from FDS for the carpet material under the 60 kW/m² and 75 kW/m² radiant exposures using parameters obtained from the stochastic hill-climber algorithm with non-competing goals.

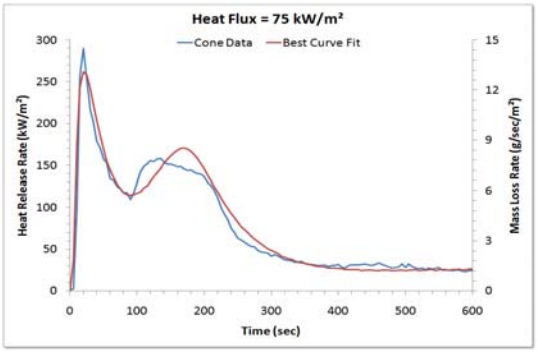

Figure 13-1. Comparison of the Heat Release Rate from Cone Calorimetry and the Mass Loss Rate from FDS for the Carpet Material under a 75 kW/m² Radiant Exposure using Parameters Obtained from a Stochastic Hill-Climber Algorithm with Non-Competing Goals

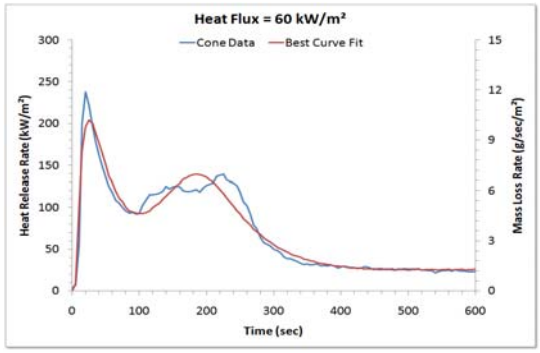

Figure 13-2. Comparison of the Heat Release Rate from Cone Calorimetry and the Mass Loss Rate from FDS for the Carpet Material under a 60 kW/m² Radiant Exposure using Parameters Obtained from a Stochastic Hill-Climber Algorithm with Non-Competing Goals

The R-squared values of Goals 1 & 2 for the carpet material are greater than 96%.

The following figures compare the heat release rate from cone calorimetry and the mass loss rate from FDS for the carpet material under range of radiant exposures using parameters obtained from calibrating the 75 kW/m² and 60 kW/m² exposures.

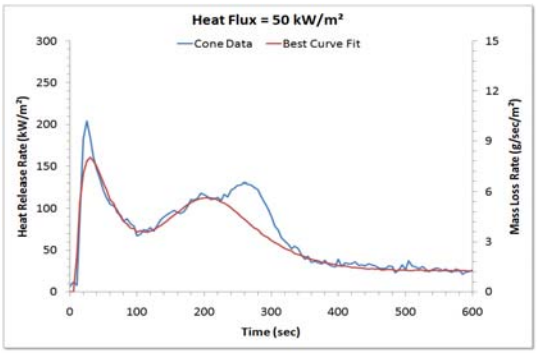

Figure 13-3. Comparison of the Heat Release Rate from Cone Calorimetry and the Mass Loss Rate from FDS for the Carpet Material under a 50 kW/m² Radiant Exposure using Parameters Obtained from calibrating the 75 kW/m² and 60 kW/m² Exposures

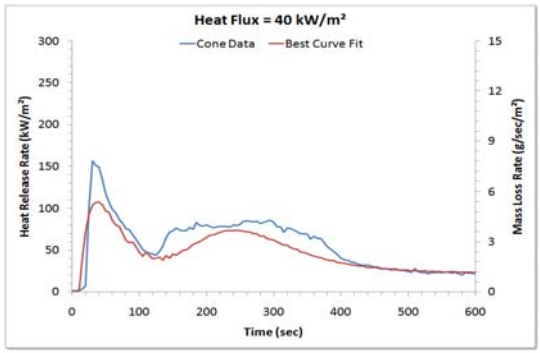

Figure 13-4. Comparison of the Heat Release Rate from Cone Calorimetry and the Mass Loss Rate from FDS for the Carpet Material under a 40 kW/m² Radiant Exposure using Parameters Obtained from calibrating the 75 kW/m² and 60 kW/m² Exposures

The results for the carpet material extrapolate well with exposure heat flux.

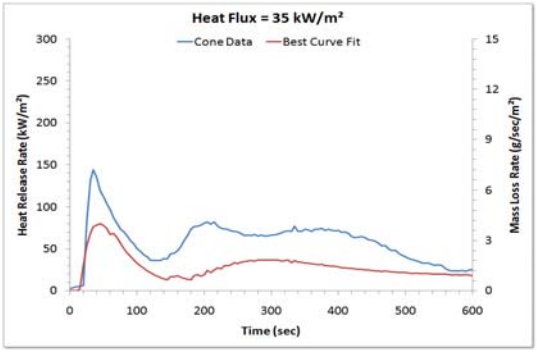

Figure 13-5. Comparison of the Heat Release Rate from Cone Calorimetry and the Mass Loss Rate from FDS for the Carpet Material under a 35 kW/m² Radiant Exposure using Parameters Obtained from calibrating the 75 kW/m² and 60 kW/m² Exposures

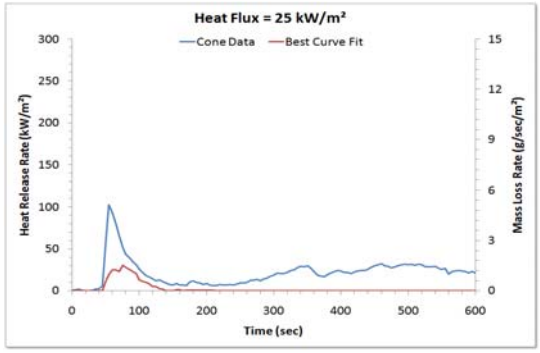

Figure 13-6. Comparison of the Heat Release Rate from Cone Calorimetry and the Mass Loss Rate from FDS for the Carpet Material under a 25 kW/m² Radiant Exposure using Parameters Obtained from calibrating the 75 kW/m² and 60 kW/m² Exposures

It is clear that the error is more pronounced the greater the extrapolation from calibrated exposures. Following are the FDS input parameters used for extrapolation.

VIRGIN MATERIAL	REACTION	RESIDUE MATERIAL
DENSITY=5.246E+02	HEAT_OF_REACTION=4.198E+01	DENSITY=5.364E+02
SPECIFIC_HEAT=5.086E-01	NU_FUEL=4.369E-01	**SPECIFIC_HEAT=1.165E+01**
CONDUCTIVITY=3.789E-01	THRESHOLD_TEMPERATURE=4.041E+02	CONDUCTIVITY=4.981E-02
EMISSIVITY=1.259E+00	A=1.912E+00	EMISSIVITY=1.995E-01
THICKNESS=1.521E-02	E=2.595E+04	

Figure 13-7. FDS Input Parameters Obtained by the Stochastic Hill-Climber Algorithm for the Carpet Material Under 65 kW/m² and 75 kW/m² Radiant Exposures

In the figures above, no targets were defined, and select "highly unrealistic" values are shown in red. The actual carpet material sample thickness in the present study was approximately 6.0 mm, and the virgin material density was approximately 450 kg/m³.

13.2 Wall Material

The following figures compare the heat release rate from cone calorimetry and the mass loss rate from FDS for the wall material under the 65 kW/m² and 80 kW/m² radiant exposures using parameters obtained from the stochastic hill-climber algorithm with non-competing goals.

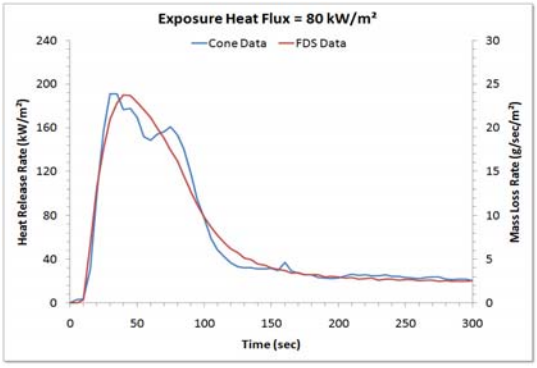

Figure 13-8. Comparison of the Heat Release Rate from Cone Calorimetry and the Mass Loss Rate from FDS for the Wall Material under a 80 kW/m² Radiant Exposure using Parameters Obtained from a Stochastic Hill-Climber Algorithm with Non-Competing Goals

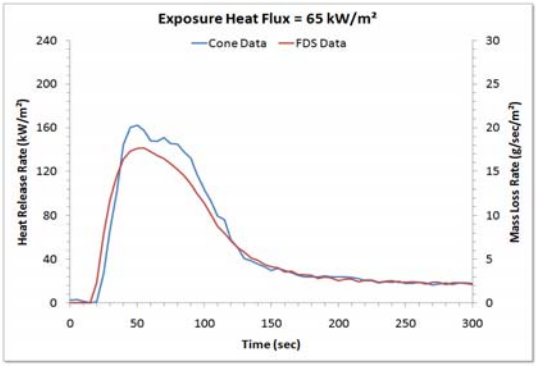

Figure 13-9. Comparison of the Heat Release Rate from Cone Calorimetry and the Mass Loss Rate from FDS for the Wall Material under a 65 kW/m² Radiant Exposure using Parameters Obtained from a Stochastic Hill-Climber Algorithm with Non-Competing Goals

The R-squared values of Goals 1 & 2 for the wall material are greater than 96%.

The following figures compare the heat release rate from cone calorimetry and the mass loss rate from FDS for the wall material under range of radiant exposures using parameters obtained from calibrating the 80 kW/m² and 65 kW/m² exposures.

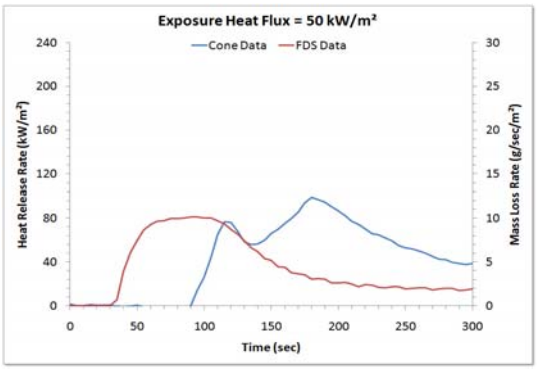

Figure 13-10. Comparison of the Heat Release Rate from Cone Calorimetry and the Mass Loss Rate from FDS for the Wall Material under a 50 kW/m² Radiant Exposure using Parameters Obtained from calibrating the 80 kW/m² and 65 kW/m² Exposures

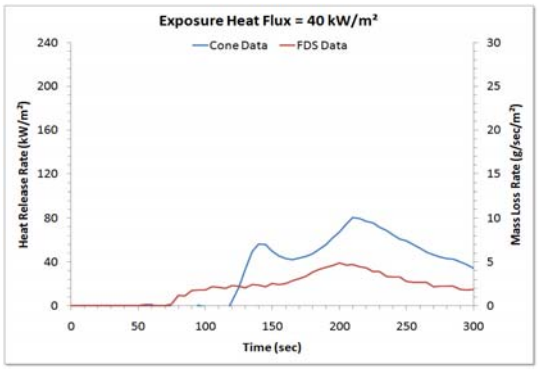

Figure 13-11. Comparison of the Heat Release Rate from Cone Calorimetry and the Mass Loss Rate from FDS for the Wall Material under a 40 kW/m² Radiant Exposure using Parameters Obtained from calibrating the 80 kW/m² and 65 kW/m² Exposures

The results for the wall material extrapolate well with exposure heat flux, but the characteristics of the second peak are only marginally differentiable. Again, the error in the timing of ignition at mid-range heat flux is most likely because of an error in data collection.

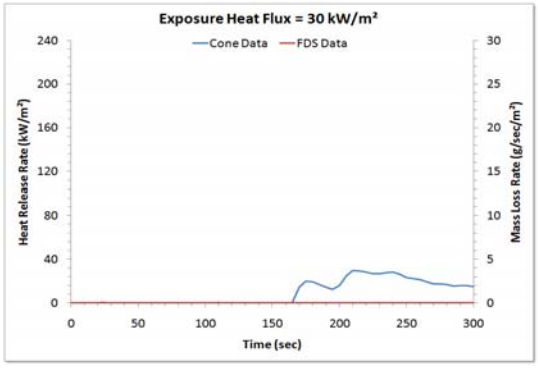

Figure 13-12. Comparison of the Heat Release Rate from Cone Calorimetry and the Mass Loss Rate from FDS for the Wall Material under a 30 kW/m² Radiant Exposure using Parameters Obtained from calibrating the 80 kW/m² and 65 kW/m² Exposures

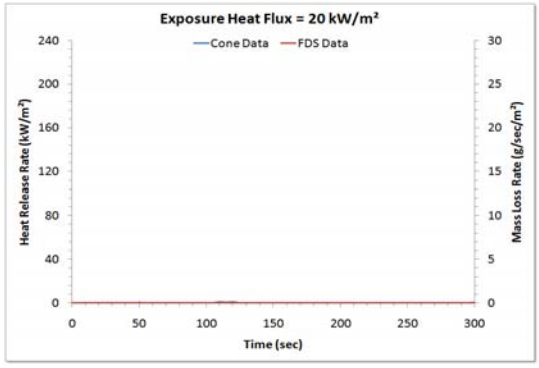

Figure 13-13. Comparison of the Heat Release Rate from Cone Calorimetry and the Mass Loss Rate from FDS for the Wall Material under a 20 kW/m² Radiant Exposure using Parameters Obtained from calibrating the 80 kW/m² and 65 kW/m² Exposures

Again, the extrapolation was not able to predict the critical heat flux, as quantified by the threshold temperature. Following are the FDS input parameters used for extrapolation.

VIRGIN MATERIAL	REACTION	RESIDUE MATERIAL
DENSITY=2.720E+02	HEAT_OF_REACTION=9.363E+02	DENSITY=7.649E+02
SPECIFIC_HEAT=6.566E-01	NU_FUEL=9.863E-01	SPECIFIC_HEAT=6.576E-02
CONDUCTIVITY=5.434E-01	THRESHOLD_TEMPERATURE=5.902E+02	CONDUCTIVITY=8.649E-02
EMISSIVITY=1.027E+00	A=4.251E-01	**EMISSIVITY=2.022E+00**
THICKNESS=9.784E-03	E=1.253E+04	

Figure 13-14. FDS Input Parameters Obtained by the Stochastic Hill-Climber Algorithm for the Wall Material Under 65 kW/m² and 80 kW/m² Radiant Exposures

In the figures above, no targets were defined, and select "highly unrealistic" values are shown in red. The actual wall material sample thickness in the present study was approximately 2.4 mm, and the virgin material density was approximately 2,000 kg/m³.

13.3 Panel Material

The following figures compare the heat release rate from cone calorimetry and the mass loss rate from FDS for the panel material under the 60 kW/m² and 75 kW/m² radiant exposures using parameters obtained from the stochastic hill-climber algorithm with non-competing goals.

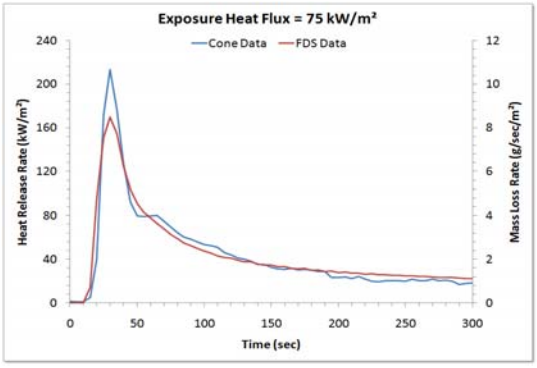

Figure 13-15. Comparison of the Heat Release Rate from Cone Calorimetry and the Mass Loss Rate from FDS for the Panel Material under a 75 kW/m² Radiant Exposure using Parameters Obtained from a Stochastic Hill-Climber Algorithm with Non-Competing Goals

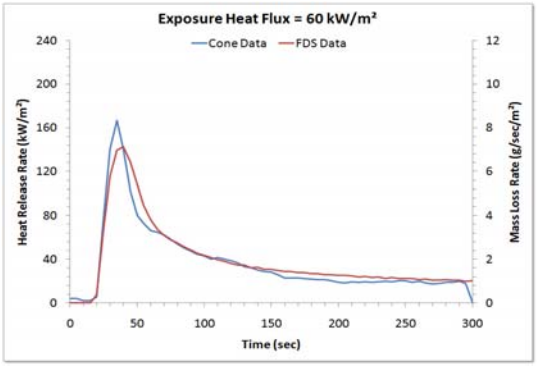

Figure 13-16. Comparison of the Heat Release Rate from Cone Calorimetry and the Mass Loss Rate from FDS for the Panel Material under a 60 kW/m² Radiant Exposure using Parameters Obtained from a Stochastic Hill-Climber Algorithm with Non-Competing Goals

The R-squared values of Goals 1 & 2 for the panel material are greater than 96%.

The following figures compare the heat release rate from cone calorimetry and the mass loss rate from FDS for the panel material under range of radiant exposures using parameters obtained from calibrating the 75 kW/m² and 60 kW/m² exposures.

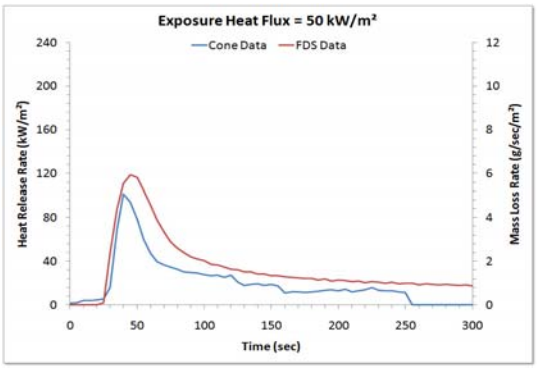

Figure 13-17. Comparison of the Heat Release Rate from Cone Calorimetry and the Mass Loss Rate from FDS for the Panel Material under a 50 kW/m² Radiant Exposure using Parameters Obtained from calibrating the 75 kW/m² and 60 kW/m² Exposures

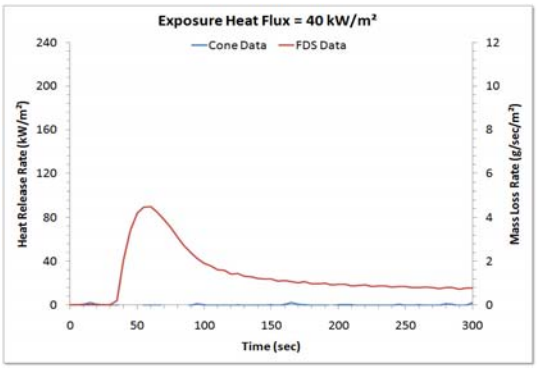

Figure 13-18. Comparison of the Heat Release Rate from Cone Calorimetry and the Mass Loss Rate from FDS for the Panel Material under a 40 kW/m² Radiant Exposure using Parameters Obtained from calibrating the 75 kW/m² and 60 kW/m² Exposures

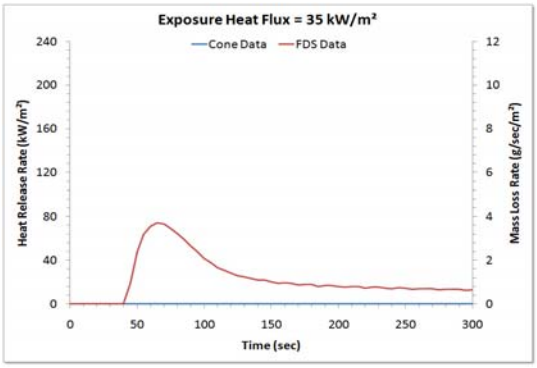

Figure 13-19. Comparison of the Heat Release Rate from Cone Calorimetry and the Mass Loss Rate from FDS for the Panel Material under a 35 kW/m² Radiant Exposure using Parameters Obtained from calibrating the 75 kW/m² and 60 kW/m² Exposures

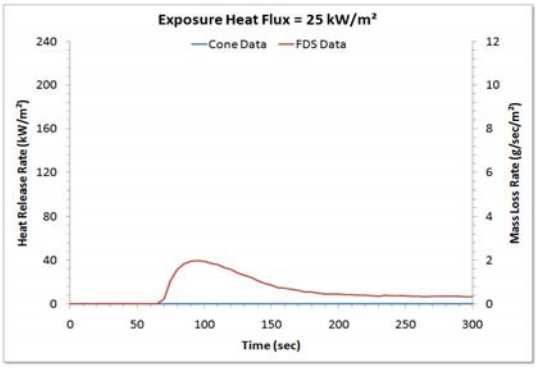

Figure 13-20. Comparison of the Heat Release Rate from Cone Calorimetry and the Mass Loss Rate from FDS for the Panel Material under a 25 kW/m² Radiant Exposure using Parameters Obtained from calibrating the 75 kW/m² and 60 kW/m² Exposures

The results for the wall material extrapolate well with exposure heat flux, but the extrapolation was not able to predict the critical heat flux, as quantified by the threshold temperature. Following are the FDS input parameters used for extrapolation.

```
VIRGIN MATERIAL                 REACTION                              RESIDUE MATERIAL
DENSITY=4.008E+02               HEAT_OF_REACTION=1.517E+03            DENSITY=4.257E+03
SPECIFIC_HEAT=1.640E+00         NU_FUEL=3.747E-01                     SPECIFIC_HEAT=3.735E-01
CONDUCTIVITY=7.047E-01          THRESHOLD_TEMPERATURE=3.825E+02       CONDUCTIVITY=6.433E-02
EMISSIVITY=9.010E-01            A=4.056E+07                           EMISSIVITY=4.054E-01
THICKNESS=4.886E-03             E=1.124E+05
```

Figure 13-21. FDS Input Parameters Obtained by the Stochastic Hill-Climber Algorithm for the Panel Material Under 60 kW/m² and 75 kW/m² Radiant Exposures

In the figures above, no targets were defined, and select "highly unrealistic" values are shown in red. The actual wall material sample thickness in the present study was approximately 6.0 mm, and the virgin material density was approximately 315 kg/m³.

Chapter 14. Stability and Resolution

For FDS simulations (without pyrolysis), the initial time step is estimated, and subsequent time steps are governed by the CFL criterion. The CFL criterion is a gas phase criterion which adjusts the time step based on velocities present in the domain:

$$\Delta t \max\left(\frac{|u|}{\Delta x}, \frac{|v|}{\Delta y}, \frac{|w|}{\Delta z}\right) < 1 \qquad (14\text{-}23)$$

Simply stated, the CFL criterion adjusts the time step so that it takes on a maximum value equal to the time it takes for gases to traverse a single cell. Cell size is a user defined quantity, and is usually restricted by available computer capacity.

Because pyrolysis modeling in FDS is still in its infancy, it is the responsibility of the user to choose both the solid phase cell size (Δx) and the constant time step (Δt) necessary to produce stable well-resolved results. In the present study cell size is assumed constant. The only criterion currently imposed is that the cell size is equal to the square root of the virgin material diffusivity, multiplied by the cell size factor; a user defined quantity with units of $\sec^{1/2}$. The default value for the cell size factor (csf) is 1.

$$\Delta x = csf\sqrt{\alpha} \qquad (14\text{-}24)$$

Stability and resolution are customarily expressed in terms of the grid Fourier Number:

$$F = \frac{\alpha \Delta t}{\Delta x^2} = \frac{\Delta t}{csf^2} \qquad (14\text{-}25)$$

The time step and cell size required for stability and resolution were determined automatically by the algorithm used in the present study. The typical value for time step was approximately 0.1 sec. The typical value for cell size factor was approximately 0.1. The following plots qualitatively illustrate the consequences of increasing cell size or time step.

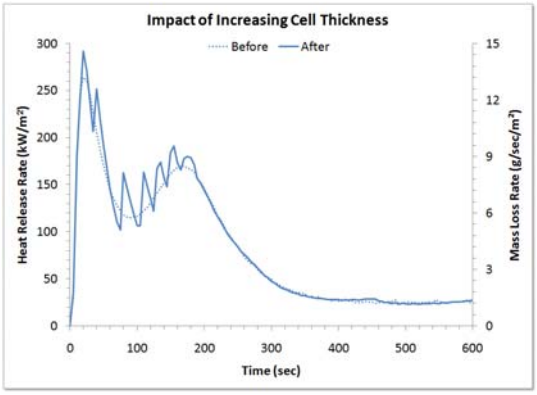

Figure 14-1. Qualitative Impact of Increasing Cell Size on the Characteristic Mass Loss Rate Curve

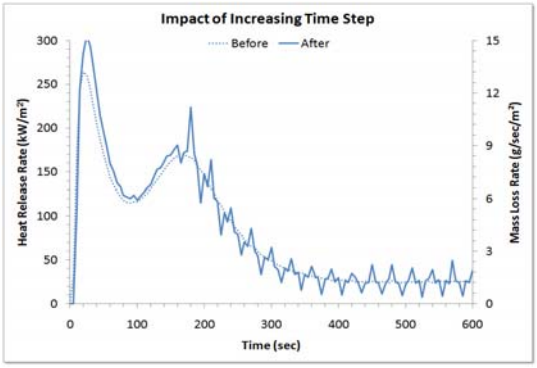

Figure 14-2. Qualitative Impact of Increasing Time Step on the Characteristic Mass Loss Rate Curve

To be relevant, stability and resolution criteria imposed must be able to address: (1) why does increasing the time step increase the magnitude of fluctuations of the mass loss rate curve, (2) why does increasing the cell size increase the magnitude of fluctuations of the mass loss rate curve, (3) why does increasing the time step only cause fluctuations later time steps, and (4) why does increasing the cell size only cause fluctuations in the early time steps?

14.2 Numerical Stability

The rate of heat diffusion in FDS is governed by a one-dimensional form of the transient heat conduction equation, as follows:

$$\rho c \frac{\partial T}{\partial t} = \frac{\partial}{\partial x}\left(k \frac{\partial T}{\partial x} \right) \tag{14-26}$$

In FDS, both conductivity (k) and specific heat (c) can be functions of temperature. However, in the present study, constant thermophysical properties are assumed, yielding:

$$\frac{\partial T}{\partial t} = \alpha \frac{\partial^2 T}{\partial x^2} \tag{14-27}$$

Internal solid temperatures in FDS are updated in time using an implicit Crank-Nicolson scheme [23]. The Crank-Nicolson scheme can be viewed as the average of the forward Euler method at n and the backward Euler method at n+1, as follows:

$$\frac{T_i^{n+1} - T_i^n}{\Delta t} = \frac{1}{2}\left(\alpha \frac{\partial^2 T}{\partial x^2}\bigg|^{n+1} + \alpha \frac{\partial^2 T}{\partial x^2}\bigg|^{n} \right) \tag{14-28}$$

where:

$$\frac{\partial^2 T}{\partial x^2} \approx \frac{1}{\Delta x^2}\left(T_{i+1} - 2T_i + T_{i-1} \right) \tag{14-29}$$

The present work uses a Von-Neumann stability analysis to check for regions of instability in the finite difference heat equation, with the stability characteristic $T_i^n = \xi^n e^{I\alpha i \Delta x}$. Following is the modified equation for transient heat conduction, where the grid Fourier number is $F = \alpha \Delta t / \Delta x^2$.

$$\frac{\rho c}{\Delta t}\left(T_i^{n+1} - T_i^n \right) = \frac{k}{\Delta x^2}\left[\frac{1}{2}\begin{pmatrix} T_{i+1}^{n+1} - 2T_i^{n+1} + T_{i-1}^{n+1} \\ + T_{i+1}^{n} - 2T_i^{n} + T_{i-1}^{n} \end{pmatrix} \right] \tag{14-30}$$

$$\frac{\rho c}{\Delta t}\left[\xi^n \left(\xi - 1 \right) e^{I\alpha i \Delta x} \right] = \frac{k}{\Delta x^2}\left[-2\xi^n \left(\xi + 1 \right)\left(\sin^2 \alpha \Delta x \right) e^{I\alpha i \Delta x} \right] \tag{14-31}$$

$$1 = \frac{\frac{k}{\Delta x^2}\left[-2\xi^n\left(\xi+1\right)\left(\sin^2\alpha\Delta x\right)e^{I\alpha i\Delta x}\right]}{\frac{\rho c}{\Delta t}\left[\xi^n\left(\xi-1\right)e^{I\alpha i\Delta x}\right]} \tag{14-32}$$

$$1 = -2F\frac{\left(\xi+1\right)}{\left(\xi-1\right)} \tag{14-33}$$

$$\text{stable for } \left|\xi\right| \le 1 \;\rightarrow\; 0 \le F < \infty \tag{14-34}$$

This demonstrates why the implicit Crank-Nicolson scheme is unconditionally stable for all realistic values of the grid Fourier number.

14.2.2 Crank-Nicolson Method with Heat Generation

Considering a one-dimensional form of the transient heat conduction equation with internal heat generation:

$$\rho c\frac{\partial T}{\partial t} = \frac{\partial}{\partial x}\left(k\frac{\partial T}{\partial x}\right) + \dot{q}'''_{gen} \tag{14-35}$$

Solid phase temperatures in FDS are updated in time using an implicit Crank-Nicolson scheme, and the heat generation source term is updated explicitly [4] as follows:

$$\frac{T_i^{n+1} - T_i^n}{\Delta t} = \frac{1}{2}\left(\alpha\frac{\partial^2 T}{\partial x^2}\bigg|^{n+1} + \alpha\frac{\partial^2 T}{\partial x^2}\bigg|^{n}\right) + \frac{\dot{q}'''_{gen}\big|_i^n}{\rho c} \tag{14-36}$$

Again, using Von-Neumann stability analysis to check for regions of instability:

$$1 = \frac{\frac{k}{\Delta x^2}\left[-2\xi^n\left(\xi+1\right)\left(\sin^2\alpha\Delta x\right)e^{I\alpha i\Delta x}\right]}{\frac{\rho c}{\Delta t}\left[\xi^n\left(\xi-1\right)e^{I\alpha i\Delta x}\right]} + \frac{\dot{q}'''_{gen}\Delta t}{\rho c\Delta T} \tag{14-37}$$

$$1 = -2F\frac{\left(\xi+1\right)}{\left(\xi-1\right)} + \frac{\dot{q}'''_{gen}\Delta t}{\rho c\Delta T} \tag{14-38}$$

$$\text{stable for } \left|\xi\right| \le 1 \;\rightarrow\; \dot{q}'''_{gen} < \frac{\rho c\Delta T}{\Delta t} \tag{14-39}$$

and similarly,

$$\frac{\frac{\rho c}{\Delta t}\left[\xi^n\left(\xi-1\right)e^{I\alpha i\Delta x}\right]}{\frac{k}{\Delta x^2}\left[-2\xi^n\left(\xi+1\right)\left(\sin^2\alpha\Delta x\right)e^{I\alpha i\Delta x}\right]}=1+\frac{\dot{q}'''_{gen}\Delta x^2}{k\Delta T} \tag{14-40}$$

$$\frac{-1}{2F}\frac{\left(\xi-1\right)}{\left(\xi+1\right)}=1+\frac{\dot{q}'''_{gen}\Delta x^2}{k\Delta T} \tag{14-41}$$

$$\text{stable for } \left|\xi\right|\le 1 \;\rightarrow\; -\frac{k\Delta T}{\Delta x^2}<\dot{q}'''_{gen} \tag{14-42}$$

The criteria above suggest the following stability conditions: (1) the rate that heat is generated internally ($\dot{q}'''_{gen}$) cannot be greater than the capacity to store that heat ($\rho c\,\partial T/\partial t$), insuring forward heat diffusion, and (2) if the rate that heat is generated internally ($\dot{q}'''_{gen}$) is negative (as in the case of pyrolysis), then its magnitude cannot be greater than the rate of heat diffusion, insuring only positive changes in temperature with respect to time. Otherwise stated,

$$\dot{q}'''_{reac}\le k\frac{\partial^2 T}{\partial x^2} \tag{14-43}$$

14.2.3 Mass Loss Rate

The rate of mass loss from a layer due to pyrolysis in FDS is a function of temperature, governed by the Arrhenius equation, as follows:

$$\dot{m}'''=-\eta\frac{\partial\rho}{\partial t}=\eta\rho_0 YA_0\exp\left(-\frac{E}{RT}\right)\max\left[0,T-T_{thr}\right]^0 \tag{14-44}$$

Consequently, the rate of change fuel mass per unit volume at temperatures greater than the threshold temperature is expressed as:

$$\frac{\partial\rho}{\partial t}=-\rho Ae^{(-E/RT)} \tag{14-45}$$

In FDS, solid fuel mass fractions are updated explicitly in time as follows:

$$\frac{\rho_i^{n+1} - \rho_i^n}{\Delta t} = -\rho_i^n A e^{\left(-E/RT_i^n\right)} \tag{14-46}$$

$$\text{stable for } 0 < \Delta t A e^{\left(-E/RT_i^n\right)} < \infty \tag{14-47}$$

This criterion ensures that the fuel mass fraction decreases with time. Therefore, the value of the fuel mass fraction is unconditionally stable. Additionally, the fuel mass loss rate ($\dot{m}'''$) is conditionally stable for positive changes in temperature with respect to time:

$$\text{stable for } T_i^{n+1} \geq T_i^n \tag{14-48}$$

14.3 Resolution Criteria

The Crank-Nicolson scheme was shown to be conditionally stable in terms of the temperature. The stability condition is that heat loss to pyrolysis cannot dominate the heat transfer process. The Arrhenius equation was shown to be conditionally stable in terms of the mass loss rate. The stability condition for mass loss is that the heat equation must be stable.

However, it is reasonable to consider the possibility that heat loss to pyrolysis can dominate heat transfer; when individual cells reach the threshold temperature $\partial T/\partial t \approx 0$, and when multiple adjacent cells reach the threshold temperature $\partial^2 T/\partial x^2 \approx 0$.

14.3.1 Critical Time Step

The following figures illustrate the impact of a large time step on the mass loss rate curve and the internal solid temperature.

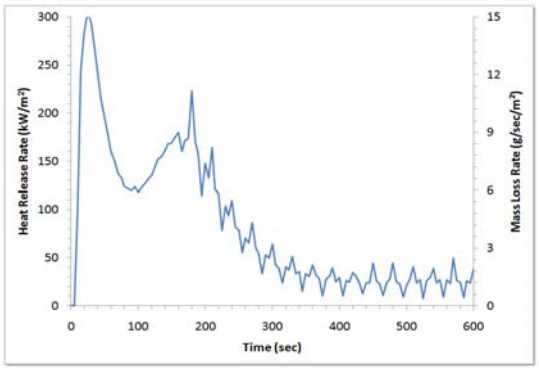

Figure 14-3. Mass Loss Rate Curve for the Carpet Material under a 75 kW/m² Radiant Exposure with a Large Time Step

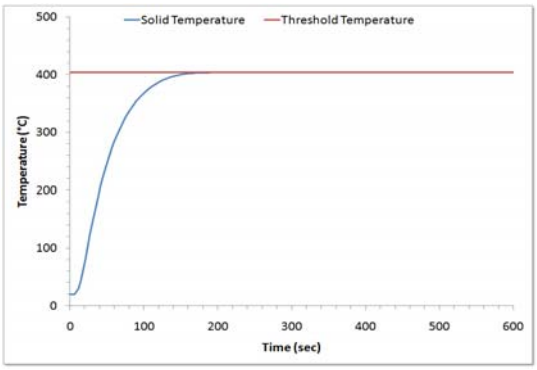

Figure 14-4. Back Surface Temperature for the Carpet Material under a 75 kW/m² Radiant Exposure with a Large Time Step

The above figures are for the carpet material with a 75 kW/m² exposure. The time step is 3.0 sec and the cell size factor is 0.10 ($\Delta x = 120\mu m$). The threshold temperature is 404.1°C. From the figures above, it is difficult to claim that the instabilities in the mass loss rate are a result of temperature instabilities, because the temperature appears to be very stable. However, upon closer examination of the same data, oscillations in the solid temperature are more apparent:

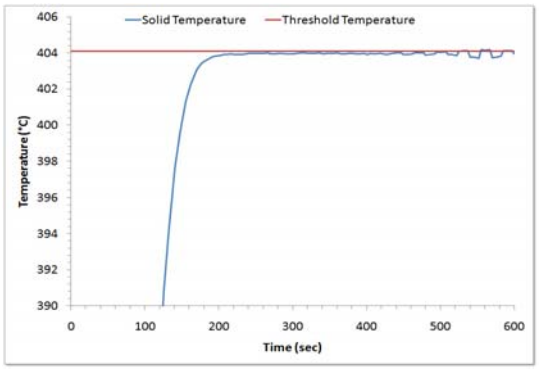

Figure 14-5. Internal Temperature for the Carpet Material under a 75 kW/m² Radiant Exposure with a Large Time Step (View 1)

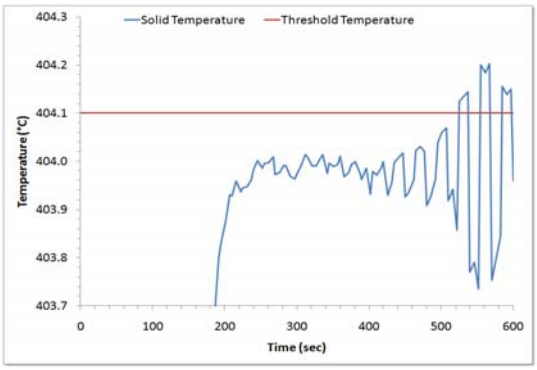

Figure 14-6. Internal Temperature for the Carpet Material under a 75 kW/m² Radiant Exposure with a Large Time Step (View 2)

In the figures above, solid temperature is measured at a depth of 0.01000 meters, and the modeled thickness is 0.01521 meters. FDS output frequency is 5 seconds.

It was established previously that the implicit Crank-Nicolson scheme was only conditionally stable. It appears that in this example, the limits of the region of stability have been exceeded, resulting in an oscillation with increasing amplitude.

As directed by the stability criteria, it is postulated that the fluctuations after the second peak in the mass loss rate are caused by multiple adjacent cells at the threshold temperature. The assumption that the solution converges toward spatially steady conditions (i.e. $\partial^2 T/\partial x^2 \approx 0$) provides a plausible explanation for instabilities observed after the second peak in mass loss rate, because this is when the back boundary temperature reaches a steady magnitude equal to the threshold temperature.

As a significant portion of the material thickness converges on the threshold temperature, the heat equation effectively loses its diffusive term as follows:

$$\rho c \frac{\partial T}{\partial t} = -\dot{q}'''_{reac} \tag{14-49}$$

and the finite form of the heat equation loses its implicit nature, and becomes unconditionally unstable, toggling between the following two conditions on alternate time steps:

$$\frac{T_i^{n+1} - T_i^n}{\Delta t} = -\frac{\dot{q}'''_{reac}\big|_i^n}{\rho c} \tag{14-50}$$

$$\frac{T_i^{n+1} - T_i^n}{\Delta t} = \frac{1}{2}\left(\alpha \frac{\partial^2 T}{\partial x^2}\bigg|^{n+1} + \alpha \frac{\partial^2 T}{\partial x^2}\bigg|^{n} \right) \tag{14-51}$$

Because the heat equation converges toward unconditionally unstable conditions, there are no actual stability criteria. Consequently, it is necessary to decide how much instability is acceptable, or equivalently, what temperature fluctuation magnitude is

acceptable. The maximum magnitude of the drop in temperature after a cell reaches the threshold temperature is as follows:

$$\Delta T_{thr} = \frac{\dot{q}'''_{reac}}{\rho c}\Delta t \tag{14-52}$$

where:

$$\dot{q}'''_{reac} = \eta \rho_0 A_0 e^{(-E/RT_{thr})} \Delta H_R \tag{14-53}$$

Therefore, to reduce the magnitude of the temperature fluctuation, it is necessary to reduce the time step. A characteristic time can be taken from our stability criteria, as follows:

$$\Delta t \sim \frac{\rho c \Delta T}{\dot{q}'''_{reac}} \approx \frac{\rho_0 c \Delta T}{\rho_0 A_0 e^{(-E/RT_{thr})} \Delta H_R} \tag{14-54}$$

and assuming linear scaling,

$$\Delta t = \frac{c \Delta T}{n A_0 e^{(-E/RT_{thr})} \Delta H_R} \tag{14-55}$$

where $\Delta T \approx \left(G/\sigma + T_\infty{}^4\right)^{1/4} - T_{thr}$, G is the irradiation level (exposure heat flux), σ is the Stefan-Boltzmann constant and n is a characteristic time scale factor. This equation can be interpreted as: the amount of energy required for pyrolysis must be small in comparison to the amount of energy available, limiting the magnitude of the inherent temperature fluctuations caused by numerical instabilities as the solution converges toward spatially steady conditions. The following figures illustrate the resolving power of characteristic time scale factor (n):

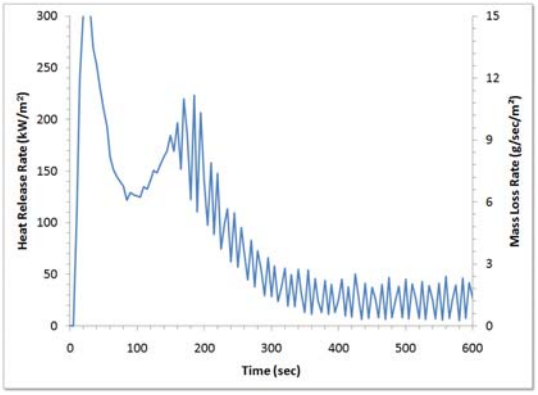

Figure 14-7. Mass Loss Rate for the Carpet Material under a 75 kW/m² Radiant Exposure with a Time Scale Factor of n = 100

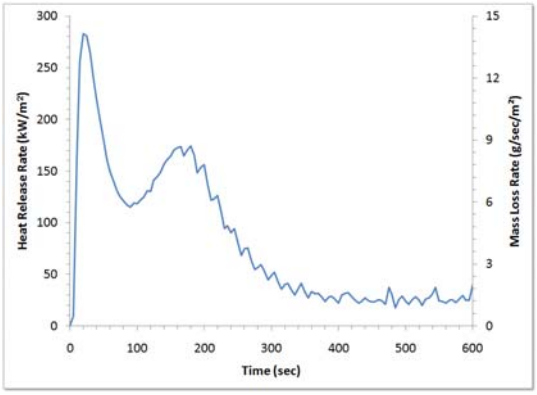

Figure 14-8. Mass Loss Rate for the Carpet Material under a 75 kW/m² Radiant Exposure with a Time Scale Factor of n = 300

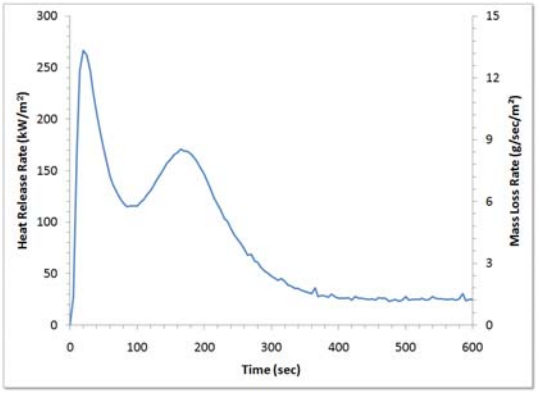

Figure 14-9. Mass Loss Rate for the Carpet Material under a 75 kW/m² Radiant Exposure with a Time Scale Factor of n = 1000

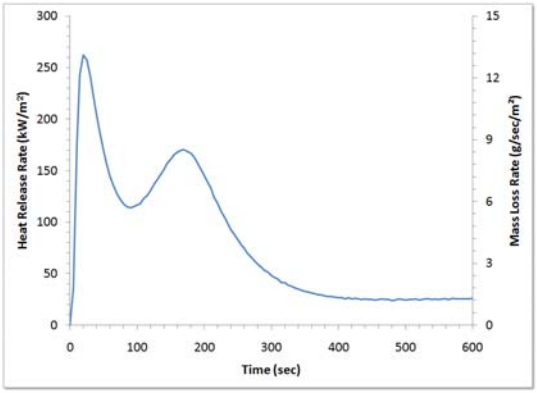

Figure 14-10. Mass Loss Rate for the Carpet Material under a 75 kW/m² Radiant Exposure with a Time Scale Factor of n = 3000

The above figures demonstrate that if the characteristic time scale factor is greater than or equal to 3000, then the instabilities associated with convergence toward spatially steady conditions are well resolved, yielding:

$$\Delta t = \frac{c\Delta T}{3000\, A_0 e^{(-E/RT_{thr})} \Delta H_R} \qquad (14\text{-}56)$$

14.3.2 Critical Cell Size

The rate of mass loss from a layer due to pyrolysis in FDS is a function of temperature, governed by the Arrhenius equation. The following expression of the mass loss rate illustrates the Arrhenius equation as it is implemented in FDS.

$$\dot{m}''' = \eta \rho_0 Y A_0 \exp\left(-\frac{E}{RT}\right) \max\left[0, T - T_{thr}\right]^0 \qquad (14\text{-}57)$$

From the Arrhenius equation, it is apparent that the mass loss rate increases as the temperature of the cell increases in time. Also, the mass loss rate decreases as the fuel mass fraction decreases in time. For the present study, the exponential nt has been set to zero, imposing an inherent discontinuity at the threshold temperature. The combination of these factors contributes to the characteristic shape of the mass loss rate curve.

It was previously documented that increasing the cell size contributes to fluctuations in the mass loss rate curve. It is the contention of the present study that the source of these fluctuations lies in the application of the Arrhenius equation, as opposed to instabilities of the heat equation, with each peak corresponding to the time that a new cell reaches the threshold temperature, and each drop associated with a reduction in the fuel mass fraction.

The assumption that the early fluctuations are caused by the Arrhenius equation is supported by the finding that they cease to exist at the time of the second peak in the mass loss rate curve, or equivalently, when the back surface reaches the threshold temperature. At this time, heat has fully penetrated the depth of the specimen. The following figures illustrate the character of early fluctuations caused by a large cell size.

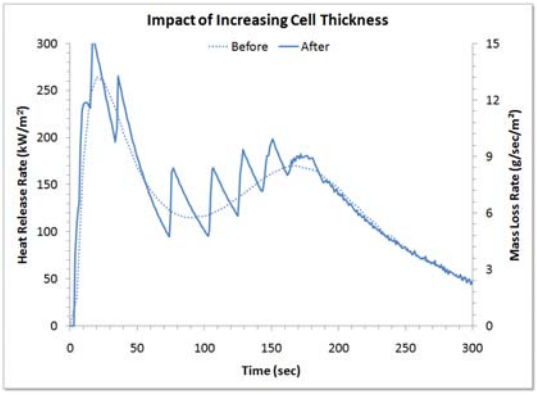

Figure 14-11. Mass Loss Rate Curve for the Carpet Material under a 75 kW/m² Radiant Exposure with a Large Cell Size (View 1)

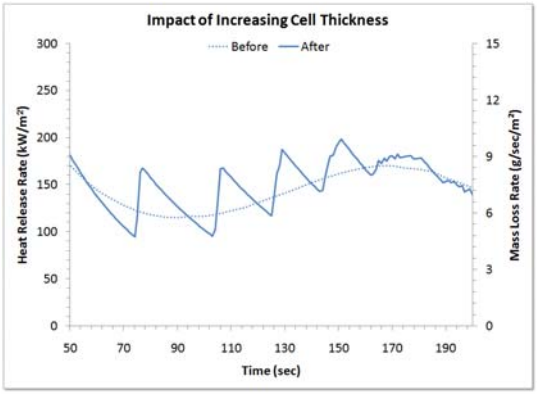

Figure 14-12. Mass Loss Rate Curve for the Carpet Material under a 75 kW/m² Radiant Exposure with a Large Time Step (View 2)

The above figures are for the carpet material with a 75 kW/m² exposure. The time step is 0.1 sec and the cell size factor is 1.0 ($\Delta x = 1200 \mu m$).

The magnitude of the change in mass loss rate for a cell at the threshold temperature is as follows:

$$\dot{m}''_{thr} = \frac{\dot{q}'''_{reac}}{\Delta H_R} \Delta x \qquad (14\text{-}58)$$

where:

$$\dot{q}'''_{reac} = \eta \rho_0 A_0 e^{(-E/RT_{thr})} \Delta H_R \qquad (14\text{-}59)$$

From the above expression, it is clear that in order to decrease the magnitude of the discontinuity in the mass loss rate when a cell reaches the threshold temperature, the cell size must be decreased. The goals of the resolving criteria proposed in the present study are to reduce the magnitude of the fluctuations to a point where their individual contribution is indistinguishable in the overall mass loss rate curve.

To make the contribution of the fluctuations indistinguishable, the cell size must be very small. A characteristic heat penetration depth is calculated from the stability criteria as follows:

$$\Delta x \sim \sqrt{\frac{k\Delta T}{\dot{q}'''_{reac}}} \approx \sqrt{\alpha \Delta t} \tag{14-60}$$

assuming linear scaling,

$$\Delta x = m\sqrt{\alpha \Delta t} \tag{14-61}$$

where m is our characteristic cell size factor. Solving for FDS cell size factor (csf),

$$csf = m\sqrt{\Delta t} \tag{14-62}$$

The following figures illustrate the resolving power of increasing the characteristic cell size factor (m):

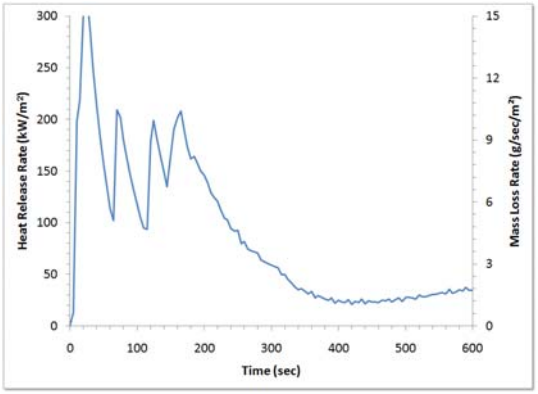

Figure 14-13. Mass Loss Rate for the Carpet Material under a 75 kW/m² Radiant Exposure with a Characteristic Cell Size Factor of m = 4

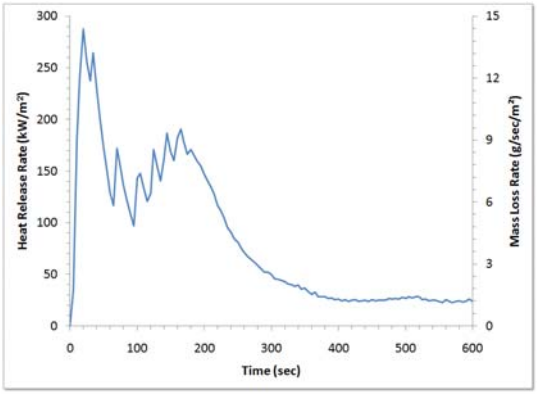

Figure 14-14. Mass Loss Rate for the Carpet Material under a 75 kW/m² Radiant Exposure with a Characteristic Cell Size Factor of m = 2

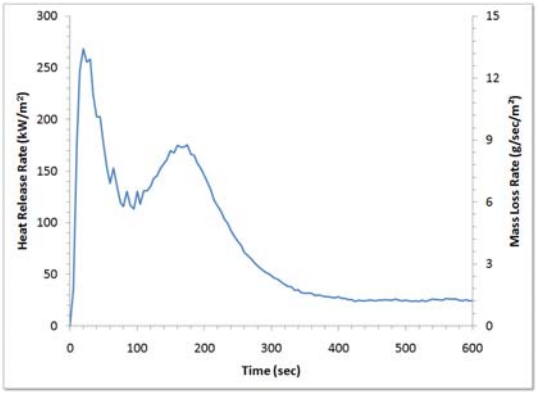

Figure 14-15. Mass Loss Rate for the Carpet Material under a 75 kW/m² Radiant Exposure with a Characteristic Cell Size Factor of m = 1

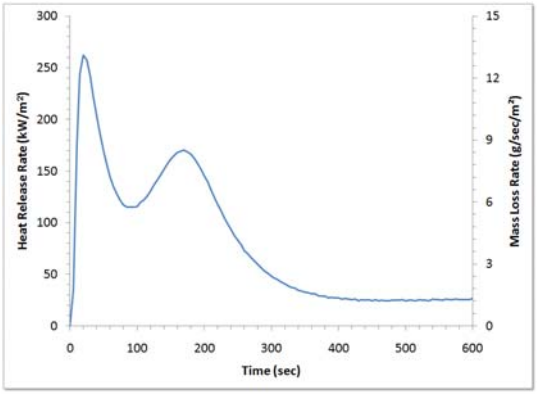

Figure 14-16. Mass Loss Rate for the Carpet Material under a 75 kW/m² Radiant Exposure with a Characteristic Cell Size Factor of m = 0.25

The above figures demonstrate that if the characteristic cell size factor is less than or equal to 0.25, then the inherent fluctuations associated with the characteristics of the Arrhenius equation are well resolved, yielding:

$$\Delta x = 0.25\sqrt{\alpha \Delta t} \tag{14-63}$$

and

$$csf = 0.25\sqrt{\Delta t} \tag{14-64}$$

Chapter 15. Limitations

This chapter is provided to document limitations of the model used in the present study. It should be noted that the limitations of the present study do not necessarily apply to all applications of the FDS program [7].

15.1.1 Mass Diffusion

FDS assumes no mass diffusion, i.e. no mass flow within the solid. Fuel vapors created within the solid are transported directly to the solid surface. This assumption could have a substantial impact on modeling of charring materials. Charring materials can form an outer layer that inhibits the diffusion of fuel vapor, resulting in a critical decay in mass loss rate, even when there is mass yet to pyrolyze.

For materials containing absorbed moisture (i.e. cellulose), or those materials that don't transition directly to fuel vapor from solid (i.e. thermoplastics), thermal effects associated with migration of the fluid within the solid may lead to significant deviation from temperatures calculated on the assumption that heat conduction alone is occurring.

15.1.2 Radiation

Radiation may also be important in these materials. An example where radiation is an important mode of heat transfer within a “solid” is in a low-density porous, smoldering material (i.e. the panel material) or in porous char. The forward transmission of heat, which is necessary for the spread of smoldering combustion, against a thermally

induced gas flow through the porous material occurs almost entirely by radiation across the pores, not by conduction through the solid pore walls.

15.1.3 Unimolecular Reaction Assumption

Although not explicitly stated in the technical manual, FDS uses a unimolecular reaction assumption. This assumption neglects the impact of additional molecules with which the reacting species may collide. The error in this assumption is magnified at low pressures or when a finite volume contains multiple species.

15.1.4 Stability

It was established that the implicit Crank-Nicolson scheme was unconditionally stable. However, it is also true that the approximate solutions can still contain spurious oscillations, another source of numerical instability not addressed in the present study.

Chapter 16. Conclusions

The results of this analysis indicate that the stochastic hill-climber algorithm, HC-PYRO was much better suited to the problem of pyrolysis parameter optimization than the genetic algorithm.

By specifying target parameter values, solution parameter sets were shown to be highly over-specified. By plotting the normalized impact of parameter mutation it was evident that the contributions of many solution set parameters were indistinguishable. Additionally, when parameter sets are not restricted in range, then highly unrealistic parameter values result. The combination of these factors supports the conclusion that the parameter values should not be considered as representative of any physical properties.

Regardless of the accuracy of a single fit mass loss rate curve under a known exposure, extrapolation was shown to produce results with a high degree of error. Experience suggests that competing goals, such as those common in most genetic algorithm applications were strongly biased toward local optimum conditions.

An algorithm was proposed that was resistive against arriving at local optimum conditions. This algorithm utilized a set of non-competing goals in a nested loop configuration. The nested loop algorithm was shown to be highly successful in matching secondary goals without sacrificing the accuracy of the primary goals. Consequently, the nested loop algorithm produced mass loss rate curves which extrapolated well to other exposures, with limitations.

The nested loop algorithm was not capable of predicting the impact of mechanisms whose characteristics were not well defined in the data used for analysis. Such mechanisms include influence of the back boundary, time to extinction, and critical heat flux / ignition temperature.

In cases where the characteristics of critical mechanisms were present in the test data, results indicate that the mass loss rate curves were well representative of test data, and extrapolate with high accuracy.

Chapter 17. Direction for Further Analysis

Based on the results of the stability analysis provided in the present study, more work needs to be done on resolving the quickly changing fuel mass loss rate. This can be accomplished by either changing the heat generation (pyrolysis) source term scheme from an explicit one to an implicit one, or by imposing the condition restricting heat loss to pyrolysis so that a cell cannot drop below the threshold temperature. The standard practice when using the Crank-Nicolson scheme is to integrate all source terms implicitly.

A common tool used in engineering problems where there are too many unknowns is lumped parameter analysis, which doesn't preclude the use of finite elements. Based on this findings of the present study, it appears that the FDS pyrolysis model could be well specified by a small number of measurable quantities and curve fit coefficients. It is suggested that, in the absence of knowledge of the actual mechanisms producing the observed fuel mass loss rate curves, additional studies should be focused on reducing the complexity of the model, rather than increasing it.

However, recent studies by Stoliarov, Lyon, and others [24, 25] suggest that several parameters used in comprehensive models (i.e. fuel yield, heat of reaction, etc.) can be derived from molecular structure. If future studies in this area support the claims of Stoliarov and Lyon, then there many be limited need for parameter optimization.

Appendix A. Model Input Syntax

In FDS, a solid object might contain multiple layers with multiple material components per layer. The solid object is described by a SURF line which contains the names of the various MATLs it is composed of. Each MATL can undergo several reactions that may occur at different temperatures and consume different amounts of heat. Each individual reaction can produce a solid RESIDUE, water vapor, and/or fuel gas. The following lines illustrate the FDS syntax for describing surfaces, layers, materials, and reactions.

```
&SURF ID='MY SURF'                          / Surface ID
      MATL_ID(1,1:2) = 'MATL A','MATL B'    / Materials in Layer 1
      MATL_MASS_FRACTION(1,1:2) = 0.70,0.3  / Mass Fractions of MATLs
      MATL_ID(2,1) = 'MATL C'               / Materials in Layer 2
      THICKNESS(1:2) = 0.01,0.01            / Thicknesses of Layers

&MATL ID = 'MATL A'                         / Material ID
      N_REACTIONS = 2                       / Number of Reactions
      A(1:2) = 1.3E10, 3.23E14              / Pre-Exponential Factors
      E(1:2) = 1.505E5, 1.965E5             / Activation Energy
      NU_RESIDUE(1:2) = 0.35, 0.0           / Residue Yields
      RESIDUE(1:2) = 'MATL D','MATL E'      / Residue MATLs
      N_S(1) = 1.0                          / Mass fraction exponent
      THRESHOLD_TEMPERATURE(1) = 273.15     / Threshold temperature
      N_T(1) = 0                            / Temperature exponent
```

FDS Input Limitations

There are a maximum of 20 solid phase reactions permitted in each FDS input file. There are a maximum of 10 solid reactions permitted per material. Each reaction can produce a maximum of 1 residue. There is a maximum of 1 combustion reaction permitted per FDS input file.

Sample FDS Input File

```
&HEAD CHID='carpet' TITLE='Iterations for carpet Parameters' /
&MESH IJK=3 3 4 XB=-0.15 0.15 -0.15 0.15 0.0 0.4 /
&MESH IJK=3 3 4 XB=-0.15 0.15 -0.15 0.15 1.0 1.4 /
&MESH IJK=3 3 4 XB=-0.15 0.15 -0.15 0.15 2.0 2.4 /
&MESH IJK=3 3 4 XB=-0.15 0.15 -0.15 0.15 3.0 3.4 /
&MESH IJK=3 3 4 XB=-0.15 0.15 -0.15 0.15 4.0 4.4 /
&MESH IJK=3 3 4 XB=-0.15 0.15 -0.15 0.15 5.0 5.4 /
&TIME T_END=600 WALL_INCREMENT=1 DT=1.00E-01 /
&MISC SOLID_PHASE_ONLY=.TRUE. /
&MATL ID='Virgin_1' DENSITY=4.51E+02 SPECIFIC_HEAT=6.04E-01
      CONDUCTIVITY=5.12E-01 EMISSIVITY=8.42E-01 N_REACTIONS=1
      RESIDUE='Residue_1' HEAT_OF_REACTION=1.09E+02 NU_FUEL=4.93E-01
      NU_RESIDUE=5.07E-01 THRESHOLD_TEMPERATURE=3.64E+02 A=6.69E+09
      E=1.40E+05 /
&MATL ID='Residue_1' DENSITY=5.28E+03 SPECIFIC_HEAT=4.24E+01
      CONDUCTIVITY=1.06E-01 EMISSIVITY=9.74E-01 /
&SURF ID='carpet_25' MATL_ID='Virgin_1' EXTERNAL_FLUX=25.
      THICKNESS=1.73E-02 BACKING='INSULATED' STRETCH_FACTOR=1.
      CELL_SIZE_FACTOR=1.00E-01 /
&SURF ID='carpet_35' MATL_ID='Virgin_1' EXTERNAL_FLUX=35.
      THICKNESS=1.73E-02 BACKING='INSULATED' STRETCH_FACTOR=1.
      CELL_SIZE_FACTOR=1.00E-01 /
&SURF ID='carpet_40' MATL_ID='Virgin_1' EXTERNAL_FLUX=40.
      THICKNESS=1.73E-02 BACKING='INSULATED' STRETCH_FACTOR=1.
      CELL_SIZE_FACTOR=1.00E-01 /
&SURF ID='carpet_50' MATL_ID='Virgin_1' EXTERNAL_FLUX=50.
      THICKNESS=1.73E-02 BACKING='INSULATED' STRETCH_FACTOR=1.
      CELL_SIZE_FACTOR=1.00E-01 /
&SURF ID='carpet_60' MATL_ID='Virgin_1' EXTERNAL_FLUX=60.
      THICKNESS=1.73E-02 BACKING='INSULATED' STRETCH_FACTOR=1.
      CELL_SIZE_FACTOR=1.00E-01 /
&SURF ID='carpet_75' MATL_ID='Virgin_1' EXTERNAL_FLUX=75.
      THICKNESS=1.73E-02 BACKING='INSULATED' STRETCH_FACTOR=1.
      CELL_SIZE_FACTOR=1.00E-01 /
&VENT XB=-0.05 0.05 -0.05 0.05 0.0 0.0 SURF_ID='carpet_25' /
&VENT XB=-0.05 0.05 -0.05 0.05 1.0 1.0 SURF_ID='carpet_35' /
&VENT XB=-0.05 0.05 -0.05 0.05 2.0 2.0 SURF_ID='carpet_40' /
&VENT XB=-0.05 0.05 -0.05 0.05 3.0 3.0 SURF_ID='carpet_50' /
&VENT XB=-0.05 0.05 -0.05 0.05 4.0 4.0 SURF_ID='carpet_60' /
&VENT XB=-0.05 0.05 -0.05 0.05 5.0 5.0 SURF_ID='carpet_75' /
&VENT MB='XMIN' SURF_ID='OPEN' /
&VENT MB='XMAX' SURF_ID='OPEN' /
&VENT MB='YMIN' SURF_ID='OPEN' /
&VENT MB='YMAX' SURF_ID='OPEN' /
&VENT MB='ZMAX' SURF_ID='OPEN' /
&DUMP NFRAMES=0 DT_DEVC=5.0 SMOKE3D=.FALSE. MASS_FILE=.FALSE.
      DT_PL3D=100000. /
&DEVC XYZ=0.0 0.0 0.0 IOR=3 QUANTITY='BURNING_RATE' ID='25 kW/m2' /
&DEVC XYZ=0.0 0.0 1.0 IOR=3 QUANTITY='BURNING_RATE' ID='35 kW/m2' /
&DEVC XYZ=0.0 0.0 2.0 IOR=3 QUANTITY='BURNING_RATE' ID='40 kW/m2' /
&DEVC XYZ=0.0 0.0 3.0 IOR=3 QUANTITY='BURNING_RATE' ID='50 kW/m2' /
&DEVC XYZ=0.0 0.0 4.0 IOR=3 QUANTITY='BURNING_RATE' ID='60 kW/m2' /
&DEVC XYZ=0.0 0.0 5.0 IOR=3 QUANTITY='BURNING_RATE' ID='75 kW/m2' /
&TAIL /
```

Appendix B. HC-PYRO Source Code

```
;;; Main Routine

(defun c:hc ()
  (vl-load-com)
  (initialize)
;;;   Skip if already fit
  (fit_1st)
;;;
  (get_2nd)
  (accept)
  (repeat 1000
    (set_random_target)
    (fit_1st)
    (get_2nd)
;;; if not targeting
    (if (> nr1 pr1)
      (accept)
      (reject)
    )
;;;
;;; if targeting
;;;    (accept)
;;;
  )
  (princ)
)

(defun write_batch_file       ()
  (setq file (strcat "C:\\HC-PYRO\\RUN_FDS.bat"))
  (setq filew (open file "w"))
  (write-line "cd\\" filew)
  (write-line "cd C:\\HC-PYRO" filew)
  (write-line
    (strcat
      "start \"FDS\" /B /LOW /WAIT "
      "\"C:\\Program Files\\FDS\\FDS5\\bin\\fds5.exe\""
      " \"C:\\HC-PYRO\\"
      matl
      ".fds\""
     )
    filew
  )
  (close filew)
)

;;; Initialize Parameters

(defun initialize ()
  (setvar "cmdecho" 0)
  (setvar "osmode" 16635)
  (setq co 0)
  (setq matl "Carpet")
  (write_batch_file)
  (setq t_end 600)
  (setq dt_devc 5.0)
  (setq fluxes '(25 35 40 50 60 75))
  (setq goal1 '(6 5 4 3 2 1))
  (setq goal2 '(6 5 4 3 2 1))
  (setq parameter_set
        (list "rho1"  "cp1"    "k1"     "emi1"   "hor"    "nu"     "temp"
              "rr"    "drr"    "rho2"   "cp2"    "k2"     "emi2"   "thk"
```

```
            )
  )
;;; wall with one goal
;;;   (setq initial_set
;;;           (list 7.878E+02     5.028E-01     4.076E-01     5.058E-01
;;;                 4.036E+01     4.173E-01     3.804E+02     2.187E-02
;;;                 1.000E-04     6.310E+02     1.615E+01     5.609E-02
;;;                 9.898E+00     1.619E-02
;;;                )
;;;   )
;;; panel with non-competing goals
;;;  (setq     initial_set
;;;     (list 4.008E+02     1.640E+00          7.047E-01    9.010E-01
;;;           1.517E+03     3.747E-01          3.825E+02    4.482E-02
;;;           1.430E-03     4.257E+03          3.735E-01    6.433E-02
;;;           4.054E-01     4.886E-03
;;;          )
;;;  )
;;; carpet with competing goals
;;;  (setq     initial_set
;;;     (list 4.187E+02     6.121E-01          3.426E-01    9.443E-01
;;;           1.946E+02     3.817E-01          4.059E+02    1.872E-02
;;;           1.180E-03     5.622E+02          7.751E+00    1.115E-01
;;;           1.837E+00     1.558E-02
;;;          )
;;;  )
;;; carpet with non-competing goals
  (setq initial_set
        (list 5.246E+02     5.086E-01          3.789E-01    1.259E+00
              4.198E+01     4.369E-01          4.041E+02    1.907E-02
              1.300E-04     5.364E+02          1.165E+01    4.981E-02
              1.995E-01     1.521E-02
             )
  )
;;; wall with non-competing goals
;;;   (setq initial_set
;;;           (list 2.720E+02     6.566E-01     5.434E-01     1.027E+00
;;;                 9.363E+02     9.863E-01     5.902E+02     7.421E-02
;;;                 1.500E-04     7.649E+02     6.576E-02     8.649E-02
;;;                 2.022E+00     9.784E-03
;;;                )
;;;   )
;;; wall with one goal - low flux
;;;   (setq initial_set
;;;           (list 3.210E+02     8.327E-01     2.980E+00     9.848E-01
;;;                 6.938E+02     9.592E-01     5.740E+02     6.089E-02
;;;                 1.600E-04     6.056E+02     1.109E-02     1.331E-01
;;;                 1.515E+00     1.571E-02
;;;                )
;;;   )
;;; carpet with one goal, several targets
;;;   (setq initial_set
;;;           (list 4.500E+02     1.342E+00     1.209E-01     9.000E-01
;;;                 2.126E+02     9.000E-01     4.000E+02     1.127E-02
;;;                 1.100E-04     4.217E+01     2.900E+02     4.427E-02
;;;                 1.261E+01     6.000E-03
;;;                )
;;;   )
;;;   panel temp
;;;   (setq initial_set
;;;           (list 2.452E+02     1.035E+00     9.428E-01     6.484E-01
;;;                 1.431E+03     6.677E-01     5.766E+02     2.324E-01
;;;                 5.186E-04     1.610E+03     8.144E-01     7.976E-02
;;;                 4.146E-01     5.422E-03
;;;                )
;;;   )
;;; panel demo start point
;;;  (setq     initial_set
;;;     (list 4.008E+02     1.640E+00          7.047E-01    9.010E-01
;;;           1.517E+03     2.000E-01          3.825E+02    4.482E-02
;;;           1.430E-03     4.257E+03          3.735E-01    6.433E-02
```

```
;;;           4.054E-01     4.886E-03
;;;          )
;;;  )
;;; carpet with one goal
;;;  (setq     initial_set
;;;     (list 5.294E+02     4.205E-01          4.087E-01    8.509E-01
;;;           6.965E+01     4.318E-01          4.374E+02    2.619E-02
;;;           6.913E-04     3.697E+03          3.911E+01    1.285E-01
;;;           1.760E+00     1.619E-02
;;;          )
;;;  )
;;;  carpet material, target thickness
;;;  (setq     initial_set
;;;     (list 8.332E+02     7.286E-01          1.693E-01    8.509E-01
;;;           4.366E+01     6.560E-01          3.293E+02    2.107E-02
;;;           1.167E-04     2.565E+02          4.110E-01    2.167E-03
;;;           1.994E-01     6.000E-03
;;;          )
;;;  )
  (mapcar '(lambda (x1 x2) (set (read x1) x2))
          parameter_set
          initial_set
  )
  (foreach a parameter_set
    (set (read (strcat "t" a)) nil)
    (set (read (strcat "n" a)) (eval (read a)))
    (set (read (strcat "p" a)) 0.0)
  )
;;; carpet
  (setq cone_data (list       3.67E-05     1.27E-04    9.78E-05     3.37E-04
                      1.62E-04     6.32E-05    6.59E-05     1.80E-04
                      6.37E-05     5.76E-04    3.52E-04     1.37E-04
                      1.08E-04     2.48E-04    1.31E-04     4.06E-04
                      2.72E-03     5.04E-03    4.63E-05     2.75E-04
                      1.58E-04     4.53E-03    9.98E-03     1.28E-02
                      0.00E+00     3.24E-04    3.88E-04     9.14E-03
                      1.19E-02     1.45E-02    0.00E+00     4.18E-03
                      5.10E-03     1.02E-02    1.11E-02     1.26E-02
                      2.50E-05     6.54E-03    7.82E-03     9.18E-03
                      9.88E-03     1.08E-02    9.76E-05     7.18E-03
                      7.57E-03     8.09E-03    8.97E-03     1.01E-02
                      1.11E-04     6.70E-03    7.46E-03     7.27E-03
                      8.12E-03     8.94E-03    2.66E-04     5.96E-03
                      6.70E-03     6.67E-03    7.41E-03     8.52E-03
                      3.02E-03     5.60E-03    5.86E-03     6.03E-03
                      6.76E-03     7.85E-03    5.14E-03     5.22E-03
                      5.42E-03     5.63E-03    6.26E-03     7.64E-03
                      4.67E-03     4.86E-03    4.95E-03     5.25E-03
                      5.90E-03     6.70E-03    4.01E-03     4.34E-03
                      4.74E-03     5.16E-03    5.42E-03     6.59E-03
                      3.27E-03     4.02E-03    4.32E-03     4.91E-03
                      5.26E-03     6.24E-03    2.60E-03     3.68E-03
                      4.12E-03     4.50E-03    4.98E-03     6.09E-03
                      2.17E-03     3.54E-03    3.81E-03     4.23E-03
                      4.79E-03     5.89E-03    1.98E-03     3.30E-03
                      3.73E-03     4.37E-03    4.67E-03     5.89E-03
                      1.74E-03     3.00E-03    3.42E-03     4.08E-03
                      4.71E-03     5.49E-03    1.56E-03     2.79E-03
                      3.15E-03     3.96E-03    4.62E-03     5.90E-03
                      1.31E-03     2.53E-03    2.88E-03     3.36E-03
                      4.64E-03     6.43E-03    1.10E-03     2.36E-03
                      2.55E-03     3.44E-03    5.13E-03     7.08E-03
                      9.12E-04     2.16E-03    2.40E-03     3.72E-03
                      5.44E-03     7.44E-03    7.97E-04     2.02E-03
                      2.35E-03     3.67E-03    5.76E-03     7.60E-03
                      7.29E-04     1.84E-03    2.26E-03     3.85E-03
                      5.78E-03     7.78E-03    5.83E-04     1.81E-03
                      2.21E-03     3.64E-03    5.79E-03     7.71E-03
                      6.56E-04     1.81E-03    2.44E-03     3.97E-03
                      5.85E-03     7.87E-03    5.38E-04     1.82E-03
                      2.76E-03     4.32E-03    5.98E-03     7.89E-03
```

4.70E-04	1.92E-03	3.23E-03	4.47E-03
6.25E-03	7.72E-03	3.65E-04	1.89E-03
3.58E-03	4.64E-03	6.11E-03	7.56E-03
3.55E-04	2.21E-03	3.69E-03	4.75E-03
6.22E-03	7.56E-03	4.35E-04	2.25E-03
3.82E-03	4.87E-03	6.25E-03	7.51E-03
3.39E-04	2.39E-03	3.71E-03	4.74E-03
6.24E-03	7.41E-03	3.40E-04	2.62E-03
3.67E-03	4.69E-03	6.00E-03	7.43E-03
3.16E-04	2.99E-03	3.67E-03	4.83E-03
5.94E-03	7.27E-03	5.40E-04	3.29E-03
3.87E-03	5.10E-03	5.94E-03	7.20E-03
5.88E-04	3.68E-03	3.76E-03	5.52E-03
6.02E-03	7.21E-03	5.04E-04	3.81E-03
4.17E-03	5.49E-03	6.07E-03	7.10E-03
4.63E-04	3.87E-03	3.99E-03	5.61E-03
5.93E-03	7.01E-03	3.87E-04	3.91E-03
3.97E-03	5.91E-03	6.17E-03	6.98E-03
4.44E-04	4.05E-03	4.01E-03	5.80E-03
6.32E-03	6.83E-03	3.45E-04	4.10E-03
3.93E-03	5.72E-03	6.39E-03	6.50E-03
3.14E-04	3.97E-03	3.86E-03	5.52E-03
6.46E-03	6.32E-03	3.06E-04	4.09E-03
3.89E-03	5.56E-03	6.87E-03	6.01E-03
3.66E-04	3.87E-03	3.94E-03	5.65E-03
6.91E-03	5.57E-03	3.41E-04	3.73E-03
3.93E-03	5.46E-03	6.97E-03	4.99E-03
3.39E-04	3.70E-03	3.93E-03	5.85E-03
6.63E-03	4.64E-03	3.67E-04	3.66E-03
3.91E-03	5.68E-03	6.55E-03	4.31E-03
3.45E-04	3.57E-03	4.02E-03	6.10E-03
6.46E-03	3.78E-03	4.10E-04	3.56E-03
3.99E-03	6.21E-03	6.29E-03	3.49E-03
4.76E-04	3.52E-03	4.06E-03	6.36E-03
5.92E-03	3.19E-03	4.67E-04	3.43E-03
4.23E-03	6.40E-03	5.32E-03	3.04E-03
4.97E-04	3.29E-03	4.26E-03	6.52E-03
5.10E-03	2.93E-03	6.18E-04	3.32E-03
4.23E-03	6.44E-03	4.58E-03	2.76E-03
6.21E-04	3.31E-03	4.20E-03	6.40E-03
4.00E-03	2.68E-03	6.89E-04	3.35E-03
4.25E-03	6.24E-03	3.71E-03	2.64E-03
5.83E-04	3.25E-03	4.12E-03	6.13E-03
3.21E-03	2.44E-03	7.12E-04	3.34E-03
4.16E-03	5.70E-03	2.90E-03	2.33E-03
7.44E-04	3.25E-03	4.25E-03	5.38E-03
2.80E-03	2.29E-03	8.87E-04	3.28E-03
4.29E-03	5.01E-03	2.72E-03	2.27E-03
9.48E-04	3.33E-03	4.17E-03	4.55E-03
2.51E-03	2.10E-03	1.05E-03	3.33E-03
3.91E-03	3.96E-03	2.43E-03	2.18E-03
1.02E-03	3.38E-03	3.91E-03	3.70E-03
2.27E-03	2.10E-03	1.04E-03	3.45E-03
3.59E-03	3.25E-03	2.07E-03	1.99E-03
1.09E-03	3.54E-03	3.82E-03	3.03E-03
1.93E-03	1.87E-03	1.20E-03	3.59E-03
3.79E-03	2.85E-03	1.93E-03	1.85E-03
1.24E-03	3.54E-03	3.72E-03	2.59E-03
1.83E-03	1.82E-03	1.37E-03	3.85E-03
3.63E-03	2.74E-03	1.78E-03	1.72E-03
1.45E-03	3.55E-03	3.49E-03	2.62E-03
1.65E-03	1.74E-03	1.43E-03	3.56E-03
3.48E-03	2.20E-03	1.58E-03	1.77E-03
1.50E-03	3.68E-03	3.47E-03	1.96E-03
1.61E-03	1.65E-03	1.36E-03	3.64E-03
3.18E-03	2.14E-03	1.57E-03	1.59E-03
1.14E-03	3.54E-03	3.35E-03	1.76E-03
1.59E-03	1.58E-03	9.39E-04	3.66E-03
3.22E-03	1.82E-03	1.61E-03	1.56E-03
8.57E-04	3.66E-03	3.21E-03	1.74E-03
1.50E-03	1.54E-03	8.27E-04	3.74E-03

```
                    2.93E-03    1.66E-03    1.53E-03    1.54E-03
                    9.61E-04    3.62E-03    2.71E-03    1.88E-03
                    1.51E-03    1.56E-03    1.07E-03    3.67E-03
                    2.56E-03    1.63E-03    1.55E-03    1.47E-03
                    1.14E-03    3.61E-03    2.40E-03    1.56E-03
                    1.51E-03    1.54E-03    1.21E-03    3.59E-03
                    2.20E-03    1.50E-03    1.39E-03    1.51E-03
                    1.19E-03    3.60E-03    2.02E-03    1.97E-03
                    1.44E-03    1.60E-03    1.10E-03    3.49E-03
                    1.93E-03    1.52E-03    1.50E-03    1.44E-03
                    1.08E-03    3.52E-03    1.90E-03    1.73E-03
                    1.43E-03    1.38E-03    1.03E-03    3.41E-03
                    1.78E-03    1.67E-03    1.41E-03    1.54E-03
                    1.12E-03    3.24E-03    1.79E-03    1.67E-03
                    1.40E-03    1.56E-03    1.19E-03    3.17E-03
                    1.69E-03    1.80E-03    1.35E-03    1.57E-03
                    1.20E-03    3.20E-03    1.63E-03    1.59E-03
                    1.39E-03    1.57E-03    1.22E-03    3.23E-03
                    1.59E-03    1.62E-03    1.47E-03    1.59E-03
                    1.28E-03    3.17E-03    1.63E-03    1.54E-03
                    1.44E-03    1.61E-03    1.40E-03    3.05E-03
                    1.57E-03    1.67E-03    1.36E-03    1.55E-03
                    1.48E-03    3.02E-03    1.51E-03    1.62E-03
                    1.29E-03    1.54E-03    1.56E-03    2.96E-03
                    1.51E-03    1.55E-03    1.33E-03    1.60E-03
                    1.62E-03    2.83E-03    1.39E-03    1.42E-03
                    1.36E-03    1.68E-03    1.48E-03    2.68E-03
                    1.41E-03    1.40E-03    1.27E-03    1.60E-03
                    1.46E-03    2.70E-03    1.38E-03    1.41E-03
                    1.28E-03    1.51E-03    1.37E-03    2.50E-03
                    1.30E-03    1.55E-03    1.35E-03    1.44E-03
                    1.42E-03    2.40E-03    1.39E-03    1.51E-03
                    1.29E-03    1.37E-03    1.51E-03    2.42E-03
                    1.35E-03    1.16E-03    1.30E-03    1.40E-03
                    1.56E-03    2.25E-03    1.27E-03    1.31E-03
                    1.31E-03    1.43E-03    1.59E-03    2.12E-03
                    1.29E-03    1.62E-03    1.35E-03    1.62E-03
                    1.55E-03    2.02E-03    1.22E-03    1.32E-03
                    1.31E-03    1.41E-03    1.59E-03    1.94E-03
                    1.18E-03    1.87E-03    1.32E-03    1.62E-03
                    1.54E-03    1.86E-03    1.40E-03    1.55E-03
                    1.31E-03    1.45E-03    1.59E-03    1.81E-03
                    1.22E-03    1.48E-03    1.33E-03    1.38E-03
                    1.55E-03    1.74E-03    1.14E-03    1.38E-03
                    1.24E-03    1.35E-03    1.44E-03    1.65E-03
                    1.16E-03    1.51E-03    1.26E-03    1.37E-03
                    1.43E-03    1.65E-03    1.09E-03    1.35E-03
                    1.23E-03    1.28E-03    1.42E-03    1.64E-03
                    1.16E-03    1.20E-03    1.21E-03    1.36E-03
                    1.45E-03    1.56E-03    1.15E-03    1.32E-03
                    1.11E-03    1.31E-03    1.35E-03    1.53E-03
                    1.18E-03    1.43E-03    1.17E-03    1.38E-03
                    1.29E-03    1.56E-03    1.15E-03    1.40E-03
                    1.21E-03    1.39E-03    1.35E-03    1.48E-03
                    1.17E-03    1.26E-03    1.23E-03    1.26E-03
                    9.90E-04    1.31E-03    1.18E-03    1.36E-03
                    1.26E-03    1.23E-03    1.16E-03    1.20E-03
                    1.11E-03    1.22E-03    1.20E-03    1.24E-03
                    1.19E-03    1.19E-03    1.17E-03    1.17E-03
                    1.29E-03    1.21E-03    1.20E-03    1.18E-03
                    1.09E-03    1.37E-03    1.23E-03    1.26E-03
                    1.18E-03    1.17E-03    1.04E-03    1.29E-03
                    1.18E-03    1.23E-03    1.14E-03    1.22E-03
                    1.15E-03    1.06E-03    1.18E-03    1.18E-03
                    1.07E-03    1.14E-03    1.13E-03    1.19E-03
                    1.17E-03    1.14E-03    1.16E-03    1.25E-03
                    1.11E-03    1.22E-03    1.17E-03    1.20E-03
                    1.05E-03    1.24E-03    1.10E-03    1.30E-03
                    1.15E-03    1.20E-03
                   )
)
```

```
;;; wall
;;;  (setq     cone_data (list        0.00E+00     0.00E+00    0.00E+00     1.61E-04
;;;                      3.31E-04     0.00E+00    0.00E+00     3.33E-05
;;;                      0.00E+00     1.14E-05    3.98E-04     3.32E-04
;;;                      0.00E+00     4.09E-05    3.90E-05     0.00E+00
;;;                      2.06E-04     4.42E-04    0.00E+00     4.44E-05
;;;                      0.00E+00     1.29E-04    1.88E-05     3.80E-03
;;;                      0.00E+00     3.27E-05    0.00E+00     4.59E-05
;;;                      1.65E-04     1.22E-02    4.48E-06     7.02E-05
;;;                      0.00E+00     5.29E-05    3.34E-03     1.97E-02
;;;                      4.39E-06     0.00E+00    0.00E+00     7.19E-05
;;;                      8.43E-03     2.39E-02    0.00E+00     0.00E+00
;;;                      0.00E+00     0.00E+00    1.28E-02     2.39E-02
;;;                      0.00E+00     0.00E+00    0.00E+00     0.00E+00
;;;                      1.80E-02     2.21E-02    0.00E+00     0.00E+00
;;;                      0.00E+00     0.00E+00    2.00E-02     2.22E-02
;;;                      6.63E-05     0.00E+00    0.00E+00     7.10E-05
;;;                      2.03E-02     2.12E-02    0.00E+00     0.00E+00
;;;                      1.21E-04     0.00E+00    1.97E-02     1.90E-02
;;;                      0.00E+00     0.00E+00    1.25E-04     0.00E+00
;;;                      1.85E-02     1.86E-02    0.00E+00     0.00E+00
;;;                      0.00E+00     0.00E+00    1.84E-02     1.92E-02
;;;                      0.00E+00     0.00E+00    0.00E+00     0.00E+00
;;;                      1.89E-02     1.95E-02    0.00E+00     0.00E+00
;;;                      0.00E+00     0.00E+00    1.82E-02     2.01E-02
;;;                      0.00E+00     0.00E+00    0.00E+00     0.00E+00
;;;                      1.81E-02     1.92E-02    0.00E+00     0.00E+00
;;;                      0.00E+00     0.00E+00    1.73E-02     1.76E-02
;;;                      0.00E+00     0.00E+00    0.00E+00     2.54E-05
;;;                      1.65E-02     1.48E-02    3.46E-05     0.00E+00
;;;                      5.57E-05     1.76E-03    1.46E-02     1.19E-02
;;;                      0.00E+00     0.00E+00    0.00E+00     3.27E-03
;;;                      1.30E-02     9.72E-03    0.00E+00     0.00E+00
;;;                      0.00E+00     5.57E-03    1.16E-02     7.34E-03
;;;                      1.32E-04     6.03E-05    0.00E+00     8.12E-03
;;;                      9.96E-03     6.03E-03    9.26E-05     0.00E+00
;;;                      0.00E+00     9.55E-03    9.52E-03     5.25E-03
;;;                      1.07E-04     0.00E+00    5.27E-04     9.52E-03
;;;                      7.24E-03     4.59E-03    0.00E+00     0.00E+00
;;;                      2.13E-03     8.43E-03    6.32E-03     4.13E-03
;;;                      0.00E+00     0.00E+00    4.18E-03     7.30E-03
;;;                      5.11E-03     4.03E-03    0.00E+00     0.00E+00
;;;                      6.17E-03     6.95E-03    4.84E-03     3.99E-03
;;;                      0.00E+00     0.00E+00    7.07E-03     7.05E-03
;;;                      4.45E-03     3.91E-03    0.00E+00     0.00E+00
;;;                      7.03E-03     7.48E-03    4.15E-03     3.90E-03
;;;                      0.00E+00     0.00E+00    6.28E-03     8.18E-03
;;;                      3.72E-03     3.93E-03    0.00E+00     0.00E+00
;;;                      5.68E-03     8.72E-03    3.99E-03     3.68E-03
;;;                      0.00E+00     0.00E+00    5.37E-03     9.40E-03
;;;                      3.70E-03     4.63E-03    0.00E+00     5.05E-05
;;;                      5.27E-03     9.94E-03    3.47E-03     3.61E-03
;;;                      0.00E+00     1.82E-03    5.43E-03     1.07E-02
;;;                      3.17E-03     3.36E-03    0.00E+00     2.47E-03
;;;                      5.62E-03     1.17E-02    2.95E-03     3.21E-03
;;;                      0.00E+00     2.43E-03    5.93E-03     1.24E-02
;;;                      2.97E-03     3.18E-03    0.00E+00     2.12E-03
;;;                      6.45E-03     1.21E-02    3.01E-03     2.88E-03
;;;                      0.00E+00     1.79E-03    7.01E-03     1.18E-02
;;;                      3.10E-03     2.81E-03    0.00E+00     1.55E-03
;;;                      7.75E-03     1.13E-02    3.00E-03     2.79E-03
;;;                      0.00E+00     1.99E-03    8.43E-03     1.08E-02
;;;                      2.97E-03     2.85E-03    0.00E+00     3.10E-03
;;;                      9.33E-03     1.03E-02    2.98E-03     3.09E-03
;;;                      0.00E+00     3.73E-03    1.01E-02     9.64E-03
;;;                      2.94E-03     3.26E-03    0.00E+00     3.67E-03
;;;                      9.98E-03     9.27E-03    2.78E-03     3.15E-03
;;;                      0.00E+00     3.55E-03    9.66E-03     8.75E-03
;;;                      2.55E-03     3.22E-03    0.00E+00     3.35E-03
;;;                      9.46E-03     8.21E-03    2.56E-03     3.11E-03
;;;                      0.00E+00     3.39E-03    9.00E-03     8.08E-03
```

```
;;;                     2.33E-03     3.11E-03    0.00E+00     3.48E-03
;;;                     8.64E-03     7.72E-03    2.41E-03     3.18E-03
;;;                     0.00E+00     3.51E-03    8.09E-03     7.39E-03
;;;                     2.35E-03     3.02E-03    0.00E+00     3.27E-03
;;;                     7.64E-03     6.87E-03    2.51E-03     3.01E-03
;;;                     0.00E+00     2.95E-03    7.47E-03     6.58E-03
;;;                     2.25E-03     2.92E-03    0.00E+00     2.78E-03
;;;                     7.02E-03     6.49E-03    2.27E-03     2.85E-03
;;;                     0.00E+00     2.66E-03    6.59E-03     6.22E-03
;;;                     2.35E-03     2.80E-03    0.00E+00     2.42E-03
;;;                     6.17E-03     6.00E-03    2.31E-03     2.89E-03
;;;                     0.00E+00     2.20E-03    5.83E-03     5.62E-03
;;;                     2.07E-03     2.95E-03    0.00E+00     2.20E-03
;;;                     5.60E-03     5.32E-03    2.18E-03     2.95E-03
;;;                     0.00E+00     2.10E-03    5.42E-03     5.23E-03
;;;                     2.30E-03     2.73E-03    0.00E+00     1.93E-03
;;;                     5.35E-03     4.96E-03    2.11E-03     2.66E-03
;;;                     0.00E+00     1.98E-03    5.04E-03     4.79E-03
;;;                     2.29E-03     2.70E-03    1.24E-05     2.01E-03
;;;                     4.73E-03     4.72E-03    2.31E-03     2.69E-03
;;;                     8.84E-05     1.87E-03    4.28E-03     4.80E-03
;;;                     2.25E-03     2.54E-03
;;;                    )
;;;  )
;;; panel
;;;  (setq     cone_data (list        0.00E+00     0.00E+00    0.00E+00     8.09E-05
;;;                     2.09E-04     9.64E-05    0.00E+00     0.00E+00
;;;                     0.00E+00     9.84E-05    1.93E-04     7.61E-05
;;;                     0.00E+00     0.00E+00    0.00E+00     1.90E-04
;;;                     1.00E-04     6.51E-05    0.00E+00     0.00E+00
;;;                     0.00E+00     1.90E-04    1.08E-04     2.59E-04
;;;                     0.00E+00     0.00E+00    0.00E+00     2.12E-04
;;;                     2.68E-04     1.98E-03    0.00E+00     0.00E+00
;;;                     0.00E+00     2.81E-04    3.94E-03     8.58E-03
;;;                     0.00E+00     0.00E+00    0.00E+00     8.04E-04
;;;                     7.04E-03     1.07E-02    0.00E+00     0.00E+00
;;;                     0.00E+00     3.45E-03    8.35E-03     8.80E-03
;;;                     0.00E+00     0.00E+00    0.00E+00     5.07E-03
;;;                     7.00E-03     6.40E-03    0.00E+00     0.00E+00
;;;                     0.00E+00     4.69E-03    5.12E-03     4.63E-03
;;;                     0.00E+00     0.00E+00    0.00E+00     3.91E-03
;;;                     4.02E-03     4.00E-03    0.00E+00     0.00E+00
;;;                     0.00E+00     2.98E-03    3.63E-03     3.96E-03
;;;                     0.00E+00     0.00E+00    0.00E+00     2.36E-03
;;;                     3.32E-03     3.99E-03    0.00E+00     0.00E+00
;;;                     0.00E+00     1.99E-03    3.23E-03     4.01E-03
;;;                     0.00E+00     0.00E+00    0.00E+00     1.84E-03
;;;                     3.11E-03     3.75E-03    0.00E+00     0.00E+00
;;;                     0.00E+00     1.73E-03    2.93E-03     3.49E-03
;;;                     0.00E+00     0.00E+00    0.00E+00     1.63E-03
;;;                     2.70E-03     3.22E-03    0.00E+00     0.00E+00
;;;                     0.00E+00     1.51E-03    2.53E-03     3.02E-03
;;;                     0.00E+00     0.00E+00    0.00E+00     1.49E-03
;;;                     2.38E-03     2.92E-03    0.00E+00     0.00E+00
;;;                     0.00E+00     1.46E-03    2.22E-03     2.81E-03
;;;                     0.00E+00     0.00E+00    0.00E+00     1.40E-03
;;;                     2.14E-03     2.69E-03    0.00E+00     0.00E+00
;;;                     0.00E+00     1.34E-03    2.01E-03     2.63E-03
;;;                     0.00E+00     0.00E+00    0.00E+00     1.36E-03
;;;                     2.08E-03     2.56E-03    0.00E+00     0.00E+00
;;;                     0.00E+00     1.27E-03    2.01E-03     2.31E-03
;;;                     0.00E+00     0.00E+00    0.00E+00     1.36E-03
;;;                     1.94E-03     2.20E-03    0.00E+00     0.00E+00
;;;                     0.00E+00     1.03E-03    1.83E-03     2.07E-03
;;;                     0.00E+00     0.00E+00    0.00E+00     8.93E-04
;;;                     1.65E-03     2.01E-03    0.00E+00     0.00E+00
;;;                     0.00E+00     9.41E-04    1.60E-03     1.91E-03
;;;                     0.00E+00     0.00E+00    0.00E+00     9.67E-04
;;;                     1.51E-03     1.78E-03    0.00E+00     0.00E+00
;;;                     0.00E+00     8.95E-04    1.43E-03     1.76E-03
;;;                     0.00E+00     0.00E+00    0.00E+00     9.36E-04
```

```
;;;                     1.41E-03     1.64E-03    0.00E+00     0.00E+00
;;;                     0.00E+00     8.77E-04    1.28E-03     1.56E-03
;;;                     0.00E+00     0.00E+00    0.00E+00     5.39E-04
;;;                     1.13E-03     1.55E-03    0.00E+00     0.00E+00
;;;                     0.00E+00     6.01E-04    1.14E-03     1.60E-03
;;;                     0.00E+00     0.00E+00    0.00E+00     6.03E-04
;;;                     1.14E-03     1.52E-03    0.00E+00     0.00E+00
;;;                     0.00E+00     5.75E-04    1.11E-03     1.55E-03
;;;                     0.00E+00     0.00E+00    0.00E+00     5.88E-04
;;;                     1.08E-03     1.52E-03    0.00E+00     0.00E+00
;;;                     0.00E+00     6.13E-04    1.08E-03     1.44E-03
;;;                     0.00E+00     0.00E+00    0.00E+00     6.74E-04
;;;                     1.06E-03     1.45E-03    0.00E+00     0.00E+00
;;;                     0.00E+00     6.96E-04    1.01E-03     1.18E-03
;;;                     0.00E+00     0.00E+00    0.00E+00     6.54E-04
;;;                     9.39E-04     1.19E-03    0.00E+00     0.00E+00
;;;                     0.00E+00     7.28E-04    9.21E-04     1.21E-03
;;;                     0.00E+00     0.00E+00    0.00E+00     5.91E-04
;;;                     9.70E-04     1.13E-03    0.00E+00     0.00E+00
;;;                     0.00E+00     6.33E-04    9.31E-04     1.22E-03
;;;                     0.00E+00     0.00E+00    0.00E+00     6.94E-04
;;;                     9.56E-04     1.11E-03    0.00E+00     0.00E+00
;;;                     0.00E+00     8.03E-04    9.30E-04     1.00E-03
;;;                     0.00E+00     0.00E+00    0.00E+00     6.76E-04
;;;                     9.60E-04     9.90E-04    0.00E+00     0.00E+00
;;;                     0.00E+00     6.48E-04    9.95E-04     1.03E-03
;;;                     0.00E+00     0.00E+00    0.00E+00     6.52E-04
;;;                     9.75E-04     1.03E-03    0.00E+00     0.00E+00
;;;                     0.00E+00     5.98E-04    1.03E-03     1.04E-03
;;;                     0.00E+00     0.00E+00    0.00E+00     5.74E-04
;;;                     1.02E-03     1.00E-03    0.00E+00     0.00E+00
;;;                     0.00E+00     0.00E+00    9.47E-04     1.11E-03
;;;                     0.00E+00     0.00E+00    0.00E+00     0.00E+00
;;;                     1.00E-03     1.03E-03    0.00E+00     0.00E+00
;;;                     0.00E+00     0.00E+00    9.28E-04     1.02E-03
;;;                     0.00E+00     0.00E+00    0.00E+00     0.00E+00
;;;                     8.65E-04     1.10E-03    0.00E+00     0.00E+00
;;;                     0.00E+00     0.00E+00    8.91E-04     1.03E-03
;;;                     0.00E+00     0.00E+00    0.00E+00     0.00E+00
;;;                     9.30E-04     1.04E-03    0.00E+00     0.00E+00
;;;                     0.00E+00     0.00E+00    9.30E-04     1.01E-03
;;;                     0.00E+00     0.00E+00    0.00E+00     0.00E+00
;;;                     9.86E-04     8.57E-04    0.00E+00     0.00E+00
;;;                     0.00E+00     0.00E+00    8.82E-04     9.04E-04
;;;                     0.00E+00     0.00E+00    0.00E+00     0.00E+00
;;;                     0.00E+00     9.22E-04
;;;                    )
;;;  )
;;;  (make_stable)
  (setq pr1 0.0)
)

;;;

(defun accept ()
  (foreach a parameter_set
    (set (read (strcat "p" a)) (eval (read (strcat "n" a))))
  )
  (setq pr1 nr1)
)

;;;

(defun reject ()
  (foreach a parameter_set
    (set (read (strcat "n" a)) (eval (read (strcat "p" a))))
  )
)

;;; Set a random target
```

```
(defun set_random_target ()
  (setq nr1 pr1)
  (setq r1 nr1)
  (foreach a parameter_set
    (set (read (strcat "n" a)) (eval (read (strcat "p" a))))
  )
  (foreach a parameter_set
    (set (read a) (eval (read (strcat "p" a))))
  )
  (foreach a parameter_set (set (read (strcat "t" a)) nil))
;;; if not targeting
  (setq a (nth (fix (* (rnd) (* (length parameter_set) 0.99)))
               parameter_set
          )
  )
  (normalize a (* (rnd) 0.50))
  (set (read (strcat "t" a))
       (increment (eval (read (strcat "p" a)))
                  (eval (read (strcat "m" a)))
                  (expt 10 (* (1- (* (fix (* (rnd) 1.99)) 2)) 99.0))
       )
  )
  (setq a nil)
;;; if targeting
;;;  (setq a "thk")
;;;  (normalize a (* (rnd) 0.50))
;;;  (set (read (strcat "t" a))
;;;       (increment (eval (read (strcat "p" a)))
;;;                  (eval (read (strcat "m" a)))
;;;                  0.006
;;;       )
;;;  )
;;;  (setq a nil)
;;;
  (setq tthk 0.006)
;;;
  (force_new)
  (run_fds)
  (setq fds_data (read_fds_output))
  (get_r1 goal2)
  (princ (strcat "\n " (rtos (* r1 100) 2 2) "%"))
)


;;; Determine how well secondary goal is met

(defun get_2nd ()
  (foreach a parameter_set
    (set (read a) (eval (read (strcat "n" a))))
  )
  (run_fds)
  (setq fds_data (read_fds_output))
  (get_r1 goal2)
  (setq nr1 r1)
)

;;; Curve fit to 1st goal

(defun fit_1st ()
  (foreach a parameter_set (set (read (strcat "m" a)) 1))
  (run_fds)
  (setq fds_data (read_fds_output))
  (drawmlr_all)
  (get_r1 goal1)
  (setq nr1 r1)
  (setq co 0)
  (output_results)
  (normalize_all)
  (curve_fit)
)
```

```
;;; Forces a new best parameter solution set

(defun force_new ()
  (increment_all)
  (run_fds)
  (drawmlr_all)
  (get_r1 goal1)
  (setq nr1 r1)
  (output_results)
)

;;; Stochastic Hill-Climber Algorithm

(defun curve_fit ()
  (setq beepnext 1)
  (setq co 0)
  (while (< co 50)
    (mutate_all)
    (run_fds)
    (if (= beepnext 1)
      (drawmlr_all)
    )
    (setq beepnext 0)
    (setq fds_data (read_fds_output))
    (get_r1 goal1)
    (if (> r1 nr1)
      (progn (setq beepnext 1)
             (setq ro 1)
             (foreach a       parameter_set
               (set (read (strcat "n" a)) (eval (read a)))
             )
             (setq nr1 r1)
;;;                (save_best)
             (setq co (max 0 (- co 10)))
      )
      (setq co (1+ co))
    )
    (output_results)
  )
;;;  (make_stable)
)

;;; reserves the current data as the best so far

(defun save_best ()
  (vl-file-delete
    (strcat "c:\\HC-PYRO\\" matl "_devc_BEST.csv")
  )
  (vl-file-copy
    (strcat "c:\\HC-PYRO\\" matl "_devc.csv")
    (strcat "c:\\HC-PYRO\\" matl "_devc_BEST.csv")
  )
  (vl-file-delete (strcat "c:\\HC-PYRO\\" matl "_BEST.fds"))
  (vl-file-copy
    (strcat "c:\\HC-PYRO\\" matl ".fds")
    (strcat "c:\\HC-PYRO\\" matl "_BEST.fds")
  )
)

;;; draws all MLR curves to the screen

(defun drawmlr_all ()
  (command "undo" "be")
  (vlr-beep-reaction)
  (command "erase" "all" "")
  (drawmlr cone_data cone_data)
  (drawmlr fds_data cone_data)
  (command "zoom" "e" "zoom" "0.9x")
;;;  (command "_EXPORT"
;;;        (strcat "c:\\HC-PYRO\\IMG_"
;;;                (SUBSTR (RTOS (GETVAR "CDATE") 2 8) 7 2)
```

```
;;;               (SUBSTR (RTOS (GETVAR "CDATE") 2 8) 10)
;;;               ".bmp"
;;;        )
;;;        "all"
;;;        ""
;;;  )
  (command "undo" "e")
)

;;; random number generator

(defun rnd ()
  (if (not seed)
    (setq seed (getvar "DATE"))
  )
  (setq seed (rem (+ (* 25173 seed) 13849) 65536))
  (/ seed 65536)
)

;;; mutates a single parameter

(defun mutate (x1 x2 / x1 x2)
  (*
    x1
    (expt (1+
           (/ (* (* (+ (* 0.0004 co co) (* -0.04 co) 1.0) (expt 2.0 x2))
                 (rnd)
              )
              100
           )
         )
         (1- (* (fix (* (rnd) 1.9999)) 2))
    )
  )
)

;;; increments a single parameter in the direction of the target value

(defun increment (x1 x2 x3 / x1 x2 x3)
  (if (<= (/ (abs (- x1 x3)) x1) (/ (expt 2.0 x2) 100))
    x3
    (* x1
       (expt (1+ (/ (expt 2.0 x2) 100))
             (if (>= x3 x1)
               1
               -1
             )
       )
    )
  )
)

;;; reads in MLR time history from fds output

(defun read_fds_output (/ fds_data file filer char point)
  (setq fds_data nil)
  (setq file (strcat "C:\\HC-PYRO\\" matl "_devc.csv"))
  (setq filer (open file "r"))
  (read-line filer)
  (read-line filer)
  (setq char 0)
  (while (/= char nil)
    (setq char (read-char filer))
    (setq point "")
    (while (and (/= char 44) (/= char nil))
      (setq point (strcat point (chr char)))
      (setq char (read-char filer))
    )
    (setq fds_data (append fds_data (list (atof point))))
  )
  (close filer)
```

```
  (cdr fds_data)
)

;;; outputs the parameter sets and the r-squared values to a comma delimited
;;; file

(defun output_results (/ file filea)
  (setq file (strcat "C:\\HC-PYRO\\" matl ".csv"))
  (if (findfile file)
    (setq filea (open file "a"))
    (progn
      (setq filea (open file "a"))
      (setq str "")
      (write-line
       (progn
         (foreach a parameter_set (setq str (strcat str a ",")))
         (foreach a parameter_set (setq str (strcat str "n" a ",")))
         (foreach a parameter_set (setq str (strcat str "p" a ",")))
         (foreach a parameter_set (setq str (strcat str "m" a ",")))
         (foreach a parameter_set (setq str (strcat str "t" a ",")))
         (strcat str "dx,dt,r1,nr1,pr1")
       )
       filea
      )
    )
  )
  (setq str "")
  (write-line
    (strcat
      (progn (foreach a       parameter_set
               (setq str (strcat str (rtos (eval (read a)) 1 3) ","))
             )
             (foreach a       parameter_set
               (setq
                 str
                  (strcat str (rtos (eval (read (strcat "n" a))) 1 3) ",")
               )
             )
             (foreach a       parameter_set
               (setq
                 str
                  (strcat str (rtos (eval (read (strcat "p" a))) 1 3) ",")
               )
             )
             (foreach a       parameter_set
               (setq
                 str
                  (strcat str (rtos (eval (read (strcat "m" a))) 1 3) ",")
               )
             )
             (foreach a       parameter_set
               (setq str (strcat str
                                 (if (eval (read (strcat "t" a)))
                                   (rtos (eval (read (strcat "t" a))) 1 3)
                                   ""
                                 )
                                 ","
                         )
               )
             )
             (strcat str
                     (rtos dx 1 4)
                     ","
                     (rtos dt 1 4)
                     ","
                     (rtos r1 1 4)
                     ","
                     (rtos nr1 1 4)
                     ","
                     (rtos pr1 1 4)
                     ","
```

```
            )
      )
    )
    filea
  )
  (princ (strcat "\n"
                 (itoa co)
                 "\t"
                 (rtos (* r1 100) 2 2)
                 "%"
                 "\t"
                 (rtos (* nr1 100) 2 2)
                 "%"
                 "\t"
                 (rtos (* pr1 100) 2 2)
                 "%"
         )
  )
  (close filea)
)

;;; returns the cumulative sum of the values in list x1

(defun sum (x1 / x1 x2 x3)
  (setq x3 0.0)
  (foreach x2 x1 (setq x3 (+ x3 x2)))
  x3
)

;;; increments all parameters with target values

(defun increment_all ()
  (foreach a parameter_set
    (if (eval (read (strcat "t" a)))
      (set (read (strcat "n" a))
           (increment (eval (read (strcat "n" a)))
                      (eval (read (strcat "m" a)))
                      (eval (read (strcat "t" a)))
           )
      )
    )
    (set (read a) (eval (read (strcat "n" a))))
  )
)

;;; mutates all parameters without target values

(defun mutate_all ()
  (foreach a parameter_set
    (if (not (eval (read (strcat "t" a))))
      (set (read a)
           (mutate (eval (read (strcat "n" a)))
                   (eval (read (strcat "m" a)))
           )
      )
    )
  )
)

;;; normalizes all parameters

(defun normalize_all ()
  (princ "\n Normalizing Parameters... \n")
  (setq no 1)
  (foreach a parameter_set (normalize a 0.05))
)

;;; determines the % change in a parameter that
;;; produces a % change in the accuracy of the solution

(defun normalize (a b / a b)
```

```
  (foreach a parameter_set
    (set (read a) (eval (read (strcat "n" a))))
  )
  (set (read (strcat "m" a)) 1)
  (princ "\n")
  (while (and (< (abs (/ (- r1 nr1) nr1)) b)
              (< (eval (read (strcat "m" a))) 7)
         )
    (set (read (strcat "m" a))
         (1+ (eval (read (strcat "m" a))))
    )
    (set (read a)
         (* (eval (read a))
            (/ 100.0 (+ (expt 2 (eval (read (strcat "m" a)))) 100.0))
         )
    )
    (run_fds)
    (setq fds_data (read_fds_output))
    (get_r1 goal1)
    (set (read a) (eval (read (strcat "n" a))))
    (princ (strcat "\r m"
                   a
                   "= "
                   (itoa (1- (eval (read (strcat "m" a)))))
                   "    "
           )
    )
  )
  (set (read (strcat "m" a))
       (1- (eval (read (strcat "m" a))))
  )
  (setq r1 nr1)
)

;;; draws the MLR time history to the screen

(defun drawmlr (mlr mlr2)
  (setq mo 0)
  (while (< mo (- (length mlr) (length fluxes)))
    (setq col (1+ (rem mo (length fluxes))))
    (command "-color" col)
    (if (member col goal2)
      (command
       "line"
       (list (/ (/ mo (length fluxes))
                (/ (/ (length mlr) (length fluxes)) 2.0)
             )
             (/ (nth mo mlr) (car (vl-sort mlr2 '>)))
       )
       (list
         (/ (1+ (/ mo (length fluxes)))
            (/ (/ (length mlr) (length fluxes)) 2.0)
         )
         (/ (nth (+ mo (length fluxes)) mlr) (car (vl-sort mlr2 '>)))
       )
       ""
      )
    )
    (setq mo (1+ mo))
  )
)

;;; calculates the r-squared value all MLR curves

(defun get_r1 (flux)
  (setq r1 1)
  (setq fds_data_i nil)
  (setq cone_data_i nil)
  (foreach c flux
    (setq po 0)
    (while (< po (length fds_data))
```

```
      (if (= (rem (- (1+ po) c) (length fluxes)) 0)
       (progn (setq fds_data_i (append fds_data_i (list (nth po fds_data))))
              (setq cone_data_i
                    (append cone_data_i (list (nth po cone_data)))
              )
       )
      )
      (setq po (1+ po))
    )
  )
  (setq r1
        (- 1.0
           (/ (sum (mapcar '(lambda (x1 x2) (* (- x1 x2) (- x1 x2)))
                           cone_data_i
                           fds_data_i
                   )
              )
              (- (sum (mapcar '(lambda (x1) (expt x1 2.0)) cone_data_i))
                 (/ (expt (sum cone_data_i) 2.0) (length cone_data_i))
              )
           )
        )
  )
)

;;; writes and runs the fds input file

(defun run_fds (/ file filer filer line)
  (setq file (strcat "C:\\HC-PYRO\\" matl ".fds"))
  (setq filew (open file "w"))
  (write-line
    (strcat "&HEAD CHID='"       matl
            "' TITLE='Iterations for "
            matl                 " Parameters' /"
           )
    filew
  )
  (setq dt 0.1)
  (setq dx (* 0.25 (sqrt dt)))
  (setq ko 0.0)
  (foreach a fluxes
    (write-line
      (strcat "&MESH IJK=3 3 4 XB=-0.15 0.15 -0.15 0.15 "
              (rtos ko 2 1)
              " "
              (rtos (+ ko 0.4) 2 1)
              " /"
      )
      filew
    )
    (setq ko (1+ ko))
  )
  (write-line
    (strcat "&TIME T_END="
            (rtos t_end 2 0)
            " WALL_INCREMENT=1 DT="
            (rtos dt 1 3)
            " /"
    )
    filew
  )
  (write-line "&MISC SOLID_PHASE_ONLY=.TRUE. /" filew)
  (write-line
    (strcat "&MATL ID='Virgin_1' DENSITY="
            (rtos rho1 1 3)
            " SPECIFIC_HEAT="
            (rtos cp1 1 3)
            " CONDUCTIVITY="
            (rtos k1 1 3)
            " EMISSIVITY="
            (rtos emi1 1 3)
```

```
          " N_REACTIONS=1 RESIDUE='Residue_1'"
          " HEAT_OF_REACTION="
          (rtos hor 1 3)
          " NU_FUEL="
          (rtos nu 1 3)
          " NU_RESIDUE="
          (rtos (- 1.0 nu) 1 3)
          " THRESHOLD_TEMPERATURE="
          (rtos temp 1 3)
          " A="
          (rtos (/ rr
                   (exp (/ (*       -1
                              (* -1
                                 (log (/ rr (+ rr drr)))
                                 8.314
                                 (+ temp 273.15)
                                 (+ temp 274.15)
                              )
                           )
                           (* 8.314 (+ temp 273.15))
                        )
                   )
                )
                1
                3
          )
          " E="
          (rtos (* -1
                   (log (/ rr (+ rr drr)))
                   8.314
                   (+ temp 273.15)
                   (+ temp 274.15)
                )
                1
                3
          )
          " /"
  )
  filew
)
(write-line
  (strcat "&MATL ID='Residue_1' DENSITY="
          (rtos rho2 1 3)
          " SPECIFIC_HEAT="
          (rtos cp2 1 3)
          " CONDUCTIVITY="
          (rtos k2 1 3)
          " EMISSIVITY="
          (rtos emi2 1 3)
          " /"
  )
  filew
)
(foreach a fluxes
  (write-line
    (strcat "&SURF ID='"
            matl
            "_"
            (rtos a 2 0)
            "' MATL_ID='Virgin_1' EXTERNAL_FLUX="
            (rtos a 2 0)
            ". THICKNESS="
            (rtos thk 1 3)
            " BACKING='INSULATED' STRETCH_FACTOR=1. CELL_SIZE_FACTOR="
            (rtos dx 1 3)
            " /"
    )
    filew
  )
)
(setq ko 0.0)
```

```
  (foreach a fluxes
    (write-line
      (strcat "&VENT XB=-0.05 0.05 -0.05 0.05 "
              (rtos ko 2 1)
              " "
              (rtos ko 2 1)
              " SURF_ID='"
              matl
              "_"
              (rtos a 2 0)
              "' /"
      )
      filew
    )
    (setq ko (1+ ko))
  )
  (write-line "&VENT MB='XMIN' SURF_ID='OPEN' /" filew)
  (write-line "&VENT MB='XMAX' SURF_ID='OPEN' /" filew)
  (write-line "&VENT MB='YMIN' SURF_ID='OPEN' /" filew)
  (write-line "&VENT MB='YMAX' SURF_ID='OPEN' /" filew)
  (write-line "&VENT MB='ZMAX' SURF_ID='OPEN' /" filew)
  (write-line
    (strcat "&DUMP NFRAMES=0 DT_DEVC="
            (rtos dt_devc 1 3)
            " SMOKE3D=.FALSE. MASS_FILE=.FALSE. DT_PL3D=100000. /"
    )
    filew
  )
  (setq ko 0.0)
  (foreach a fluxes
    (write-line
      (strcat "&DEVC XYZ=0.0 0.0 "
              (rtos ko 2 1)
              " IOR=3 QUANTITY='BURNING_RATE' ID='"
              (rtos a 2 0)
              " kW/m2' /"
      )
      filew
    )
    (setq ko (1+ ko))
  )
  (write-line "&TAIL /" filew)
  (close filew)
  (command "RUN_FDS")
)


(defun sci_sub (a)
  (atof
    (strcat (rtos (max (1- (atof (substr (rtos a 1 0) 1 1))) 0.9) 2 2)
            (substr (rtos a 1 0) 2 4)
    )
  )
)

(defun sci_add (a)
  (atof
    (strcat (rtos (1+ (atof (substr (rtos a 1 0) 1 1))) 2 2)
            (substr (rtos a 1 0) 2 4)
    )
  )
)

(defun make_stable ()
  (princ "\n Resolving Time Step...\n")
  (foreach a parameter_set
    (set (read a) (eval (read (strcat "n" a))))
  )
  (setq dt 0.04)
  (run_fds)
  (setq fds_data (read_fds_output))
```

```
  (drawmlr_all)
  (get_r1 goal2)
  (setq nr1 r1)
  (while
    (and (< (abs (/ (- nr1 r1) nr1)) (min 0.05 (- 0.1 (* 0.1 nr1))))
        (<= dt 1.0)
    )
     (setq dt (sci_add dt))
     (run_fds)
     (setq fds_data (read_fds_output))
     (drawmlr_all)
     (get_r1 goal2)
     (princ (strcat "\r dt="
                    (rtos (sci_sub dt) 2 2)
                    " sec"
            )
     )
  )
  (setq dt (sci_sub dt))
  (run_fds)
  (setq fds_data (read_fds_output))
  (drawmlr_all)
  (get_r1 goal1)
  (setq nr1 r1)
)

;;;(defun c:sensitivity_analysis ()
;;;   (initialize)
;;;   (foreach a parameter_set
;;;      (setq matl a)
;;;      (write_batch_file)
;;;      (set (read (strcat "m" a)) 0)
;;;      (setq r1 nr1)
;;;      (while (< (/ (abs (- nr1 r1)) nr1) 0.5)
;;;         (set (read a)
;;; (* (expt (1+ (/ (expt 2.0 (eval (read (strcat "m" a))))
;;; 100))
;;;                         1
;;;;;; 1 or -1
;;;                  )
;;;                  (eval (read (strcat "n" a)))
;;;              )
;;;         )
;;;         (run_fds)
;;;         (setq fds_data (read_fds_output))
;;;         (drawmlr_all)
;;;         (get_r1 goal1)
;;;         (output_results)
;;;         (set (read (strcat "m" a))
;;;              (1+ (eval (read (strcat "m" a))))
;;;         )
;;;      )
;;;      (set (read a) (eval (read (strcat "n" a))))
;;;   )
;;;)

;;; calculates the r-squared value for least accurate MLR curve

;;;(defun get_r1 (flux)
;;;   (setq r1 1)
;;;   (foreach c flux
;;;      (setq fds_data_i nil)
;;;      (setq cone_data_i nil)
;;;      (setq po 0)
;;;      (while (< po (length fds_data))
;;;         (if (= (rem (- (1+ po) c) (length fluxes)) 0)
;;; (progn (setq fds_data_i (append fds_data_i (list (nth po
;;; fds_data))))
;;; (setq cone_data_i (append cone_data_i (list (nth po
;;; cone_data))))
;;;             )
```

```
;;;         )
;;;         (setq po (1+ po))
;;;       )
;;;       (setq r1
;;;               (min r1
;;;                    (- 1.0
;;; (/ (sum (mapcar '(lambda (x1 x2) (* (- x1 x2) (- x1
;;; x2)))
;;;                                         cone_data_i
;;;                                         fds_data_i
;;;                                )
;;;                            )
;;; (- (sum (mapcar '(lambda (x1) (expt x1 2.0))
;;; cone_data_i))
;;; (/ (expt (sum cone_data_i) 2.0) (length
;;; cone_data_i))
;;;                            )
;;;                         )
;;;                     )
;;;               )
;;;       )
;;;    )
;;;)
```

Bibliography

1. Quintiere, J., A Semi-Quantitative Model for the Burning Rate of Solid Materials, Building and Fire Research Laboratory, NISTIR 4840, National Institute of Standards and Technology, Gaithersburg, MD, 1992.
2. Moghtaderi et all, An Integral Model for the Transient Pyrolysis of Solid Materials, Fire materials, Vol. 21, p.p. 7-16, 1997
3. Di Blasi, C., Modeling and Simulation of Combustion Processes of Charring and Non–Charring Solid Fuels, Progress in Energy and Combustion Science 19: 71–104, 1993.
4. McGrattan, K., Hostikka, S., Floyd, J., Baum, H., and Rehm, R., Fire Dynamics Simulator (Version 5), Technical Reference Guide, Volume 1: Mathematical Model, NIST Special Publication 1018-5, National Institute of Standards and Technology, Gaithersburg, Maryland.
5. Lautenberger, C.A., Generalized Pyrolysis Model for Combustible Solids, PhD Thesis, University of California, Berkeley, 2007.
6. ASTM E 1354-02a, Standard Test Method for Heat and Visible Smoke Release Rates for Materials and Products Using an Oxygen Consumption Calorimeter, 2002.
7. McGrattan, K., Hostikka, S., Floyd, J., Baum, H., and Rehm, R., Fire Dynamics Simulator (Version 5), User's Guide. NIST Special Publication 1019-5, National Institute of Standards and Technology, Gaithersburg, Maryland.
8. Rockett, J., Milke, J. Conduction of Heat in Solids. The SFPE Handbook of Fire Protection Engineering, 4th Edition, 2008.
9. Staggs, J.E.J, A Theoretical Investigation into Modeling Thermal Degradation of Solids Incorporating Finite–Rate Kinetics," Combustion Science and Technology 123: 261–185, 1997.
10. Delichatsios, M.A. and Zhang, J., Pyrolysis of a Finite Thickness Composite Material, International Journal of Heat and Mass Transfer, 51:1480-1487, 2008
11. Fernandez–Pello, A.C., The Solid Phase, Combustion Fundamentals of Fire, Ed. G. Cox, pp. 31–100, Academic Press, New York, 1995.
12. Darwin, C., On the Origin of Species by Means of Natural Selection (1st edn), Murray, London, 1859.
13. Reeves, C., Rowe, J. Genetic Algorithms - Principles and Perspective, 2002.
14. Matala, A., Estimation of Solid Phase Reaction Parameters for Fire Simulation, MS Thesis, University of Techniology, Helsinki, 2008.

Bibliography
(continued)

15. Matala, A., Hostikka, S., Mangs, J., Estimation of Pyrolysis Model Parameters for Solid Materials Using Thermogravimetric Data, 9th Intl. Symposium, IAFSS, 2009, pp.1213-1223.

16. Lautenberger, C., Rein, G., Fernandez-Pello, C., The Application of a Genetic Algorithm to Estimate Material Properties for Fire Modeling from Bench-Scale Fire Test Data, Fire Safety J., 41, 2006, pp.204-214.

17. Rein, G., C. Lautenberger, C. Fernandez-Pello, J. Torero, D. Urban, "Application of genetic algorithms and thermogravimetry to determine the kinetics of polyurethane foam in smoldering combustion", Combustion and Flame 146: 95 108, 2006

18. Kim, E., Lautenberger, C., Dembsey, N., Property Estimation for Pyrolysis Modeling Applied to Polyester FRP Composites with Different Glass Contents, Composites & Polycon, American Composites Manufacturers Association, Tampa, FL, USA, 2009.

19. Wolpert, D.H., Macready, W.G., No Free Lunch Theorems for Search, Technical Report SFI-TR-95-02-010, Santa Fe Institute, 1995.

20. Wolpert, D.H., Macready, W.G., No Free Lunch Theorems for Optimization, IEEE Transactions on Evolutionary Computation 1, 67, 1997.

21. Drysdale, D., An Introduction to Fire Dynamics, 2nd Edition

22. Tewarson, A., Generation of Heat and Gaseous, Liquid, and Solid Products in Fires, The SFPE Handbook of Fire Protection Engineering, 4th Edition, 2008.

23. Crank, J., Nicolson, P., A Practical Method for Numerical Evaluation of Solutions of Partial Differential Equations of the Heat-Conduction Type, Proceedings of the Cambridge Philosophical Society, 1947

24. Lyon, R., Takemori, M., Safronava, N., Stoliarov, S., and Walters, R., A Molecular Basis for Polymer Flammability, Polymer, Volume 50, Issue 12, 5 June 2009, Pages 2608-2617.

25. Stoliarov, S., Crowley, S., Lyon, R., Linteris, G., Prediction of the burning rates of non-charring polymers, Combustion and Flame, Volume 156, Issue 5, May 2009, Pages 1068-1083.